2019

Improving reliability in the wind energy industry via field failure predictions based on life, maintenance, and dynamic data from supervisory control and data acquisition systems

Michael Stanley Czahor
Iowa State University

Improving reliability in the wind energy industry via field failure predictions based on life, maintenance, and dynamic data from supervisory control and data acquisition systems

by

Michael Stanley Czahor

A dissertation submitted to the graduate faculty

in partial fulfillment of the requirements for the degree of

DOCTOR OF PHILOSOPHY

Major: Statistics; Wind Energy Science, Engineering, and Policy (WESEP)

Program of Study Committee:
William Q. Meeker, Major Professor
Petrutza Caragea
James D. McCalley
Daniel J. Nordman
Gene Takle

The student author, whose presentation of the scholarship herein was approved by the program of study committee, is solely responsible for the content of this dissertation. The Graduate College will ensure this dissertation is globally accessible and will not permit alterations after a degree is conferred.

Iowa State University

Ames, Iowa

2019

DEDICATION

I would like to dedicate this dissertation to my brother Matthew and my late Aunt Dorothy.

TABLE OF CONTENTS

LIST OF TABLES

Page

LIST OF FIGURES

Page

ACKNOWLEDGEMENTS

I would like to personally thank some special people who have been paramount in my life since the beginning of my graduate studies at Iowa State. I would first like to thank my family and friends for dealing with me having my laptop on me 24/7 as I worked and studied over the years.

I am very grateful to have had the most supportive girlfriend and now fiance', Matyll, during my time at Iowa State. Matyll's endless support and patience during late night after late night of work has been and continues to be unbelievable.

I would like to thank my best friend since childhood, Chris Weaver, for being the most reliable and encouraging friend throughout both graduate school and my entire life.

I would like to express my sincere gratitude to the National Science Foundation for their IGERT Award 1069283. Specifically, I would like to extend my appreciation to Dr. James D. McCalley, the Principal Investigator of Iowa State's WESEP program, who was one of many that provided me with this award.

I would like to thank the Department of Statistics at Iowa State University for: providing me with multiple years of graduate assistantships, awarding me with Teaching Excellence Honors, and constantly pushing me to be an expert statistician. Specifically, I would like to thank Dr. Petrutza Caragea, Dr. Ulrike Genschel, and Dr. Anna Peterson for overseeing my teaching duties.

I would like to send a special thanks to Gary Eyles and the Ames Soccer Club for hiring me as a youth soccer coach during all of my years at Iowa State. This was a special experience that kept me busy outside of graduate school.

I would like to thank Dr. Katharina Fischer, Senior Scientist at Fraunhofer IWES Research Institute, for hiring me as a reliability statistician during an international experience in Hanover, Germany. This experience helped shape my thesis research.

I would like to thank Dr. Meg White, a former professor from Rowan University, who has continued to be one of the most supportive people that I have ever met. Looking back, Dr. White's encouragement to pursue graduate school was the best advice and mentorship that I have ever received.

I would like to thank Andy Galdi and the Philadelphia Phillies for hiring me as a Quantitative Analyst within their research and development department. This has been my dream job since I was a kid and I feel overwhelmed that it has come true.

Finally, and most importantly, I would like to express my sincere gratitude to Dr. William Q. Meeker for his constructive suggestions, enthusiasm towards my work, and inspiring work ethic. Dr. Meeker has been a mentor and friend. I feel beyond privileged to have worked under such a professional and I hope to remain in close touch with Dr. Meeker moving forward.

ABSTRACT

Many modern engineering systems are being evaluated with prognostics and health management (PHM) tools. The goal of PHM is to evaluate and predict the state of a system or product during its service life. PHM aims to predict failure in order to alleviate system risks. Many different industries, including wind energy use PHM systems. In wind power generation, PHM aims to reduce maintenance costs and extend the availability periods for each turbine. With large technological advancements, the upcoming generation of reliability field data will be abundant with valuable information to help predict future failures of many systems including wind turbines. Sensors and tools such as synchrophasors (PMUs), accelerometers, programmable logical controllers (PLCs), and so on help monitor variables such as vibration, use rate, environmental variables, and much more. Such sensors and tools provide information about component or system use, load, and operating environment over time. Such multivariate time series data are referred to as system operating/environmental data (SOE data). Wind turbines collect these data through supervisory control acquisition data (SCADA) systems. Such data, along with failure data can be used to build models that can be used to predict the remaining life of individual wind turbines. Throughout the model building process: statistical, probabilistic, and model uncertainties should be assessed to properly determine the accuracy of all predictions calculated. In this thesis, three real application problems are presented. In Chapter 2, we focus on reliability small wind turbine (SWT) reliability issues and look at recurrence data from 21 individual 100kW wind turbines. We outline a nonhomogenous Poisson process (NHPP) model with a Bayesian hierarchical power law structure in discrete-time that allows for inclusion of time-varying covariates. Data used in Chapter 2 was provided by a power systems company in the United States. In Chapter 3, we focus on developing a repairable systems simulation tool in R to assist in maintenance decisions for wind turbine owners and operators. In Chapter 4 we introduce a nonparametric algorithm for predicting future part consumption in systems that fail from multiple failure types. Chapter 5 summarizes the work in this thesis and discusses the future of these research areas.

CHAPTER 1. INTRODUCTION

1.1 Background

Due to the expanding global effort to reduce carbon emissions, today's wind energy industry need to develop new, higher technology wind turbines with improved reliability and productivity. Wind turbine manufacturers of reliable turbines can have a competitive advantage in the market, as wind turbine operations and maintenance costs can make up a large portion of the overall costs of a wind turbine. Industry and others have recognized the financial implications of improving turbine reliability and continue to expand the efforts for better technologies, as turbines are often sited in hostile environments according to Hill, Stinebaugh, and Briand (2008). Condra defines reliability as "quality over time." Achieving high reliability in the wind energy industry requires a better understanding of maintenance schedules, failure-time distributions, and dynamic covariates associated with multiple failure modes. With access to this kind of information, one can develop methodologies to predict important quantities such as system downtime, reliability, and costs. The predictions can be used to inform decision making to help minimize the financial operations and maintenance burden that is consistently troubling the wind energy industry.

With prediction as the focus, extrapolation is necessary, as it is in most applications. While parametric models are often used, non-parametric models are sometimes used when problems have complicated structures. In all statistical analysis, it is important to quantify statistical uncertainty in predictions with use of prediction intervals, which can be calibrated to attain a desired coverage probability.

1.1.1 Wind Energy Data Sources

Wind turbine reliability data consist of failure times for wind turbines that experience a failure and service times for wind turbines that undergo preventive maintenance activities (i.e., inspecting

oil). These data are highly proprietary and often require a nondisclosure agreement for outside use. Bertling and Wennerhag (2012) summarize the type of studies and data that are often used within the wind energy industry.

1.1.2 Complex Field and Dynamic Covariate Data

Wind turbine failure data becomes complex due to censoring, truncation, and multiple failure modes. In addition, older wind farms are starting to experience non-homogeneity issues, as newly installed turbines do not share the same characteristics as the older turbines. The dynamic covariate data that are logged by supervisory control and data acquisition (SCADA) systems provide great potential for characterizing individual differences among a turbine fleet. Some industry examples using such data can be seen in Sajid and Hossam (2013), Matthews and Godwin (2013), and Al-Tubi et al. (2015).

1.1.2.1 Censoring and Truncation

Right-censoring occurs when units that have not failed at the time that the data is being analyzed. For example, a wind turbine could be operational for some entire period, causing it to be right-censored. Another example of censoring is multiple censoring, which is a function of staggered entry into a fleet. For example, a new turbine can be installed on an existing wind farm. Methods to analyze such data are described in Meeker and Escobar (1998).

Truncation occurs when failure times are observed only when they take on values in a certain range. Observations that fall outside of the observation period are unknown, making the sample size unknown. Methods for dealing with truncation are described in Meeker and Escobar (1998).

1.1.2.2 Population non-homogeneity

In studies that include field data for extended periods, staggered entries or existing product evolvement can occur. For example, a wind turbine might experience a gearbox failure, leading to the installation of a new gearbox with a different design. In this case, the population would be non-

homogenous. It is important to consider population non-homogeneity through use of techniques such as stratification.

1.2 Motivation

The main purpose of this research is to develop prediction methods and R tools for repairable systems, such as wind turbines. The research is motivated by real applications in the field of wind energy, but the methods are generic and can be adapted to other applications. This section describes the motivation for the three projects in the body of this dissertation.

1.2.1 Predicting the Future Downtime Costs for Small-Scale Wind Turbines

Small-scale wind turbine (SWT) installations saw a dramatic increase between 2008 and 2012. Unfortunately, downtime events raise concerns about the reliability and availability of SWTs, which are repairable systems that return to an operational state after a failure or other downtime events. The prediction of future downtime, which leads to lost revenue, can be based on historical lifetime data and any meaningful covariates tracked by the individual turbine's SCADA systems.

In this project, we explored recurring service events and the associated cost for each event. The data were obtained from a United States power company, where the questions at hand included, given a population of wind turbines, can we predict the future downtime costs for a new wind turbine? The power company sent SCADA logs and associated service event logs from the beginning of each turbines life through the Fall of 2016. We have information on the installation dates, use rates, vibration signals, and alarm logs. We do not, however, have any information on why the turbines actually failed, only that they were serviced at a particular time.

We present a statistical procedure for predicting the future amount of downtime for existing and new turbines. The general methodology is outlined and describes issues that can arise from truncation, censoring, and population non-homogeneity. A prediction interval methodology is described to quantify the uncertainty in our predictions.

1.2.2 Evaluating Maintenance Policies with Repairable System Simulation

A repairable system's behavior over time is dependent on operational conditions, system makeup, etc. To better understand how a repairable system will operate over time, a simulation-based method can be used to evaluate and compare different maintenance policies.

This project was motivated by the data sources in Section 1.1.1, which provide more of a summary than a detailed analysis on how wind turbines operate overtime. In addition, a limited number of maintenance-based simulation software currently exists (i.e., JMP and BlockSim). An R tool was developed to extend the capabilities of commercial products and applied to data within the wind energy industry. Data were obtained from Tretton et al. (2011) and were used within an R tool called RSimmer. We study the properties of three different failure processes: renewal process, trend renewal process, and non-homogenous Poisson process, within two different models (component and subsystem). Results show that the higher/less detailed model (subsystem) provides a good approximation to the component-level model. We present an analysis and apply both models based on the Tretton et al. (2011) data.

1.2.3 Prediction of Spare Part Requirements Based on Recurrent-Event Maintenance Data

In this project, we have data from a fleet of engineering assets, which are repairable systems. The part consumption of each asset is tracked over a two year period, that does not necessarily start at the beginning of each assets lifetime. We use historical data to answer the question: "given the part consumption history for the individual assets, can we predict part consumption orders on a week-to-week basis for the fleet?"

The data have staggered entries and multiple failure modes. Upon exploratory analysis, we found that the time series structures for part consumption had complex joint distributions and therefore took a nonparametric approach. An algorithm for predicting future part consumption for each combination of week and part type is presented and applied to our dataset. In addition, we compare our approach to a simpler approach and highlight the benefits of the developed algorithm.

1.3 Dissertation Organization

This dissertation consists of three main chapters, preceded by the general introduction and followed by a general conclusion. Each of these main chapters corresponds to a journal article. Chapter 2 presents a small-scale wind turbine recurrence and cost modeling problem that is a function of operational covariates from supervisory control and data acquisition systems. Chapter 3 develops a repairable systems software tool that offers two models (subsystem and component) and showcases an application of wind turbine maintenance. Chapter 4 describes a prediction algorithm for computing future part consumption needs with multiple failure causes and part types for complicated recurrence data.

Bibliography

Al-Tubi, I., Long H., Tavner P., Shaw B.and Zhang J. (2015). Probabilistic analysis of gear flank micropitting risk in wind turbine gearbox using supervisory control and data acquisition data. *IET Renewable Power Generation 9*, 610–617.

Bertling, L. and Wennerhag, P. (2012). *Wind turbine operation and maintenance.* (Tech Rep. No. 12:41). Elforsk.

Condra, L. W. (1993). *Reliability Improvement with Design of Experiments.* New York: Marcel Dekker.

Hill, R., Stinebaugh, J., and Briand, D. (2008). Wind turbine reliability: A database and analysis approach. Technical report, 0983, Sandia National Laboratories. https://windpower.sandia.gov/other/080983.pdf. Last accessed November 21, 2018.

Matthews, P., and Godwin J. (2013). Classification and detection of wind turbine pitch faults through SCADA data analysis. *International Journal of Prognostics and Health Management, 4,* 90–100.

Meeker, W. Q., and Escobar L. A. (1998). *Statistical Methods for Reliability Data.* Wiley.

Sajid, H., and Hossam A. G. (2013). Fault diagnosis in gearbox using adaptive wavelet filtering and shock response spectrum features extraction. *Structural Health Monitoring, 12,* 169–180.

Tretton, M., Reha, M., Drunsic, M., and Keim, M. (2008). Data Collection for Current U.S. Wind Energy Projects: Component Costs, Financing, Operations, and Maintenance. Technical report, 52707, NREL. https://www.nrel.gov/docs/fy12osti/52707.pdf. Last accessed November 21, 2018.

CHAPTER 2. SMALL-SCALE WIND TURBINE RECURRENCE AND COST MODELING AS A FUNCTION OF OPERATIONAL COVARIATES FROM SUPERVISORY CONTROL AND DATA ACQUISITION SYSTEMS

A paper submitted to *the International Journal of Health and Prognostics*

Michael S. Czahor and William Q. Meeker

Department of Statistics

Iowa State University

Ames, IA, 50011, USA

Abstract

Small-scale wind turbine (SWT) installations saw a dramatic increase between 2008 and 2012. Recently, the trend within industry has shifted towards installing larger wind turbines, leaving little attention for installed SWT reliability. Unfortunately, downtime events raise concerns about the reliability and availability of the large number of installed SWTs. SWTs are repairable systems that return to an operational state after a failure and repair or other downtime events. Multiple events over time, on a single observational unit (e.g., a wind turbine) are known as recurrent events. In this paper, the reliability of a fleet of SWTs is examined based on recurrent event data from 21 individual 100 kW wind turbines. Supervisory control and data acquisition (SCADA) systems periodically record SWT dynamic covariate data in the form of a vector time series. One type of event experienced by SWTs is known as a "service event," which is a time when an SWT is put into service mode for a repair (or due to a false alarm). We explore recurring service events and the associated cost of each "service event" and propose methodologies to link dynamic covariate data to downtime costs to assist in quantifying the variation of downtime across wind turbines.

We use a nonhomogeneous Poisson process (NHPP) model with a Bayesian hierarchical power law structure to describe the counting process and an autoregressive time series use rate model with a Bayesian framework to describe cumulative downtime that results from SWT "service events." Using the posterior distribution of the parameters of the hierarchical NHPP model, we develop conditional and unconditional methods to predict downtime mean cumulative functions (MCFs) for wind turbines.

Key Words: SCADA; power law; recurrent events.

2.1 Introduction

2.1.1 Background

Enhancing the reliability of wind turbines has been a collaborative effort between industry, federal government laboratories, and academia for the past two decades. Recently, the Department of Energy (DOE) has stated their vision for achieving higher wind turbine reliability with a five-part plan that includes a well-developed database on wind farm operations under normal operating conditions. Gould (2014) summarizes DOE's *Wind Vision* report and outlines the goals set forth by the DOE, which include developing a world-class database, ensuring reliable operation in severe operating environments, and developing and documenting the best practices in the wind industry to improve reliability and increase service life. Bertling and Wennerhag (2012) provide an international perspective in contrast to the US-centric DOE reports, with a compilation of reports that survey the development and research needs for wind turbine operation and maintenance across Europe. Reports within this survey include component-specific reliability reports, maintenance strategy reports based on reliability modeling results, and database development needs for future work.

Limited work in applying reliability-based statistical methodologies to wind farm reliability data has appeared in the literature and can potentially assist in the DOE's effort. The *Reliawind* study by Wilkinson et al. (2011) identifies critical failure modes, summarizes the potential of SCADA systems, and highlights the benefits of having access to service records and alarm logs. Arifujjaman (2013) conducts a component-specific reliability analysis of grid-connected permanent

magnet generator-based wind turbines and establishes a method to relate wind speed and power losses to the reliability of power electronic converters. Fischer, Besnard, and Bertling (2011) present results on a reliability-centered maintenance (RCM) study that utilizes failure data and industry expert opinions to improve the reliability, availability, and profitability of wind turbines.

There is an abundant number of wind turbine component-specific papers that implement statistical methodologies that are not reliability-based, but can be useful for future reliability work as they convey the benefits of SCADA data. For example, Sajid and Hossam (2013) focus on predicting gearbox health using a nonlinear autoregressive model with exogenous inputs. Al-Tubi et al. (2015) investigate the probabilistic risk of gear flank micropitting risk with the use of SCADA data. Matthews and Godwin (2013) develop classification methods to detect wind turbine pitch faults using SCADA data.

2.1.2 Big Data in the Wind Energy Industry

Wind turbines are commonly outfitted with many sensors to assist in tracking operational and environmental conditions. According to Kashyap (2014), a typical wind turbine can have 125 to 200 sensors that generate data at a rate of approximately 2000 observations per minute. At this rate, a single wind turbine can generate upwards of one terabyte of data in one week. Table 1 provides an example of types of data that SCADA systems capture from wind turbines. These time series data are generally values averaged over 10-minute intervals with an attached chronological timestamp. Ciang, Lee, and Bang (2008) and Faulkner, Cutter, and Owens (Faulkner2012) describe the use of such sensor data for system health monitoring. Tautz-Weinert and Watson (2016) provide a review of using SCADA data for wind turbine condition monitoring. Analysts in industry and academia have made progress in the prognostic realm of wind energy with advances in condition monitoring techniques, wind turbine sensor placement, and communication capabilities (e.g., allowing wind turbines to use an IP address to send a live feed of data to a centralized location). Saxena et al. (2008) summarize different prognostic techniques that are being used across industries and highlight

the benefits of having historical covariate data in correspondence with life data. We use such data for SWT recurrent event analysis in this paper.

SCADA data contains information on the state of individual wind turbines. We focus on a state that indicates when a wind turbine is in service mode. Programmable logical controllers (PLCs) continuously log state data and when a component of the wind turbine exhibits unusual behavior (i.e, when values exceed predefined tolerances), the wind turbine will change states to let an owner or operator know of the event via an alarm. Such alarms or state changes may serve as a precursor to failure events and are of interest to owners and operators to minimize financial burdens that are experienced because of unplanned maintenance or catastrophic failures.

Table 2.1 Examples of data logged by SCADA systems.

Subsytem	**Data Collected**
Rotor and Blades	Pitch angle and rotor speed.
Gearbox	Oil, bearing, and hydraulic temperatures. Vibration, force, and rotational speed.
Generator	Stator and rotor voltages and currents. Power factors, rotor and grid frequencies, cabinet temperature, and generator speed.
Nacelle	Position, frame temperature, etc.

2.1.3 Operations and Maintenance Costs and Availability

According to Morthorst and Awerbuch (2009), operations and maintenance (O&M) costs typically account for 20 to 25% of a wind turbine's total levelized cost of energy (LCOE). O&M costs have gone down drastically in the last 30 years due to advances in engineering, condition monitoring

approaches, and preventive maintenance strategies. The International Renewable Energy Agency reports that O&M costs are not uniform across wind farms, suggesting that factors such as wind turbine manufacturer and turbine model influence the number and cost of downtime events. One must consider that a wind turbine's O&M costs will also change over time. The rate of occurrence of failures typically increases with age, making failures more likely to occur outside of warranty periods, which increases the cost to return wind turbines to operational status after a downtime event. See Gielen (2012) for more information on O&M costs for wind turbines.

One key O&M metric is wind turbine availability, which helps compare turbine-to-turbine performance. Wind turbine availability is usually defined as

$$A_{Time} = \frac{T_{Operation}}{T_{Total}} \tag{2.1}$$

where $T_{Operation}$ is the time that a wind turbine is operating (i.e., generating power) and T_{Total} is the total time that a wind turbine could have been operating (if the turbine never went into service mode).

Maintenance events to be considered in (2.1) include preventive maintenance, corrective maintenance, and scheduled shutdowns. These are examples of events that lower A_{Time}, because $T_{Operation}$ decreases when such maintenance events occur. Throughout this paper, we will discuss a collection of these events and provide an illustrative example of the associated cost for such events.

2.1.4 Overview

The rest of the paper is organized as follows. Section 2.2 introduces the wind turbine dataset as a motivating example. Section 2.3 introduces notation for a nonhomogeneous Poisson process (NHPP) with a power law intensity function and a model to estimate the cumulative number of events for a single wind turbine and multiple wind turbines, based on draws from posterior parameter distributions. Section 2.4 develops an autoregressive (AR) time series model for use rate for the turbines. Section 2.5 gives methods to predict the cumulative number of service-time events using results from the previous sections and provides results from a simulation study.

Section 2.6 first discusses unconditional prediction and then shows how this leads to the more useful conditional prediction intervals for the number of service-time events. We also show the value of updating posterior distributions with prior information. Section 2.7 discusses the economic benefits associated with hierarchical modeling and mentions areas for future work.

2.2 Data

2.2.1 Data from a US Power Company

The illustrative application is based on 21 wind turbines in different locations throughout the US. Data used in this work was provided from a US power systems company. The data were collected over a four-year period from 2012 through 2016. The 21 wind turbines all have the same model designation, with a generating capacity of 100 kW. All 21 wind turbines have unique starting times (install dates), but have a common data freeze date (DFD) in October 2016. During the observation period, each wind turbine had a SCADA system automatically record operational and environmental dynamic covariate data (e.g., wind speed, ambient temperature, etc.) as 10-minute averages for each variable. From the time of installation until the DFD, there is an entire covariate history. Each wind turbine's state information was also periodically recorded over the observation period, where a state code corresponds to a wind turbine's operational status during each 10-minute time interval. Because different manufacturers use different systems of state codes and because the exact coding method could be sensitive, we refer to states by name instead of code.

We focus on the "service mode" state. Being in this state implies that the wind turbine was being treated for preventive maintenance, correcting a failure event, or subject to a false alarm. Service events are recurring events that result in downtime, for which cost accrues over time. Due to the proprietary nature of the data used in this paper, different kinds of service events were combined, even though different failure modes and event types exist. For more information on state codes, see Kusiak and Verma (2010) .

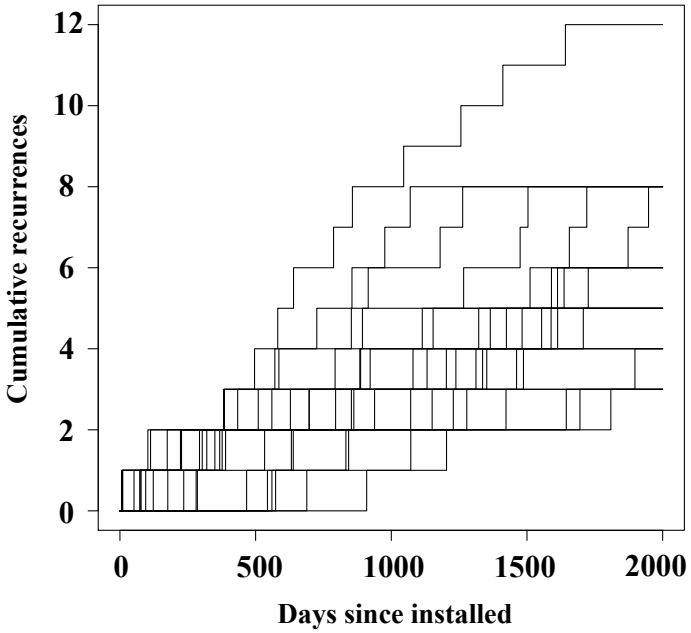

Figure 2.1 Cumulative events versus time (days since installation) for each of the 21 wind turbines.

2.3 Service Event and Cost Model

2.3.1 A Nonparametric View of the Cost and Count Data

With access to the entire life history up until the DFD, there were n_j observed service events for wind turbine j. The process for each turbine is time censored, where the end of observation time is denoted by t_{c_j}, which is computed from the real time of the DFD. Refer to Dai and Wang (2017) for more information on time censoring of recurrent data processes. The observed service events that occur for wind turbine j are $0 < t_{j1} < t_{j2} < ... < t_{c_j}$. Figure 2.1 is a plot of cumulative recurrences over time for each wind turbine. Chapter 4 of Nelson (2003) and Chapter 16 of Meeker and Escobar (1998) provide an algorithm to compute the mean cumulative function (MCF) from such data and standard errors that allow one to compute pointwise approximate confidence intervals for the population MCF.

2.3.2 Nonhomogeneous Poisson Process with a Power Law Intensity Function

Parametric statistical models for recurrent events have been studied, for example, by Bain and Engelhardt (1991) and Rigdon and Basu (2000). With minimal repair maintenance (as opposed to system renewal), the nonhomogeneous Poisson process (NHPP) model is often appropriate. An NHPP model allows for a nonconstant recurrence rate $\nu(t)$. Adapting methods used in Ryan, Hamada, and Reese (2011), we consider an NHPP with a power law intensity rate function

$$\nu(t;\phi,\eta) = \frac{\phi}{\eta}\left(\frac{t}{\eta}\right)^{\phi-1}, \phi > 0, \eta > 0 \tag{2.2}$$

with a mean cumulative function (MCF)

$$\lambda(t) = E\big[N(t)\big] = \textstyle\int_0^t \nu(u)du = \left(\frac{t}{\eta}\right)^{\phi}.$$

The likelihood function corresponding to (2.2) for turbine j is

$$\mathcal{L}(DATA_j) = \left(\tfrac{\phi_j}{\eta_j}\right)^{r} \times \textstyle\prod_{i=1}^{r} t_{ji}^{\phi_j - 1} \times \exp\big(-\lambda_i\big)$$

where $\lambda_i\big(t_{c_j};\phi_j,\eta_j\big) = \big(t_{c_j}/\eta_j\big)^{\phi_j}$ is the expected number of service events up to time t_{c_j} and r is the number of service events for turbine j. For more information on NHPP estimation procedures see Chapter 16 of Meeker and Escobar (1998) and Rigdon and Basu (2000).

2.3.3 Motivating a Bayesian Approach

For this paper, we use a Bayesian approach for modeling and estimation. Gelman (2006) summarize the four basic components of a Bayesian analysis:

1. **The prior distribution** reflects any prior knowledge about the values of parameters.
2. **The data** are the observed values from the subjects within the study.
3. **The model** relates data to the parameters.
4. **The posterior distribution** reflects the updated belief in the parameter values given the data and the model.

The prior distribution component is important, as Bayesian inference combines any new wind turbine data with what we know about the NHPP parameters from previously observed turbines. An important benefit of the Bayesian approach is posterior distributions can constantly be updated as new data become available. Added information has the potential to decrease the variability in posterior distributions, which can result in narrower confidence intervals.

Bayesian approaches have been utilized previously within the wind energy industry. Courtney, Lynch, and Sweeny (2013) use Bayesian model averaging to improve high-resolution forecasting techniques for ensemble prediction systems. Sobolewski (2015) presents probabilistic models that quantify wind farm reliability taking multiple factors into account using Bayesian networks. Wu et al. (2017) develop a novel Bayesian hierarchical modeling framework to predict time-to-failure distributions for a small wind turbine using fatigue and reliability analysis.

2.3.4 Model for a Single Wind Turbine

To provide parameters with a clearer interpretation for turbine j, we replace the parameter η_j with $\lambda_j = \lambda(t_{c_j}) = (\eta_j/c_j)^{-\phi_j}$, which is the mean number of service events up to time t_{c_j}. To move between two parameterizations for turbine j we use

$$\eta_j = c_j \lambda_j^{-1/\phi_j}.$$

The development of a single wind turbine model is the first step toward the multiple turbine model that is necessary to describe the $J = 21$ wind turbine datasets of interest. The form of the likelihood function $\mathcal{L}(DATA_j|\theta_j)$ for the time-censored data design is given in Ryan, Hamada, and Reese (2011).

Following Ryan, Hamada, and Reese (2011), direct use of Bayes' theorem results in independent posterior distributions for θ_j for turbine j that are proportional to

$$\mathcal{L}(DATA_j|\theta_j)\pi(\theta_j), \tag{2.3}$$

where θ_j is the parameter vector and $\pi_j(\theta_j)$ is the prior distribution for θ_j. Because there is little or no prior information about θ we use diffuse prior distributions. The posterior distribution in (2.3)

provides an update of information on the parameters based on the observed data. In particular, we assume no prior knowledge of the parameters and use a Jeffereys prior distribution (which tend to be diffuse) for the parameters where

$$\pi(\lambda_j, \phi_j) \propto \frac{1}{\lambda_j \phi_j} \quad j = 1, ..., J.$$

See Kass and Wasserman (1996) for more information on diffuse prior distributions.

2.3.5 Application to a Single Wind Turbine

As an example, consider Turbine 1 which experienced six service events during its 2000 days of observed service. Three separate chains were run with three different sets of starting values for the parameters, using RJAGS to implement the Gibbs sampler. Each chain produced 9,000 draws from the joint posterior distribution and the first 500 (i.e., burn-in samples) were discarded. We used time series plots of the parameter draws to determine that the chain mixed well.

As an example, Figure 2.2 displays the resulting 25,500 draws from the joint posterior distribution for λ_1 and ϕ_1. Figure 2.3 displays the marginal posterior densities for λ_1 and ϕ_1. Table 2.2 summarizes the Bayesian estimation results for Turbine 1.

Table 2.2 NHPP parameter estimates and credible intervals based on the joint distribution for Turbine 1

Parameter	Median	95% Credible interval
λ_1	5.87	[4.95, 7.08]
ϕ_1	1.11	[0.90, 1.41]

2.3.6 Multiple Wind Turbine Hierarchical Model

We now consider combining the service event data from multiple wind turbines. Similar to Ryan, Hamada, and Reese (2011), we use a hierarchical model based on an NHPP power law process for multiple repairable systems (wind turbines in our application) and simple posterior inference methods for time-truncated designs by taking the cost of service events into consideration and incorporating dynamic covariate information into the model.

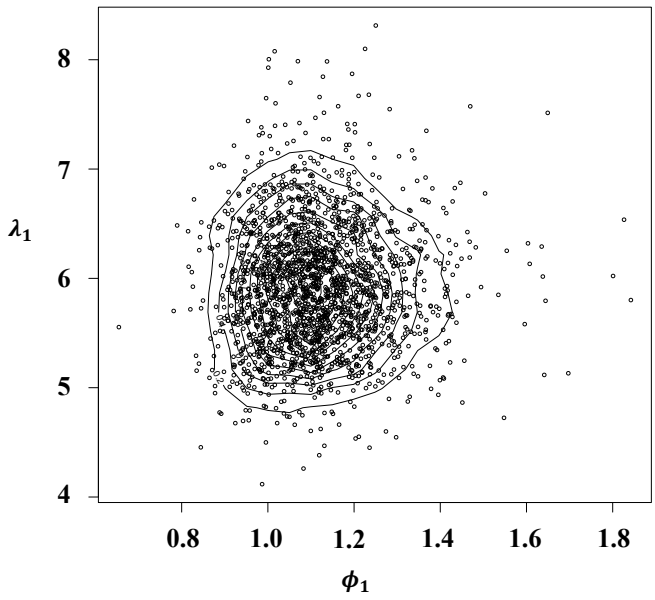

Figure 2.2 Sample draws from the NHPP joint posterior distribution for a single turbine, where the contours represent the areas with the most density from inside to out.

We start by considering the J wind turbines, which have unique install times and are observed through the time t_{c_j}, $j = 1, ...J$. We assume that the vector service event times from wind turbine j follow an intensity given in (2) and have parameters λ_j and ϕ_j. We consider a hierarchical model to allow data from all of the wind turbines to be partially pooled, and allow each of the wind turbines to have its own intensity parameters. That is, instead of estimating the 21 pairs of parameters independently, we describe variability in the parameters with a joint distribution and estimate the hyperparameters of that distribution The statistical notion of partially pooling data is commonly known as "borrowing strength" and is outlined, for example in Draper et al. (1992). This notion assists in describing relationships involving the observed data and unobserved parameters of interest.

To help choose the distribution of the parameters in the hierarchical model we first fit separate NHPP models to each of the wind turbines and compare the empirical distribution of those estimates to several distributions. Figure 2.4 displays a scatterplot of the NHPP point estimates (median

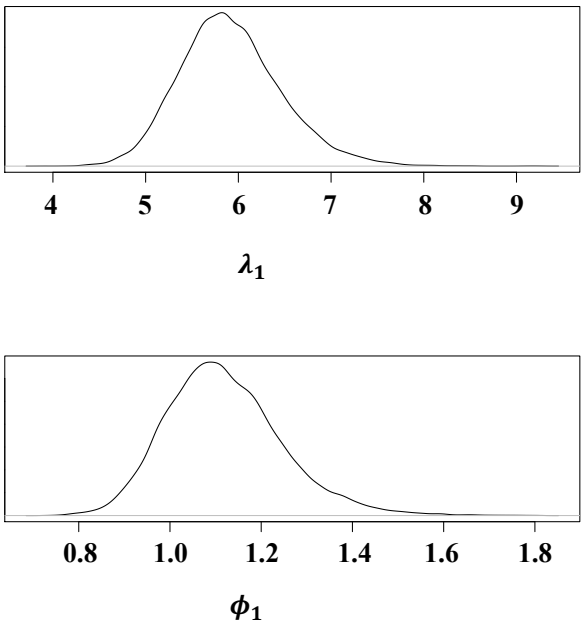

Figure 2.3 Marginal posterior distributions for the NHPP parameters.

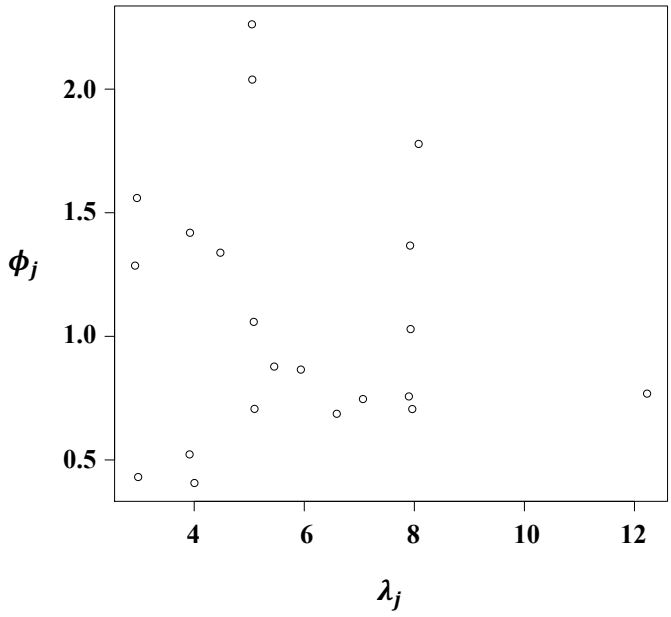

Figure 2.4 Scatterplot of the NHPP point estimates.

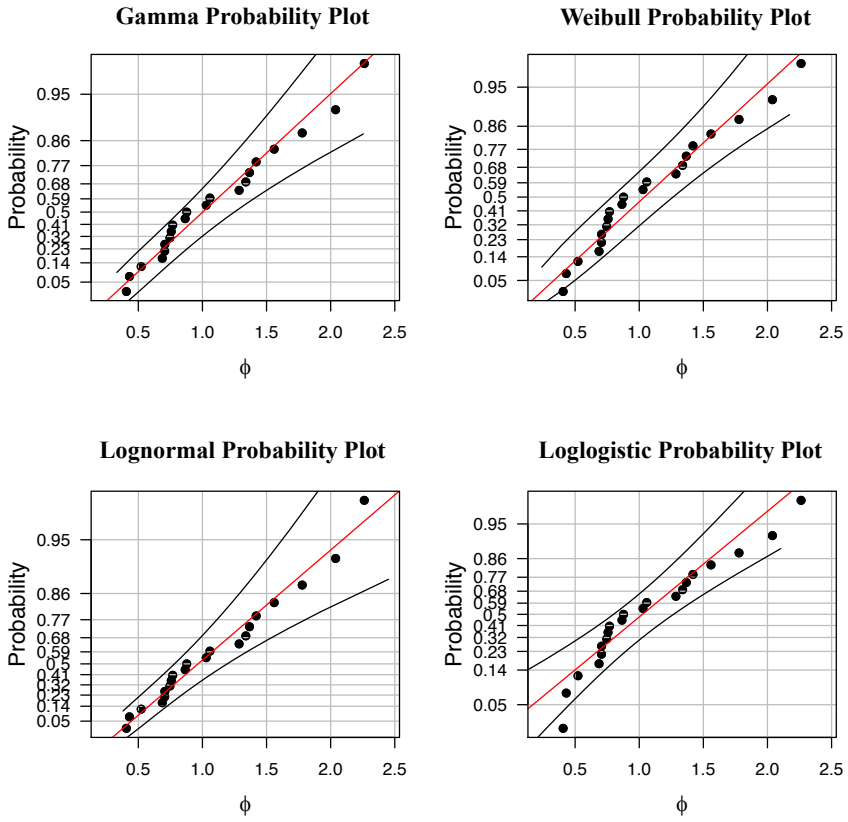

Figure 2.5 Probability plots for ϕ from four different assumed distributions.

of the respective marginal posterior distributions). Figures 2.5 and 2.6 display probability plots for the ϕ and λ parameters respectively for each of four selected distributions. Tables 2.3 and 2.4 summarize the goodness of fit for ϕ and λ respectively for each distribution. The results indicate that the Gamma distribution provides a reasonable description of the data for both parameters. We will use Gamma distributions here because they provide a good description of the parameter distributions and they will simplify computations.

Thus let the distributions for λ and ϕ be independent and identically distributed (iid) Gamma distributions denoted by

$$\lambda_j \sim \text{Gamma}(\alpha_\lambda, \beta_\lambda) \tag{2.4}$$

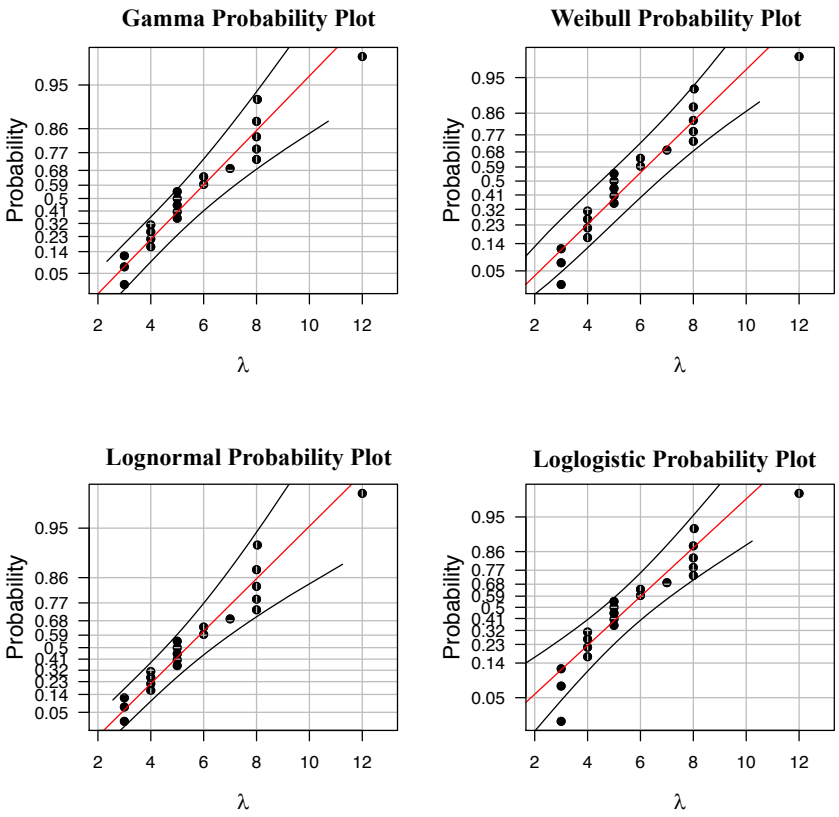

Figure 2.6 Probability plots for λ from four different assumed distributions.

$$\phi_j \sim \text{Gamma}\big(\alpha_\phi, \beta_\phi\big) \tag{2.5}$$

for $j = 1, 2, ...J = 21$. Because there is no prior information about the hyperparameters in (2.4) and (2.5), we propose

$$\alpha_\lambda \sim \text{Gamma}\big(0.001, 0.001\big),\ \beta_\lambda \sim \text{Gamma}\big(0.001, 0.001\big)$$

$$\alpha_\phi \sim \text{Gamma}\big(0.001, 0.001\big),\ \beta_\phi \sim \text{Gamma}\big(0.001, 0.001\big)$$

for α_λ, β_λ, α_ϕ, and β_ϕ. This choice of prior distributions guarantees that the parameters are positive and that the prior distributions are diffuse, allowing inferences about the $J = 21$ wind turbines to be data-driven.

Table 2.3 Goodness of fit for the distribution of ϕ

Distribution	AIC	BIC
Lognormal	30.44	32.53
Gamma	30.85	32.93
Weibull	32.30	34.39
Loglogistic	34.93	37.02

Table 2.4 Goodness of fit for the distribution of λ

Distribution	AIC	BIC
Lognormal	92.83	94.92
Gamma	93.52	95.61
Weibull	96.02	98.11
Loglogistic	97.18	99.27

Because the NHPP parameters vary from turbine-to-turbine, estimates based on the fully-pooled data are subject to large bias. If there is no pooling, we expect less bias, but an increased variance in the parameter estimates. The hierarchical model allows for a useful compromise between a completely pooled analysis and an individual turbine analysis, generally resulting in improved estimation performance Gelman (2006).

A fully specified likelihood and prior distribution for the multiple systems model can be seen in Ryan, Hamada, and Reese (2011), followed by a description of a multiple-system Metropolis-Hastings within Gibbs sampler. We use the JAGS software Depaoli, Clifton, and Cobb (2016) to generate draws from the joint posterior distribution and the RJAGS interface to R Su and Yajima (2009).

2.4 Cost and Use Rate Model

2.4.1 SCADA Data and Cost Relationship

After developing models for service event counts and corresponding costs, we are now interested in relating operating conditions to the amount of cost that results from each event. The use rate, which is defined to be a two-week average amount of use immediately before a service event, is

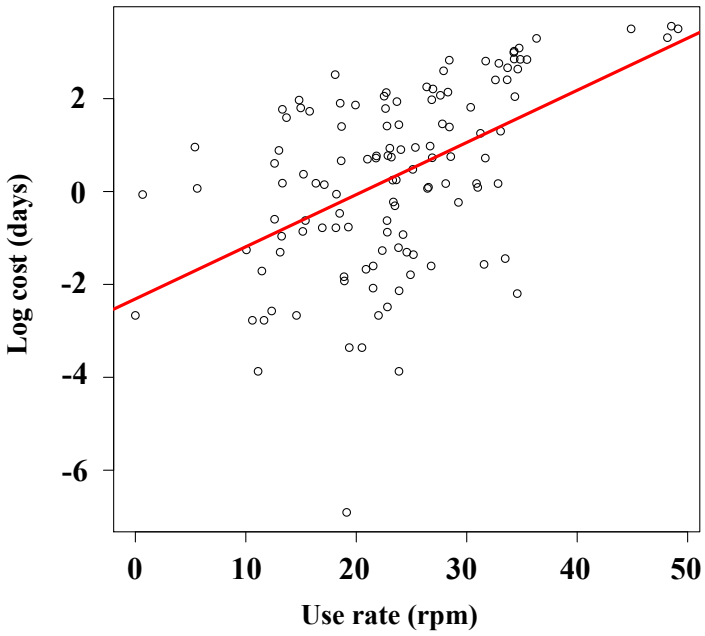

Figure 2.7 Log cost vs. use rate for $N = 121$ service events in the turbine fleet.

measured in the number of rotations per minute (rpm). We use a model that implies that there is a linear relationship between log(cost) and the use rate. Figure 2.7 is a plot of the costs (measured in days of cost on a log axis) for the $N = 121$ service events versus the corresponding use rates. The assumed relationship between cost and use rates can be expressed as

$$Z_i = \beta_0 + \beta_1 \times U_i + \epsilon_i$$

where Z_i is the log of the cost, U_i is the corresponding use rate, and β_0 and β_1 are parameters that are estimated from the data, using least squares regression.

Using standard graphical regression diagnostic checking of the usual linear model assumptions (i.e., constant variance of residuals, independence of residuals, normally distributed residuals, and a linear relationship between the explanatory and response variables) we found no evidence of serious departures. Also, we note that there is a correlation of 0.51 between Z_i and U_i. Using the data, the fitted simple linear regression model is

$$\hat{z}_i = -2.31 + 0.11 \times u_i \tag{2.6}$$

where $\hat{z}_i$ is the predicted log cost, u_i is an observed use rate for event i. Predictions of the use rate of future service events are needed to predict the corresponding costs for each event. The next section develops a time series model that will provide predictions for future use rates.

2.4.2 Autoregressive Model for Use Rate

We explore the time series structure of use rates for the $J = 21$ wind turbines. After considering alternative models we found that an AR(2) model provides an adequate description of the use rate data with parameters $\left(\gamma_1, \gamma_2, \tau^2\right)$ where

$$U_t = \gamma_1 U_{t-1} + \gamma_2 U_{t-2} + \epsilon_t, \quad \epsilon_t \sim N\left(0, \tau^2\right). \tag{2.7}$$

We centered the data by subtracting the sample mean to remove the need for an intercept term. We notice no significant turbine-to-turbine differences in the use rate distributions.

2.4.3 AR Model in JAGS via Bayesian Analysis

Similar to Section 2.3, we use a Bayesian approach by using a likelihood and prior distribution to obtain posterior distributions for the parameters of interest

$$\pi\left(\tau^2, \gamma_1, \gamma_2 | U_1, U_2, ..., U_t\right)$$

$$= f\left(U_1, U_2, ..., U_t | \tau^2, \gamma_1, \gamma_2\right) \pi\left(\tau^2\right) \pi\left(\gamma_1, \gamma_2\right)$$

where the likelihood function for (2.7) is

$$f\left(U_1, U_2, ..., U_t\right) = f\left(U_1\right) \prod_{k=2}^{t} f\left(U_k | U_1, ...U_{k-1}\right).$$

We use noninformative uniform prior distributions for γ_1 and γ_2. Because $\tau > 0$, we use a gamma prior distribution with shape and scale parameters of 0.001 and 0.001 respectively. This diffuse prior distribution lets the data from empirical observations dictate the shape of the posterior distribution. For more information on prior distributions for variance parameters, see Gelman (2006).

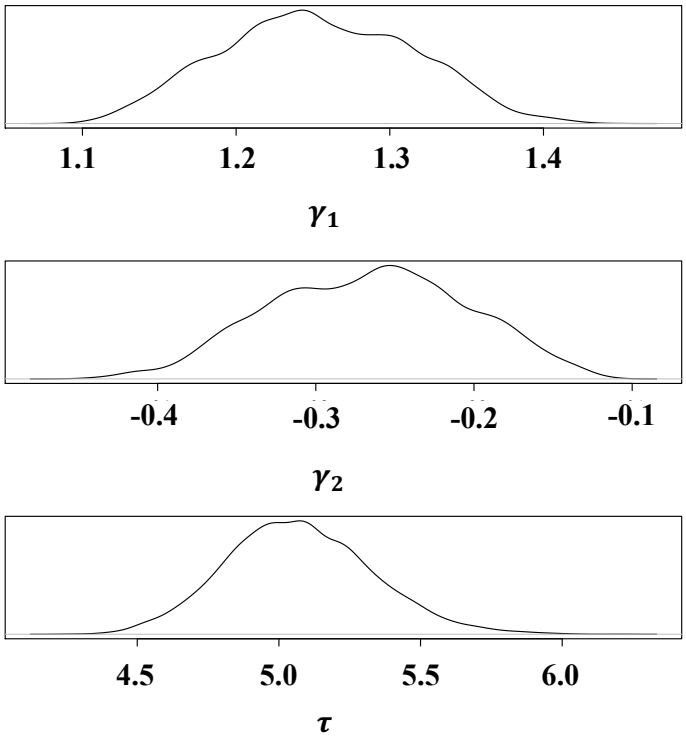

Figure 2.8 Marginal densities from use rate AR(2) model based on $N = 10,000$ draws.

We use again JAGS to compute draws from the joint posterior distribution of the parameters of the AR(2) model. Table 2.5 and Figure 2.8 provide summaries of the posterior output from JAGS.

Table 2.5 Use rate AR(2) parameter estimates

Parameter	Median	95% Credible interval
γ_1	1.25	[1.12, 1.38]
γ_2	−0.26	[−0.40, −0.14]
τ	5.06	[4.59, 5.61]

2.5 Predicting the Behavior of a New Wind Turbine

2.5.1 Assumptions

Suppose that a potential customer is considering the installation of a new wind turbine of the same type and environment populations as those under study here. In this section we use the

fitted model for the 21 available wind turbines to predict the future cost of this new turbine to be installed in the future. We call this Turbine 22.

The assumptions we use to make the cumulative cost prediction are

1. The relationship between use rates and costs in (2.6) holds for Turbine 22.
2. Recurrence rates are independent of cost parameters.
3. Turbine 22 comes from the same population as the originally observed wind turbines.

In the remainder of this section and in Section 6, we do the following. First we make predictions under the (unrealistic) "conditional" assumption that we know the event intensity function for Turbine 22. Then we make similar predictions under the "unconditional" assumption that we know nothing about those parameters, resulting in considerably wider prediction intervals. Then, in Section 6 we show how prediction precision is improved over time as operational information about Turbine 22 is accumulated.

2.5.2 Simulating Draws from Posterior Predictive Distributions

In this section we present an approach to simulate from the posterior distributions in Section 2.3.5 and 2.4.3 to generate predictions and prediction intervals for the cost as a function of time for a new wind turbine. Consider different methods: a conditional approach and an unconditional approach. For the conditional approach we fix the values of λ_{22} and ϕ_{22}, specify the end of observation time $t_{c_{22}}$, and

1. Draw the fixed values of λ_{22} and ϕ_{22} from the joint posterior distribution.
2. Draw a realization of γ_1, γ_2, and τ from an AR(2) process.
3. Simulate a sequence of NHPP events until $t_{c_{22}}$ resulting in n_{22} events
4. For each event simulate costs $z_1, ..., z_{n_{22}}$ using (2.6).
5. Compute the MCF and accumulate

6. Repeat steps 2 - 5 B times and save the results

7. For each sequence of closely-spaced times between 0 and $t_{c_{22}}$ obtain the 0.025, 0.5, and 0.975 quantiles of the predictive distribution, giving a point prediction and 95% prediction intervals for each point in time.

The unconditional approach is similar, but we would change step 6 to Repeat steps 1 - 5 B times (i.e., draw a new pair λ_{22}, ϕ_{22} from the joint posterior distribution of (λ, ϕ) for each iteration).

2.5.3 MCF Cost Function Results

After following the steps in Section 2.5.2, with $B = 10000$, we obtain a cost MCF prediction with prediction intervals. Figure 2.9 shows an example of MCF prediction results, where the solid line is the median of the draws obtained in part (g) and the values of the model parameters were $\phi_{22} = 1.05$ and $\lambda_{22} = 6.31$. We notice that distance between the upper bound and MCF prediction increases rapidly with age due to the right skew in the distribution of costs. In Figure 2.9 the observation period is $0 < t < t_{c_{22}} = 2000$ days.

The conditional distribution assumes we know the MCF parameters of Turbine 22 (which is not realistic). Unconditionally, we expect to see wider prediction intervals because the NHPP parameters vary in the unconditional algorithm (i.e., with no advanced knowledge of the turbine's reliability, there is much uncertainty in the predictions). Figure 2.10 displays the MCF cost prediction using the unconditional approach.

2.6 Value of Updating

2.6.1 A Compromise Between Conditional and Unconditional Approaches

Before we have any information about the parameters for Turbine 22, the MCF cost prediction must be dealt with unconditionally. Once Turbine 22 begins to operate, however, we can use available data to obtain a joint posterior distribution for λ_{22} and ϕ_{22} to get higher precision in our

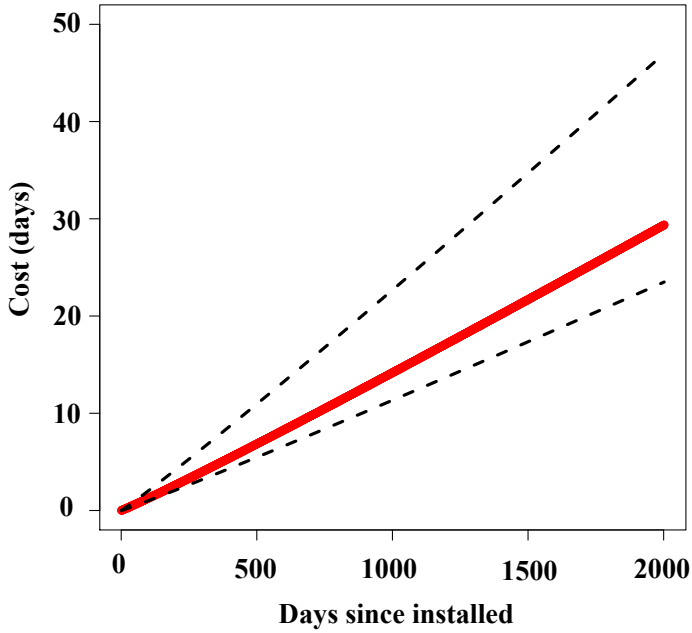

Figure 2.9 Predicted cost MCF with 95% prediction intervals, conditional on $\phi_{22} = 1.05$ and $\lambda_{22} = 6.31$.

MCF predictions. We can continually update the joint posterior distributions as more information is obtained.

2.6.2 Benefits of Linking Covariate Data to Event Data

Technological advancements, including SCADA systems, have the capability to reduce the uncertainty in predictions of reliability characteristics for wind turbines. It is desirable to have accurate reliability predictions in variable environments, such as wind farms, which are subject to various environmental and operational conditions. Having access to individual wind turbine SCADA data, in addition to lifetime data, can be extremely useful for maintenance optimization and economic planning purposes.

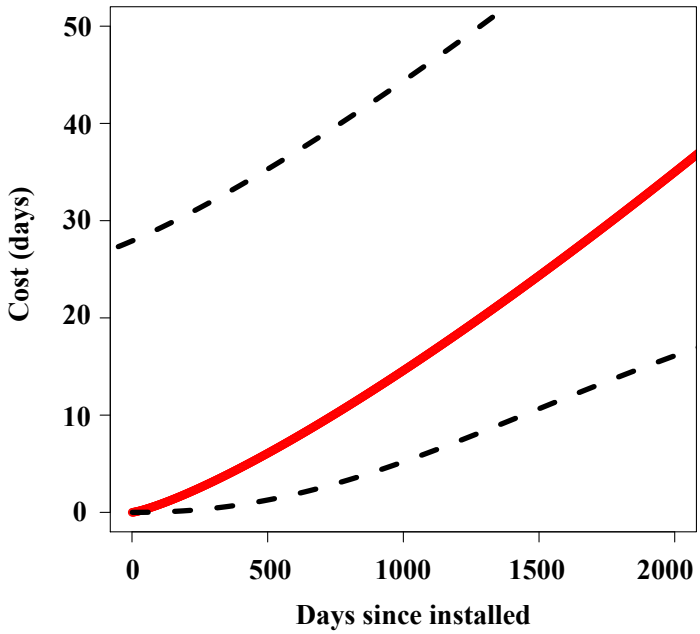

Figure 2.10 Unconditional predicted cost MCF with 95% prediction intervals.

2.6.3 Updating the Posterior Distribution

In the unconditional approach we have no specific information on the λ and ϕ parameters for a new turbine, so using the hierarchical approach we can sample from the joint posterior distribution during each iteration outlined in Section 2.5.2. When following this approach, predictions are made based only on the data from the 21 turbines used in developing the hierarchal model. If we were able to instead observe a new wind turbine for some period of its life starting at the beginning of operation, then we would have some information about its specific NHPP parameters. Longer periods of observation results in more prior information, which is expected to improve future cost predictions.

To see how accumulating data from the new turbine improves future cost predictions, we do evaluations at several times over a 2000 day period. In particular, we consider data accumulated after 0, 800, 1200, and 1600 days, where 0 days of operation is equivalent to an unconditional approach because we know nothing about a new turbine's parameters without having observed any

data. The unconditional posterior distribution for a new wind turbine's service event parameters is

$$\mathcal{L}\big(DATA_{Day=0}|\theta\big)\pi\big(\theta\big).$$

Consider observing a new wind turbine from day 0 to 800 days. After observing a new wind turbine for 800 days of service, the posterior distributions can be updated by including the observed data into (3) and obtaining

$$\mathcal{L}\big(DATA_{Day=800}|\theta\big)\pi\big(\theta\big),$$

The algorithm to make predictions about the future cost with an event history up to 800 days becomes

1. Observe $n_{Day=800}$ events up to 800 days.
2. For each event observe costs $z_1, ..., z_{n_{Day=800}}$.
3. Update the joint posterior distribution using information from steps 1 and 2.
4. Draw λ_{22} and ϕ_{22} from the updated joint posterior distribution.
5. Draw a realization of γ_1, γ_2, and τ from an AR(2) process.
6. Simulate NHPP events until $t_{c_{22}}$ resulting in n_{22} additional events after $t_{Day=800}$.
7. For each event generate costs $z_{n_{Day=800}+1}, ..., z_{n_{Day=800}+n_{22}}$ using (6).
8. Compute the MCF and accumulate.
9. Repeat steps steps 4 - 8 B times and save the results.
10. For a sequence of closely-spaced times between 0 and $t_{c_{22}}$ obtain the 0.025, 0.5, and 0.975 quantiles of the predictive distribution, giving a point prediction and 95% prediction intervals for each point in time.

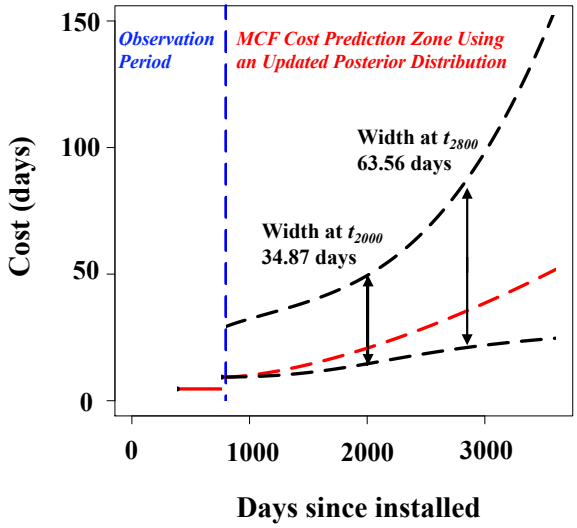

Figure 2.11 Predicted cost MCF with 95% prediction intervals after observing events at 387 and 765 days of operation, where the prediction is made after 800 days of observing the turbine.

This updated algorithm can be adjusted for any amount of previous observation time, where longer periods of observation are expected to narrow the future prediction bounds.

Figure 2.11 provides an example of using the updating algorithm to generate prediction intervals for the future cost of a wind turbine after 800 hours of operation. The vertical dashed line marks the point where we stop observing the new turbine. We notice in this illustration that up to t_{800} the turbine experiences two service events which result in an approximate 10 days of cost. We follow steps (d) through (j) in the updating algorithm to produce the prediction intervals, which are indicated by the horizontal dashed lines.

2.6.4 Prediction Results Using Early Observation Time

Using the updating algorithm in Section 2.6.3 for each of the new-turbine observation periods, we can produce figures similar to Figure 2.11. To see the benefits of incorporating early-observation information into the prediction process, consider 2000 days after the beginning of operation. We run the algorithm with $B_2 = 10000$ for several early-observation periods and obtain 95% prediction

intervals for the cumulative cost at 2000 days for each scenario, which differ only by the number of days of observed data prior to making each prediction. Table 2.6 displays the results. In Figure 2.12 we display the same results from 0 to 2000 days during each early-observation scenario.

Table 2.6 Cumulative cost prediction at 2000 days with 95% prediction intervals after different amounts of system operation

	0 days	800 days	1200 days	1600 days
95% Lower	10.06	14.59	16.64	19.45
Prediction	25.23	20.78	20.11	20.75
95% Upper	84.94	49.46	42.26	38.08
Width	74.88	34.87	25.62	18.63

In Table 2.6, we notice that the width of the 95% prediction interval width decreases by 40 days of cost when incorporating 800 days of early-observation time into the algorithm. With 1200 days of early-observation, the prediction interval width decreases by an additional 9.25 days. The difference in in the widths of the prediction intervals for cost after 1200 days of operation and 1600 days of operation is about five days. Overall, the ability to predict future cumulative costs was improved using the hierarchical approach and updating the algorithm.

2.6.5 Fleet-level Predictions

Suppose we are going to install five new wind turbines on a small farm and want to make cost predictions for the fleet. Similar to previous sections, we could generate posterior distributions for the NHPP parameters and run through the algorithm in Section 2.6.3 to update information as time passes.

We introduce service events from the fleet over time. We run the algorithm $B = 10{,}000$ times for each prior update and obtain 95% prediction intervals for the cumulative cost at 2000 days for the fleet (similar to Section 2.6.4). We display fleet level predictions in Table 2.7. Figure 2.13 displays predicted cost MCFs with 95% prediction intervals for the unconditional case and for cases where data are accumulated for different amounts of time for five new wind turbines.

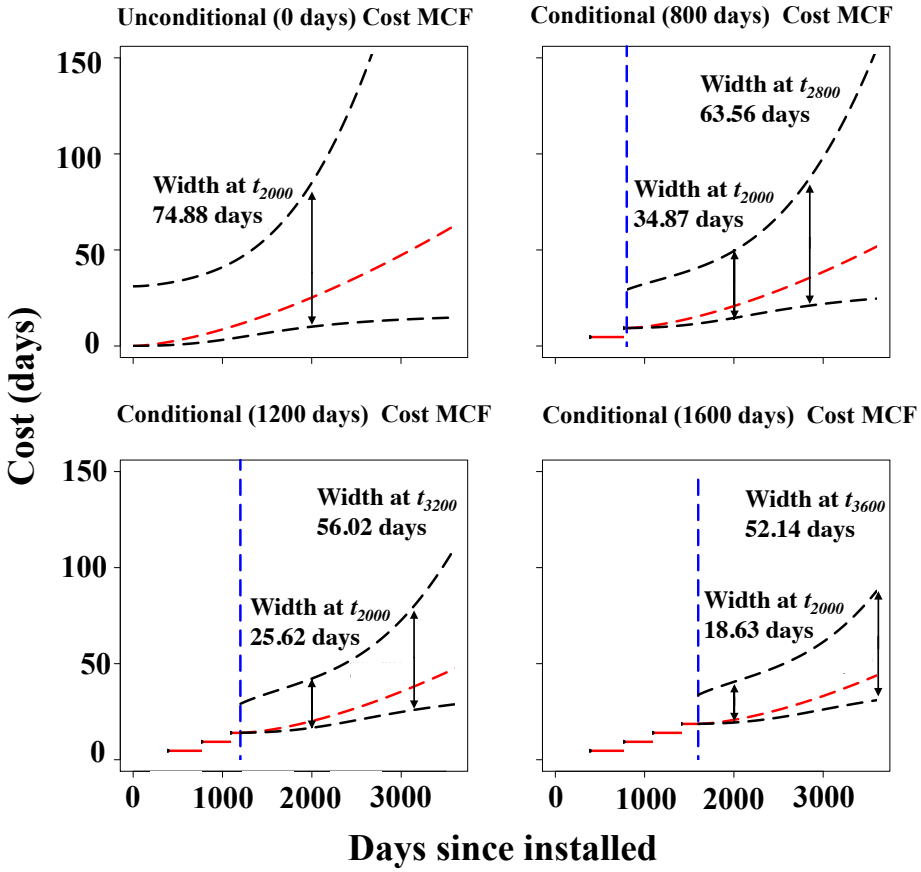

Figure 2.12 Predicted cost MCF with 95% prediction intervals for unconditional and early observation scenarios. For the unconditional (top left), we have 0 days of observation for the new wind turbine. For the early observation scenarios, we observe the turbine behavior for 800 (top right), 1200 (bottom left), and 1600 (bottom right) days before making the predictions.

In Table 2.7, we notice that 800 days of early-observation information decreases the width of the prediction interval by over 160 days. Again, the hierarchical approach and updating algorithm improved the ability to predict future costs.

Table 2.7 Prediction for cumulative cost at 2000 days with 95% prediction intervals for a fleet of five turbines.

	0 days	800 days	1200 days	1600 days
95% Lower	24.04	52.54	73.94	93.85
Prediction	60.90	65.96	81.17	96.32
95% Upper	233.47	96.43	101.61	109.56
Width	209.43	43.89	27.67	15.71

2.7 Discussion and Areas for Future Work

2.7.1 Economic Implications

According to Moloney (2014) SWTs are not popular because of their high upfront cost, but are still economically feasible in the United States because of federal tax credits. AWEA estimates that SWTs cost between $3,000 and $8,000 per kilowatt to install.

To understand how cumulative cost affects SWTs economically, one should first consider the power output from each turbine. Recall the power rating for SWTs in this paper is 100 kW. Typical generation percentages are between 25% and 35% of the year. To calculate the power output over a period of time we can use

$$Output = C \times \big(PR \times Days \times 24\, hours\big) \tag{2.8}$$

where $Output$ is measured in MWh, C is the capacity factor, and PR is the power rating measured in MW. For example, if a 100 kW turbine with a 30% capacity factor operated over a 2000 day period we would expect

$$1440 \text{ MWh} = 0.30 \times \big(0.1\text{MW} \times 2000 \times 24\big)$$

that a turbine with such characteristics would generate 1440 MWh of power over a 2000 day period.

We consider the cost predictions from Table 2.6 and use (2.8) to calculate expected power losses that result from service-event downtime after 2000 days of operation for three separate capacity factor scenarios. To gain a sense of the economic losses, we assume one could sell power for $0.10/kWh.

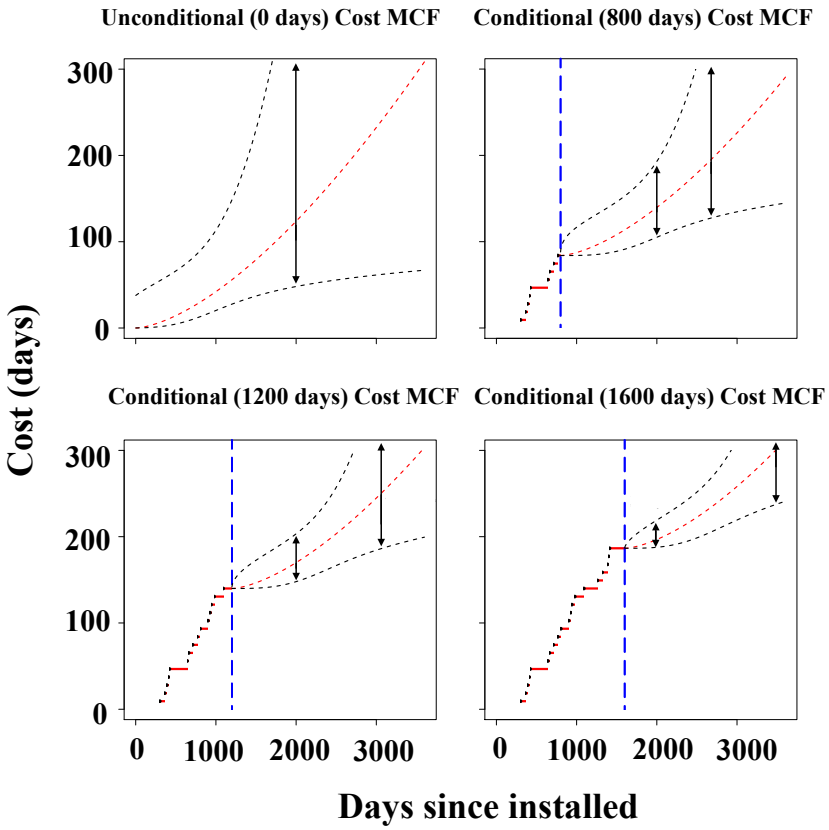

Figure 2.13 Predicted cost MCF with 95% prediction intervals for unconditional and early observation scenarios for a fleet of five wind turbines. For the unconditional (top left), we have 0 days of observation for the new wind turbine. For the early observation scenarios we observe the turbine behavior for 800 (top right), 1200 (bottom left), and 1600 (bottom right) days before making the predictions.

In Figure 2.14 we provide an example of a new wind turbine that is operating over a 2000-day period. This example assumes that the turbine has a possible capacity factors of 0.25, 0.30, 0.35 and power can be sold for \$0.10/kWh. On the x-axis we introduce historical information before predicting the lost revenue due to service event costs 2000 days after installation. The use of historical information provides improved predictions.

We notice the decrease in width of each prediction interval as more information is accumulated about the individual turbine. For example, with no information about the individual turbine, and a capacity factor of 0.25, a 95% prediction interval for economic losses resulting from service event

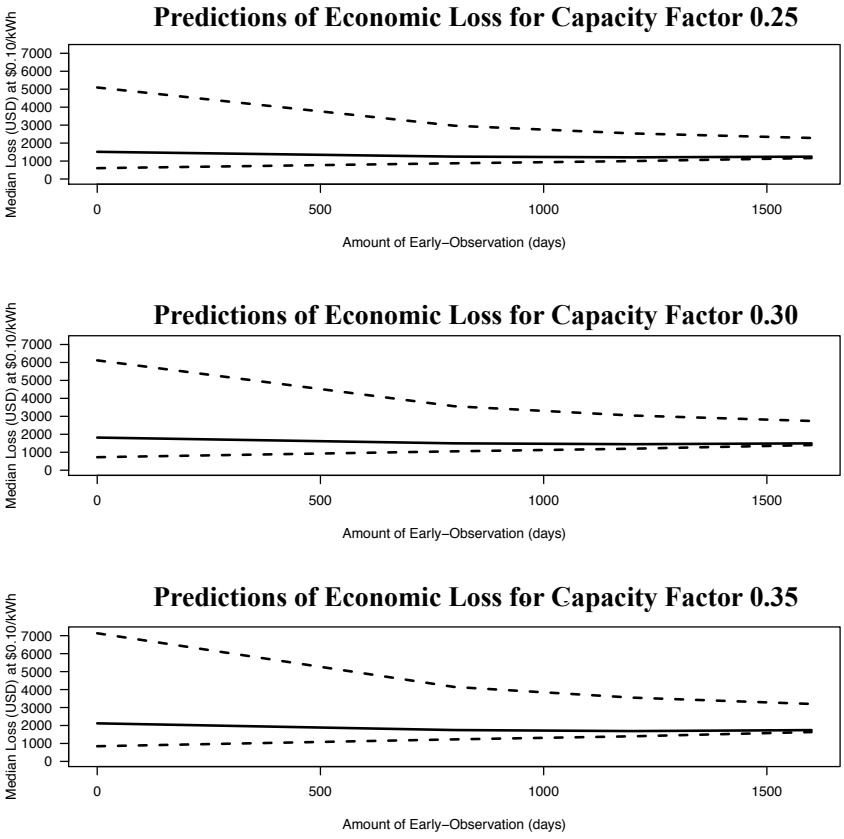

Figure 2.14 Predicted loss in revenue from unscheduled downtime after 2000 days of operation for different amounts of early observation.

cost after 2000 days of operation is [\$604, \$5096]. When the information based on 800 days of information is used to update the posterior distributions the prediction interval becomes [\$875, \$2968], which is a substantial decrease in width when one considers the potential of predicting losses for a fleet of turbines.

2.7.2 Fleet-level versus Turbine-level Predictions

Predictions in Section 2.6.4 are specific to an individual turbine, whereas Section 2.6.5 is for a small fleet of turbines. Overall one would prefer to have information at the individual unit level when possible. In this paper we considered an individual turbine (in Section 6.4) and a small fleet (in Section 6.5). We noticed improvements in predictions for both of the scenarios using early-observation data and the updating algorithms.

2.7.3 Limitations and Improvements

In this paper, we did not have access information about the cause of the service events, only whether or not a turbine was shut down for service. If one has access to component-specific data, the analyses could be separated, allowing one to make predictions for individual event types. Also, the number of turbines used to develop the hierarchical model in this paper was small. Having data from a large fleet would reduce statistical uncertainty.

With limited SCADA data, we were only able to find one covariate to link to the recurrence data. Improvements in such predictions would be possible if modeling were done conditional on additional dynamic covariate history relating to service events and it would be possible to enhance the modeling of the rate of occurrence of failures for individual wind turbines.

Acknowledgments

This work was completed under an IGERT program funded by the US National Science Foundation, Award 1069283.

Bibliography

Al-Tubi, I., Long H., Tavner P., Shaw B.and Zhang J. (2015). Probabilistic analysis of gear flank micropitting risk in wind turbine gearbox using supervisory control and data acquisition data. *IET Renewable Power Generation 9*, 610–617.

Arifujjaman, M. (2013). Reliability comparison of power electronic converters for grid-connected 1.5kw wind energy conversion system. *Renewable Energy, 57,* 348–357.

Bain, L. and Engelhardt, P. (1991). *Statistical analysis of reliability and life-testing models, theory and methods*. Marcel Dekker.

Bertling, L. and Wennerhag, P. (2012). *Wind turbine operation and maintenance.* (Tech Rep. No. 12:41). Elforsk.

Ciang, C. C., Lee, J., and Bang H. (2008). Structural health monitoring for a wind turbine system: a review of damage detection methods. *Measurement Science and Technology, 19* 12–20.

Courtney, J. F., Lynch, P., and Sweeny C. (2013). High resolution forecasting for wind energy applications using Bayesian model averaging. *Tellus A: Dynamic Meteorology and Oceanography, 65,* 19969.

Dai, H., and Wang H. (2017). *Analysis for time-to-event data under censoring and truncation* Elsevier.

Depaoli, S., Clifton, J. P., and Cobb P. R. (2016). Just another Gibbs sampler (JAGS). *Journal of Educational and Behavioral Statistics, 41,* 628–649. doi: 10.3102/1076998616664876.

Draper, D., Gaver, D. P., Greenhouse, J. B., Hedges, L. V., Morris, C. N., Tucker, J. R., and W̃aternaux, C. M.(1992). *Combining information: Statistical issues and opportunities for research* (Tech. Rep.). Committee on Applied and Theoretical Statistics. National Academy Press.

Faulkner, P., Cutter, P., and Owens A. (2012). Structural health monitoring systems in difficult environments. In *European workshop on structural health monitoring.* Dresden, Germany.

Fischer, K., Besnard, F., and Bertling, L. (2012). Reliability-centered maintenance for wind turbines based on statistical analysis and practical experience. *IEEE Transactions on Energy Conversion, 27,* 184–195.

Gelman, A. (2006). Prior distributions for variance parameters in hierarchical models. *Bayesian Analysis, 1,* 515–534.

Gielen, D. (2012). *Renewable energy technologies: cost analysis series* (Tech Rep.). International Renewable Energy Agency.

Gould, E. B. (2014). *Wind vision: updating the DOE 20 percent wind energy by 2030* (Tech Rep. No. DOE/GO-102015-4557). NREL.

Kashyap, S. (2014). *White paper: Data analytics for wind farm performance improvement* (Tech Rep.). http://algoengines.com/wind/:AlgoEngines.

Kass, R., and Wasserman L. (1996). The selection of prior distributions by formal rules. *Journal of the American Statistical Association, 91,* 1343–1370.

Kusiak, A., and Verma A. (2010). The future of wind turbine diagnostics. *Wind System Magazine* https://pdfs.semanticscholar.org/a10b/1e3135946c01e7a45aadae013988b7ce5f80.pdf. Last accessed Nov 10, 2018.

Matthews, P., and Godwin J. (2013). Classification and detection of wind turbine pitch faults through SCADA data analysis. *International Journal of Prognostics and Health Management, 4,* 90–100.

Meeker, W. Q., and Escobar L. A. (1998). *Statistical Methods for Reliability Data.* Wiley.

Moloney, C. (2014). Small wind turbine: What is the payback period? *Poplar Network.* https://www.poplarnetwork.com/news/small-wind-turbine-what-payback-period. Last accessed Nov 26, 2018.

Morthorst, P., and Awerbuch, S. (2009). *The economics of wind energy* (Tech. Rep.). EWEA. http://www.ewea.org/fileadmin/files/library/publications/reports/EconomicsofWindEnergy.pdf. Last accessed Nov 2, 2018.

Nelson, W. B. (2003). *Recurrent events data analysis for product repairs, disease recurrences, and other applications.* ASA-SIAM.

Rigdon, S.E., and Basu, A. P. (2000). *Statistical methods for the reliability of repairable systems.* John Wiley.

Ryan, K., Hamada, M., and Reese, C. (2011). A Bayesian hierarchical power law process model for multiple repairable systems with an application to supercomputer reliability. *Journal of Quality Technology, 43,* 209–223.

Sajid, H., and Hossam A. G. (2013). Fault diagnosis in gearbox using adaptive wavelet filtering and shock response spectrum features extraction. *Structural Health Monitoring, 12,* 169–180.

Saxena, A., Celaya, J., Balaban, E., Goebel, K., Saha, B., Saha, S., and Schwabacher, M. (2008). Metrics for evaluating performance of prognostic techniques. In *2008 international conference on prognostics and health management.* 1–17. doi:10.1109/PHM.2008.4711436.

Sobolewski, R. (2015). Wind farm reliability modeling using Bayesian networks and semi-Markov processes. *Acta Energetica, 3,* 71–76.

Su, Y. S., and Yajima, M. (2009). *R package "R2JAGS: A package for running JAGS from R".* https://www.researchgate.net/publication/287728027R2jagsapackageforrunningjagsJustAnotherGibbsSampler. Last accessed Nov 1, 2018.

Tautz-Weinert, J., and Watson, S. J. (2016). Using SCADA data for wind turbine condition monitoring - a review. *IET Renewable Power Generation.*

Wilkinson, M., Hendricks, B., Harman, K., Spinato, F., and van Delft, T. (2011). Measuring wind turbine reliability results of the Reliawind project. *Wind Energy, 35,* 102–109.

Wu, J., Butler, A., Mueller, M. A., and Mostafa, K. (2017). Combining fatigue analysis information into reliability analysis using Bayesian hierarchical modelling method. In *2017 annual reliability and maintainability symposium (RAMS)* 1–7. doi:10.1109/RAM.2017.7889736

CHAPTER 3. EVALUATION OF MAINTENANCE POLICIES WITH REPAIRABLE SYSTEM SIMULATION

A paper being submitted to *the Wind Energy Journal*

Michael S. Czahor and William Q. Meeker

Department of Statistics

Iowa State University

Ames, IA, 50011, USA

Abstract

Repairable system simulation can be useful for evaluating maintenance policies. Depending on system makeup, varying amounts of information may be needed to obtain a reasonable idea of how systems will perform over time. In this paper, we develop a repairable systems software tool that offers two models to understand such behavior, a subsystem-level and component-level model. Multiple algorithms are presented to assist with failure time generation with the use of the renewal process, nonhomogeneous Poisson process, and trend renewal process models. The subsystem and component-level models are applied to a moderate sized wind farm. Different parts of the software including plotting tools and summary statistics are shown within the wind farm application.

Key Words: repairable systems, trend renewal process, failure time.

3.1 Introduction and Motivation

3.1.1 Background

Studying engineering system failures is as old as engineering systems themselves. A successful engineering design is one that avoids failures and understanding such failures can help one avoid taking on burdens including increased future maintenance costs.

One example of engineering systems that are at the forefront of maintenance-based research are wind turbines. El-Thalji and Liyange (2012) report that maintenance operations make up 20-25% of the total levelized (a levelized cost is the net present value of the unit-cost of electricity over the lifetime of a generating asset) cost per kilowatt-hour (kWh) of wind turbines, making research in this area a worthwhile endeavor. Due to the large number of wind turbines in a wind farm, owners and operators are usually interested in the profitability of the entire wind farm as opposed to the prioritized reliability of individual wind turbines. This differs from conventional power systems, which impose redundancies to eliminate the risks of an asset failure.

A successful maintenance policy relies on accurate failure information, generally based on: historical failures, manufacturing specifications, and engineering expertise on the turbine type and make. Tretton et al. (2011) released a report that shares these types of information, which we use to develop a simulation-based software to predict future failures of engineering fleets. We use the software with the Tretton et al. (2011) data as an illustrative example.

3.1.2 Related work

According to Yildrim, Gebraell, and Sun (2017), current approaches to wind farm maintenance policy making include two main lines of research:

- Opportunistic maintenance methods that do no use sensor information.
- Sensor-driven methods that focus on single turbine systems.

In the first point, maintenance and operational models for wind farms rely on reactive policies and fixed time-based periodic schedules without using sensor information. There has been strong

research on time-based maintenance scheduling of wind farms. Ding and Tian (2012) develop simulation methods to evaluate opportunistic maintenance methods defined by component's age threshold values. On the second point, wind turbine maintenance scheduling uses condition monitoring information, but focuses on individual wind turbines. Yildrim, Gebraell, and Sun (2017) use sensor information to capture the interdependencies between turbines to propose a maintenance scheduling policy that integrates stochastic degradation methodologies driven by sensor information.

3.1.3 Problem formulation

This research demonstrates the importance of reliability data and the value of choosing a maintenance strategy to operate a complex system such as a wind farm. Using simulation, one can learn about the implications of maintenance decisions, for example, what will the mean cost of maintenance be for a fleet of systems? To answer this question in a generic setting, we develop a software tool in R that assists in simulating repairable systems over time.

3.1.4 Overview

The remainder of this paper is organized as follows. Section 3.2 describes repairable system models and outlines examples within the wind energy industry. Section 3.3 outlines the necessary inputs used in the simulation-based software developed in the remainder of the paper. Section 3.4 develops the framework for simulating discrete events with the repairable systems tool used in the application-based parts of this paper. Section 3.5 develops a high-level (i.e., subsystem-based) algorithm for simulating repairable systems. Section 3.6 develops a low-level (i.e., component-based) algorithm for simulating repairable systems. Section 3.7 uses the high-level and low-level models and applies the software to a moderately-sized wind farm. We compare these models in Section 3.8 and discuss areas for future research.

3.2 Repairable System Models

3.2.1 System structure

A system is a collection of interconnected components that performs some task. Systems such as wind turbines that are maintained and/or repaired after failure are known as *repairable systems*. We outline a few simple system structures that can be used to assess system (or subsystem) reliability. System structure defines the relationship between system state (operational or not) and the system's components' states. An example is the relationship between a wind turbine and the wind turbine's gearbox. If the gearbox is non-operational, the wind turbine cannot operate.

A high-level model describes repairable system reliability/availability performance as a function of subsystem reliabilities. A more complicated hierarchical model describes the relationship between system and subsystem operational state and subsystem reliability as a function of component reliabilities. We will illustrate and compare both of the approaches to repairable system modeling.

3.2.1.1 Series systems

A series system with s components works if and only if all s components work. Examples of series systems include cell phones, wind turbines, and most laptop computers. Suppose each component in a new system has a cumulative distribution function (cdf) that is denoted by $F_i = F_i(t;\theta_i)$ for component i in the system, where θ_i is a parameter vector and $R_i = 1 - F_i$ is the component reliability. A series system with s independent components has a cdf for the time to the first failure of the system is $F_T(t) = 1 - \prod_{i=1}^{s}(1 - F_i)$ and the reliability of the system is $R_T = \prod_{i=1}^{s} R_i$.

Example 1: Personal computer

Consider a personal computer, that has four main components: the power supply, motherboard, hard drive, and keyboard. This system is arranged in a series configuration, where all components must be operational for the computer to perform properly. Figure 3.1 displays a four-component series system. Suppose the components have the following reliabilities over a five year period.

1. **Power supply** $R_1 = 0.985$.
2. **Motherboard** $R_2 = 0.998$.
3. **Hard Drive** $R_3 = 0.975$.
4. **Keyboard** $R_4 = 0.997$.

Assuming that the components fail independently, the reliability of the computer (the probability that is will survive five years without a failure) is calculated as

$$\begin{aligned} R_{\text{Computer}} &= R_1 \times R_2 \times R_3 \times R_4 \\ &= 0.985 \times 0.998 \times 0.975 \times 0.997 \\ &= 0.9556. \end{aligned}$$

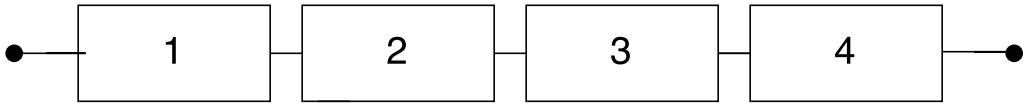

Figure 3.1 A four-component series system example.

3.2.1.2 Systems with redundancy

Sometimes redundancy can be introduced in a system if there is a weak link or a critical component (like a hard drive in a personal computer). Consider Example 3.1 and in particular the hard drive. A second hard drive can add component-redundancy to increase the reliability of the personal computer. For example, we add a parallel set with two parts to "3" in Figure 3.1. In Figure 3.2 we show the added redundancy to the hard drive. We assume the reliability of "3.1" and "3.2" are both 0.975. The reliability of the redundant hard drive subsystem is

$$
\begin{aligned}
R_{Raid} &= F_T(t) \\
&= 1 - \prod_{j=1}^{2}(1 - F_j) \\
&= 1 - \left[(1 - 0.975) \times (1 - 0.975)\right] \\
&= 0.999375.
\end{aligned}
$$

The updated reliability for the personal computer becomes

$$
\begin{aligned}
R_{\text{Computer}} &= 0.985 \times 0.998 \times 0.999375 \times 0.997 \\
&= 0.9795.
\end{aligned}
$$

Adding redundancy to the hard drive improves the computer's reliability.

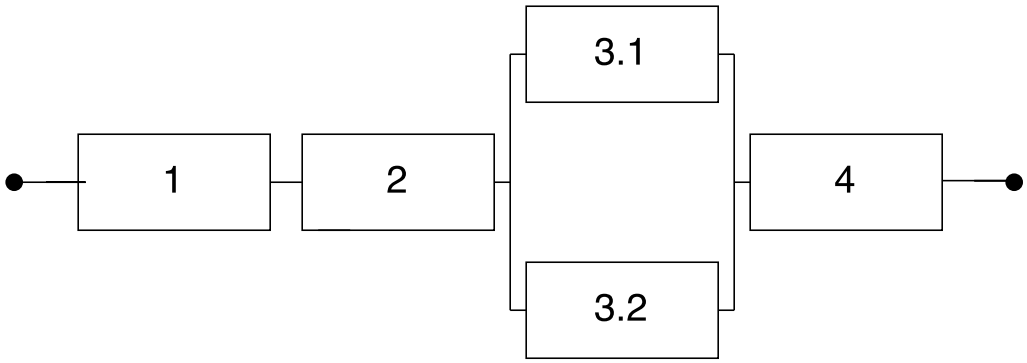

Figure 3.2 A four-component series system example with redundancy in the hard drive subsystem.

3.2.1.3 Other system structures

We will not use other system structures in this paper because they are not common in wind turbines. More details on system-level and component-level redundancy and other subsystem configurations can be found, for example, in Rausand and Hoyland (2004).

3.2.2 Repair and scheduled maintenance models

Many systems are maintained or repaired after failure. For such repairable systems, one may be interested in finding a set of operational/maintenance policies that will maximize availability (the fraction of time that a system is available for use) subject to a cost constraint or to minimize cost (subject to an availability constraint). This leads one to consider maintainability of a system, which is improving operational efficiency through scheduled maintenance (also known as preventive maintenance) techniques. Improvements in maintainability and repairability (the distribution of time to do a repair) can increase the availability of a system.

3.2.2.1 Routine maintenance

Routine maintenance includes a set of tasks that will be performed, usually periodically, regardless of the system state. An example is periodic oil change and lubrication of a vehicle or machine.

Example 2: Maintenance in the wind energy industry

Wind turbine maintenance costs can be broken into several categories. The operations costs are mostly fixed each year and include land use royalties, taxes, labor, training, and insurances. Scheduled maintenance costs are largely dependent on the maintenance policy set forth by the turbine or farm owners and operators. Corrective maintenance costs are more variable because costs are driven by failures of turbine subsystems that cannot be predicted precisely. Section 3 of Hill, Stinebaugh, and Briand (2008) summarizes costs of O&M within the wind energy industry.

3.2.2.2 Safe life replacement

Some components are automatically replaced when they reach a certain age, so that the chance of failure is minimized. An example is the replacement of an automobile timing belt after 60 or 80 thousand miles.

Example 3: Wind turbine maintenance action examples

During the first 2–5 years of a new turbine's life, it is usually under warranty from the original equipment manufacturer (OEM) and has an annual maintenance schedule. At the larger-scale (i.e., a wind farm), a "two-technician crew" is typically available to maintain a wind farm. The first crew is permanently on site to provide O&M services and the second crew is assigned from a local service center. During scheduled maintenance, the crews go through a detailed checklist that includes

- Inspection of mechanical and electrical systems
- Bolt tightening
- Check oil, grease, connections, etc.

3.2.2.3 Industry maintenance strategies

Depending on the application, industry experts plan scheduled maintenance actions in different ways. Some common strategies include

- **Time-based**: Schedule a maintenance task every N time units.
- **Meter-based (Amount)**: Schedule a maintenance task when a meter increases or decreases by a certain amount (i.e., changing tires every 40 to 60 thousand miles).
- **Meter-based (Batch)**: Schedule a maintenance task every time a machine produces/processes a certain number of units.
- **Relative to other maintenance**: Schedule a new maintenance task when an earlier task is completed.

Example 4: Siemens safe-life repair strategies

After 500 hours of use Siemens assigns technicians to conduct the first scheduled maintenance. After that initial scheduled maintenance, annual scheduled maintenance actions are performed.

The actual actions at these maintenance events vary. For example, some particular maintenance actions may not be required every year. Siemens is paid an annual fee per turbine that covers this yearly maintenance.

Siemens and other companies have a permanent data connection that goes to their monitoring centers where technicians or engineers constantly monitor the wind turbines. Approximately 75-80 percent of all turbine-trouble issues can be diagnosed from the monitoring centers. More information on Siemens maintenance strategies can be found in Trabish (2010).

It is important to note that the OEM providing maintenance is not the only option for turbine owners. The three main options are the OEM services, independent service providers, and owners who self-provide needed services.

3.2.3 Repairable system and component failure models

We note that the system cdfs derived from the RBD's like those illustrated in Figures 3.1 and 3.2 only reflect the distribution of time to *first* failure. For a repairable system, one must consider the intensity functions for stochastic processes describing recurring failures over time for particular components. We consider several failure models to describe the intensity functions. For each of the models considered, the times between failures or maintenance events are denoted by $\tau_j = T_j - T_{j-1}$, where $T_0 = 0$.

3.2.3.1 Renewal process

When a component of a system is replaced by a new component that has the same cdf after each failure, a renewal process model is appropriate. A renewal process generates a sequence of recurrences at system ages $T_1, T_2, ...$ with interrecurrence times that are assumed to be independent and identically distributed (iid). Figure 3.3 shows the conditional intensity function (the intensity at time t depends on the time of the most recent replacement) for a Weibull renewal process corresponding to

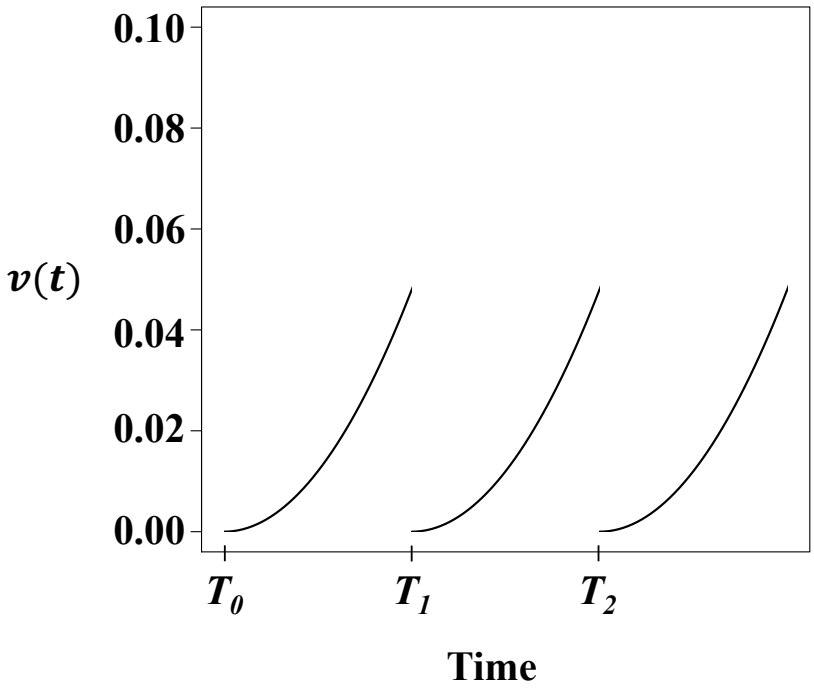

Figure 3.3 Renewal process intensity function.

$$F(t) = 1 - \exp(-t/\psi)^{\alpha} \tag{3.1}$$

and $\nu(t)$ is the Weibull hazard where α is the Weibull shape parameter and ψ is the Weibull scale parameter After each replacement, the hazard function returns to 0. Because of this repair behavior in a renewal process is said to make the repaired unit "good as new." For more information about renewal processes see Section 2.3 of Cook and Lawless (2007).

3.2.3.2 Nonhomogeneous Poisson process

A nonhomogeneous Poisson process (NHPP) model has a non-constant recurrence rate $\nu(t)$. Under the NHPP model, the number of events in any interval of time has a Poisson distribution and the number of events occurring in any two non-overlapping intervals will be independent (known as independent increments). Figure 4 shows the intensity function for a particular NHPP model. The NHPP intensity function differs dramatically from that of the renewal process. In particular,

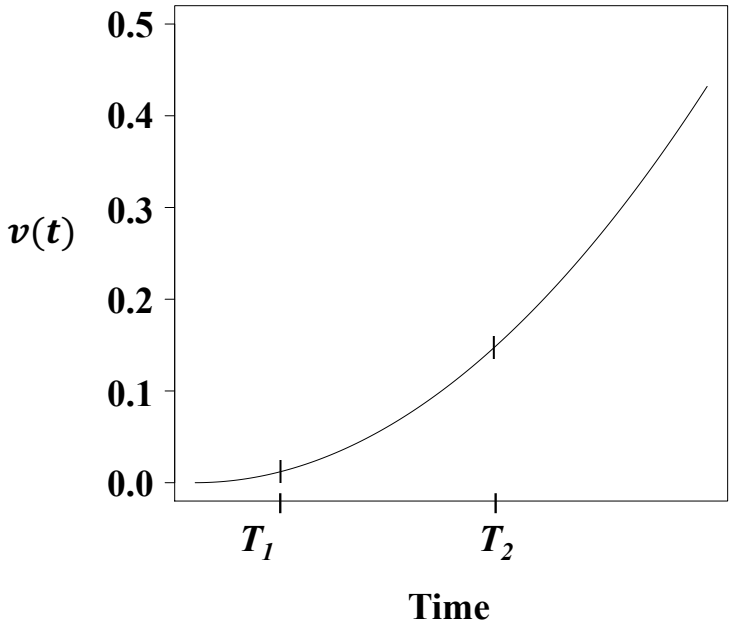

Figure 3.4 NHPP intensity function and two event times.

as shown in Figure 3.4, after each repair or other event, the intensity has the same level as just before the event occurred. For this reason, the NHPP process is referred to as "minimal repair" or "bad as old." A commonly used parametric form of $\nu(t)$ is power law process

$$\nu(t) = \lambda(t) = \frac{\beta}{\eta}\left(\frac{t}{\eta}\right)^{\beta-1}. \tag{3.2}$$

Further information about the Poisson process is given in Section 2.2 of Cook and Lawless (2007). For information on specifying $\nu(t)$ and the NHPP in general, refer to Section 16.4.3 of Meeker and Escobar (1998).

3.2.3.3 Trend renewal process

The trend renewal process (TRP) model was introduced by Lindqvist, Elvebakk, and Heggland (2003). The TRP model describes situations that are in-between the NHPP and renewal processes. Similar to a renewal process, each failure/repair or other maintenance action the intensity function

changes. The nature of the change to the intensity function depends on a trend function and the renewal hazard function.

Let $T_1, T_2, ...$ denote events from a TRP. To define the TRP process we let $\lambda(t)$ be a nonnegative trend function defined for $t \geq 0$ and let $\Lambda(t) = \int_0^t \lambda(u)du$. The process $T_1, T_2, ...$ is called TRP$(F, \lambda(.))$ if the transformed process $\Lambda(T_1), \Lambda(T_2), ...$ is a renewal process with distribution F. Thus, $\Lambda(T_i) - \Lambda(T_{i-1}), i = 1, 2, ...,$ are i.i.d. with distribution function F. The function $\lambda(.)$ is called the trend function, while F is called the renewal distribution. The conditional event intensity function is $\nu(t|H_{t^-}) = h\{\Lambda(t) - \Lambda[T_{N(t^-)}]\}\lambda(t)$ where H_{t^-} is the history of the process up until just before time t and h is the hazard function corresponding to the distribution F. Under the TRP model when there is a refurbished repair at time t, the conditional intensity function goes down to the trend value $\lambda(t)$. For example, consider the TRP$(F, \lambda(.))$ which is characterized by the power law

$$\lambda(t; \eta, \beta) = \eta\beta t^{\beta-1}, \qquad \eta > 0, \beta > 0. \tag{3.3}$$

for the trend function and Weibull distribution in (3.1) for the renewal function. Figure 3.5 exhibits this TRP intensity function over time. More information on the TRP model can be found in Chapter 5.2.2 of Cook and Lawless (2007).

The renewal and NHPP models are special cases of the TRP model. When F is an exponential distribution with mean 1, the NHPP is obtained and when $\lambda(t)$ is constant the renewal process is obtained.

3.3 Repairable System Model Specification

To explore the reliability or availability within a repairable system, one generally starts by outlining the system structure. After the system structure (product design) is established, we can define particular characteristics about the system that will allow us to simulate system performance over time. The goal of simulating a repairable system or fleet of repairable systems is to develop

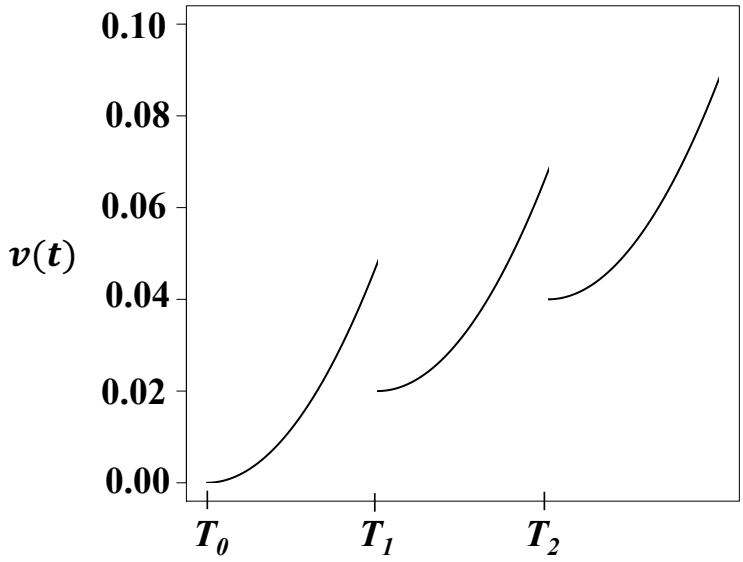

Figure 3.5 TRP intensity function and two event times.

economical maintenance policies to extend the useful life of the system and its costly components, maximize system output, and maximize profits.

3.3.1 Repairable system input definitions

Inputs needed to quantify a repairable system's operational characteristics include

- System structure, as described in Section 2.1.
- The failure-time distribution or intensity function specifications for each component.
- Parameters for the failure-time distribution or intensity function for each component.
- Specification of different types of events that will affect system operation and state.
- Specification of the distribution shape and parameters for each component repair-time distribution.

When assigning component reliability information (repair-time distributions, intensity functions, or other information), one must consider types of maintenance actions that are being done (e.g., "replace with new" or "minimal repair").

3.3.2 Operational costs

Operational cost considerations for a repairable system simulation include

- Component replacement costs.
- Labor and other repair costs.
- Lost profit from downtime costs.

3.3.3 Other inputs

Other inputs for a repairable system simulation include

- Simulation duration (e.g., how many years the system is expected to be in operation).
- Simulation time unit (i.e., hours).
- Number of simulations. A larger number of simulations will reduce Monte Carlo error.
- A random seed to allow one to reproduce results.

3.4 Repairable System Simulation

In order to make maintenance decisions with respect to cost and availability, we first need to present a method to simulate discrete events over a period of time to gain an understanding of system behavior. In this section we describe an R package that was developed to simulate discrete events for a system at the subsystem and component levels. In addition, we present some tools to perform analysis of the simulated events to help guide decisions about maintenance actions and examples to illustrate the use of the tools.

3.4.1 Simulating discrete events

Brailsford, Churilov, and Dangerfield (2014) state that discrete event simulation (DES) techniques are based upon the foundation of Monte Carlo methods and were originally developed to improve the design and operation of manufacturing plants. These DES techniques aim to model complex systems, such as wind turbine maintenance, which experience events at the subsystem and component levels. To model the behavior of a system that consists of discrete state changes we consider:

- **System State**: All of the information that describes the state of a system at a certain point in time.
- **Event**: An indicator that calls for action due to a state change.
- **Process**: A sequence of events associated with a simulation.

The DES framework is represented by entities that flow through networks of queues and activities. Brailsford, Churilov, and Dangerfield (2014) describe the fundamental building blocks of a DES model as:

- *Entities*: Individual items that flow through the system, for example, orders in a supply chain. In RSS, applications the entities are the failure events for specific subsystems/components.
- *Queues*: Areas where entities wait to be worked on, for example, inventory or waiting lists. In RSS, the queues can be thought of as a running list of work orders that are updated as failures (failure times are generally stochastic) occur or times for scheduled maintenance arise.
- *Activities*: Performance of work on entities, for example servicing a repairable system to return it to operational status. In RSS, the activities include equipment checks, partial or complete overhauls at specified points in time, oil changes, lubrication and so on. In addition, workers can record equipment deterioration so they know to replace or repair worn parts before they cause system failure.

- *Resources:* Required to be present to complete activities, for example, crew members on a maintenance team.

In Sections 3.5 and 3.6, DES modeling will focus on individual entities that flow through trajectories which consist of queues, activities, and actions. We will focus on the points in time where state changes occur. To do this, we will define an *event* as a discrete point in time at which the system state changes. *Events* often occur at irregular intervals and are followed by actions that are similar to those defined in Section 3.2.2. For more information on DES frameworks such as time handling and random sampling, see Chapter 2 of Brailsford, Churilov, and Dangerfield (2014) and Bangsow (2012).

3.4.2 Repairable system metrics

When simulating a repairable system or fleet of repairable systems, one may be interested in measuring particular system characteristics to assist in influencing future decisions (i.e., maintenance actions). Metrics that will be used in our work include:

1. *Availability*: The amount of time that a system is able to perform its intended function divided by the total amount of time in a period.

2. *Cumulative cost*: The cumulative amount of money that it takes to maintain a system over time.

3. *Waiting time*: The time it takes for a maintenance crew to reach the system to start performing maintenance actions.

4. *Resource utilization*: The proportion of time that the maintenance crew or crews are working during a given period.

3.4.3 RSimmer

Ucar and Smeets (2018) developed a process-oriented and trajectory-based DES package for the R statistical software. This R package is known as RSimmer. Using the framework of RSimmer,

we develop an extension of this package to handle RSS applications. Information on RSimmer's capabilities can be reviewed in Ucar and Smeets (2018).

3.4.4 SimmerRSS: An R tool for repairable systems

We have developed an R package SimmerRSS, building on RSimmer capabilities, to do repairable system simulation. The input to SimmerRSS is a file that defines the system to be simulated, different kinds of reliability-related events, and associated probability models and distributions, including parameters. For simplicity in this research, we focus on series systems with independent components and subsystems. Figure 3.6 displays the information that is sent from the input file to the R functions being created for repairable systems.

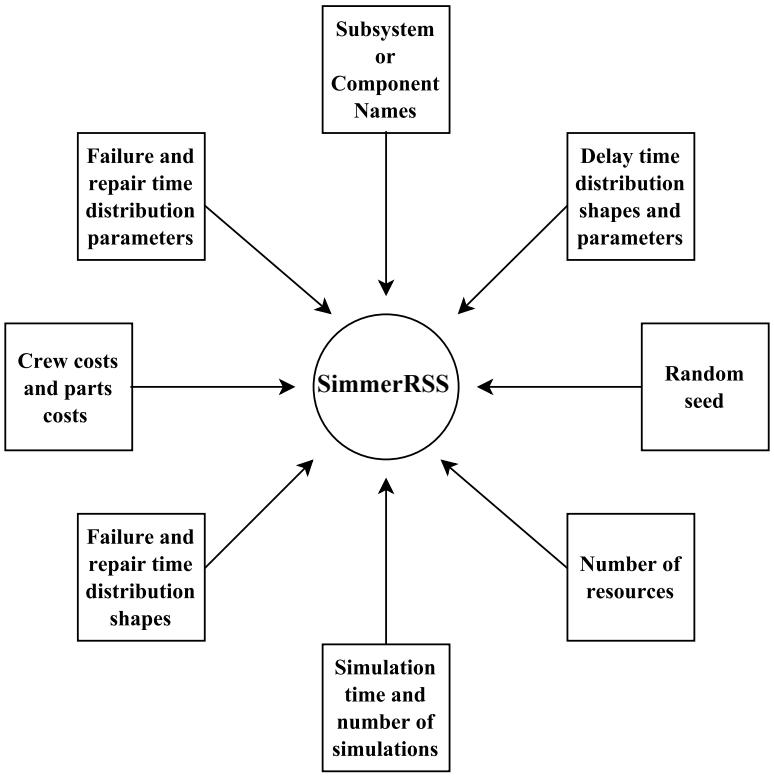

Figure 3.6 User-defined inputs for SimmerRSS functions.

3.5 Illustrative Application: A Subsystem-level Model of a Wind Turbine

3.5.1 Data

Wind turbines are repairable systems that fail and are repaired over time. Data on how frequently wind turbines fail and the corresponding costs are generally considered to be highly proprietary. A report by Tretton et al. (2011), however, provides detailed maintenance information for a fleet of 1.5 MW turbines over a 20 year period. We use the information in this report to develop illustrative examples for SimmerRSS.

3.5.2 Wind turbine subsystems

A wind turbine is generally comprised of seven subsystems. Figure 3.7 describes the seven subsystems being used in the high-level model for our example. The numbers inside each block correspond to the number of major components in each subsystem. We assume that the subsystems fail independently (e.g., the condition of one subsystem does not affect the condition of another).

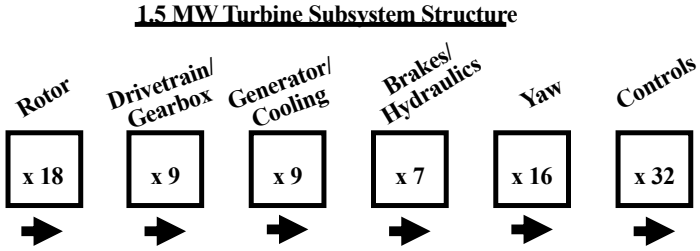

Figure 3.7 Subsystems in a 1.5 MW wind turbine.

3.5.3 Developing trajectories

RSimmer uses the concept of a trajectory tool, which is a common path in a DES model for entities (i.e., subsystems) of the same type. Trajectories are comprised of a list of actions that define some cycle of an equivalent process. For example, one could use a trajectory to define a list of actions that take place when a subsystem failure occurs in a system.

Example 5: Developing wind turbine subsystem trajectories

We begin by assigning each wind turbine subsystem a trajectory with a unique name, for example, "Rotor Path," which tells us the state of the rotor over time after it experiences a failure. All trajectories will send a message saying "the subsystem has failed." Within each trajectory, the subsystem failure time is recorded, as is the progress in the search for a maintenance crew (i.e., a resource) to come repair the subsystem. For resource deployment, SimmerRSS selects the first available maintenance team.

Once a maintenance crew is notified, the trajectory for the failed subsystem sends the message "Crew is Notified" and a delay time distribution is used to generate a time to arrival for the crew. When the maintenance crew arrives the trajectory sends the message "Crew Arrives, Begin Repair." A repair time distribution is used to generate a time to repair for the given subsystem and once complete the software displays the message "Repaired." Figure 3.8 displays a trajectory assigned to a wind turbine subsystem after a particular event. The various messages from SimmerRSS are saved in a file and can be inspected for checking and debugging.

3.5.4 Generating failure times at the subsystem level

At the subsystem level we will consider two different types of repairs, "Minimal Repair," which leads to an NHPP model and "refurbished," corresponding to a TRP model. Section 2.3.2 defines the failure intensity function for subsystem i to be the well-known power law model

$$\lambda_i(t) = \frac{\beta_i}{\eta_i}\left(\frac{t}{\eta_i}\right)^{\beta_i - 1}. \tag{3.4}$$

We use a simple algorithm from Chapter 16.7 of Meeker and Escobar (1998) to generate NHPP failure times recursively for each of the I subsystems. An explicit formula for this algorithm using the intensity in (3.4) is

$$t_j = \left[t_{j-1}^{\beta_i} - \eta_i^{\beta_i} \times \log\left(U_j\right)\right]^{1/\beta_i} \tag{3.5}$$

where $t_0 = 0$ and U_j, $j = 1, ...$ is a pseudorandom sample from a UNIF(0,1).

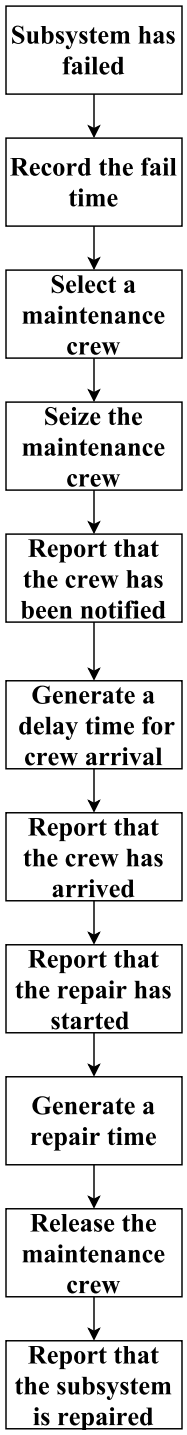

Figure 3.8 Subsystem failure/repair trajectory example.

Using the result from (3.5), we develop an algorithm that generates a sequence of failure times for subsystems that have either NHPP or TRP failure intensities (depending on the subsystem's cost, failure rate, and application), where the TRP renewal distribution is defined as $1 - \exp\big[-(\Gamma(1+1/\gamma)x)^{\gamma}\big], \gamma > 0$ (see Lindqvist et al. 2003). Next, we describe an algorithm for simulating the failures and repairs for a single subsystem over the period of the simulation. We first define the terms in the algorithm:

- τ_{ik} is the time of refurbished repair k for subsystem i and $\tau_{i0} = 0$.
- ζ_{ik} is the cumulative number of repairs (minimal and refurbished) at the time of refurbished repair k for subsystem i and $\zeta_{i0} = 0$.
- tol_i is the intensity tolerance for subsystem i. When a subsystem failure occurs at a time t where $\lambda_i(t) > tol_i$, a refurbished repair is performed on subsystem i and if a failure occurs at a time t where $\lambda_i(t) < tol_i$, a minimal repair is performed.
- b_k is the number minimal repairs between times $\tau_{i,k-1}$ and τ_{ik}.
- $W_{i\ell}$ represents the random repair time for failure ℓ for subsystem i.
- $\omega_{i\ell}$ represents the sum of $W_{i\ell}$ values prior to failure ℓ of subsystem i.

For subsystem $i = 1, ..., I$,

1. Recursively generate NHPP failure times using (3.5) until $\lambda_i(t) > tol_i$.
2. Denote the ordered times from Step 1 by $t_{1+\zeta_{ik}}, ..., t_{b_k+\zeta_{ik}}$. The repairs at $t_{1+\zeta_{ik}}, ..., t_{b_{k-1}+\zeta_{ik}} + \omega_{b_{k-1}+\zeta_{ik}}$ are times of "minimal repair" and $t_{b_k+\zeta_{ik}} + \omega_{b_k+\zeta_{ik}}$ is a "refurbished" repair time. For each failure, we adjust the vector of ordered times by adding the cumulative repair times up until the time of the most recent failure.
3. When a refurbished repair occurs, the failed subsystem's intensity returns to the trend value at $\lambda_i(t_{b_k+\zeta_{ik}} + \omega_{b_k+\zeta_{ik}}; \eta_i, \beta_i)$ where $TRP(F, \lambda(.))$ is defined in (3.3).

4. After a refurbished repair is effected, set the cumulative number of repairs to $\zeta_{ik} = \zeta_{i,k-1} + b_k$ and record the time of the k^{th} refurbished repair as $\tau_{ik} = \tau_{i,k-1} + t_{b_k+\zeta_{ik}}$.

5. Repeat Steps 1 through 4 until $\tau_{ik} + \omega_{b_k+\zeta_{ik}} > SIMTIME$, where $SIMTIME$ is the length of the simulation.

After $\sum_{i=1}^{I} \zeta_{ik}$ failure times are generated for the I subsystems, they are ordered and then sent to their respective trajectories where each subsystem failure is treated based on the unique subsystem trajectories defined by the user.

3.5.5 Single turbine simulation (subsystem-level model)

As an example of using trajectories and generated NHPP times, we run a 20-year simulation for a single turbine using the trajectory from Figure 3.8 for all of the subsystems in the overall system. The subsystem intensity function parameters for the power rule model were obtained from Tretton et al. (2011) and are given in Table 3.1.

Table 3.1 Subsystem power rule intensity parameters (η_i and β_i) and lognormal repair–time parameters (μ_i and σ_i).

Subsystem	i	η_i	β_i	μ_i	σ_i
Rotor	1	6.4	2.6	3.7	0.3
Gearbox	2	10.1	2.7	3.4	0.7
Generator	3	5.4	1.8	2.7	0.6
Brakes	4	4.8	2.4	1.6	0.2
Yaw	5	4	1.9	2.1	0.4
Control	6	7.4	2	1.6	0.4
Grid	7	14.5	2	1.9	0.3

Under the subsystem-level model, we fix crew costs by taking a weighted average of crew costs within each subsystem from the observed failures for the 100 turbines over 20 years, given in Tretton et al. (2011). Because there is a lot of variability in part costs within subsystems (i.e., a rotor pitch gear that costs $7,000 compared to a structural blade repair that can cost upwards of $200,000) we sample part costs from subsystem-specific lognormal distributions. For the repair times for each failure, we sample from a lognormal distribution with parameters μ_i and σ_i (mean and standard

deviation of the log repair times, respectively) for each of the I subsystems. Parameters for μ_i and σ_i for this simulation were selected by observing the empirical distributions of repair times from each subsystem in Tretton et al. (2011). During each simulation, an internal list of events is maintained. Table 3.2 displays the first 10 lines of internal logging from our software for a single turbine simulation at the subsystem level.

The user can inspect line-by-line actions throughout the simulation for debugging purposes. We provide the line-by-line logging for line 1 of Table 3.2. For each subsystem failure, the user can see the times (in years) at which each part of the trajectory takes place. The messages saved for each subsystem failure are:

- 6.35307: Turbine 1 has experienced a yaw failure 1: Subsystem has failed.
- 6.35307: Turbine 1 yaw failure 1: Crew is Notified.
- 6.35381: Turbine 1 yaw failure 1: Crew Arrives.
- 6.35381: Turbine 1 yaw failure 1: Begin Repair.
- 6.35445: Turbine 1 yaw failure 1: Repaired.
- 6.35448: Turbine 1 yaw failure 1: System is Operating.

Table 3.2 Example output from a subsystem-model simulation.

Failure	Start (years)	End (years)	Repair Time (hours)	Crew Cost (USD)	Part Cost (USD)
Yaw 1	6.353	6.355	12.03	800	11901
Brakes 1	6.371	6.372	17.42	551	3313
Brakes 2	7.243	7.245	18.96	551	2528
Yaw 2	7.355	7.357	17.42	800	1445
Yaw 3	7.373	7.376	23.27	800	1168
Yaw 4	7.468	7.472	29.67	800	1655
Yaw 5	7.474	7.480	50.53	800	1054
Rotor 1	7.851	7.853	19.48	1253	8402
Generator 1	7.934	7.938	35.43	585	2541
Yaw 6	8.185	8.186	12.14	800	1120

These raw event logs are used to summarize the output from each simulation.

3.5.6 Crane consideration at the subsystem level

According to Vachon (2006), the major needs for cranes during wind turbine maintenance are

- Nacelle lift or removal.
- Gearbox replacement (note that high-speed bearings can be replaced without the need for a crane).
- Structural blade damage.
- Generator replacement (note that generator bearings can often be replaced without the need for a crane).
- Tower damage (rare).

Crane costs are one of the biggest financial burdens in wind turbine maintenance and if possible, one should try to repair without using a crane. Vachon (2006) reports that crane mobilization/demobilization costs range between \$50,000 to \$100,000 and a typical four days of use of a crane would range between \$130,000 and \$200,000.

For simplicity, assume that if a crane is needed for a subsystem repair it will have a fixed cost of \$150,000. We consider the data from Tretton et al. (2011) and notice that the three subsystems that experienced crane events were the rotor, gearbox, and generator failure.

Within each trajectory, we sample from a Bernoulli distribution with a given p to determine whether a crane is needed or not. The crane-need probabilities for each subsystem are obtained by taking the observed number of crane events within each subsystem and dividing by the total number of events in the same subsystem. These observed events were reported for a fleet of 100 wind turbines over a 20–year period in Tretton et al. (2011). The estimated p's are

$$\hat{p}_{Rotor} = \frac{15+13}{15+60+547+13+142+468} = 0.0225$$

$$\hat{p}_{Gearbox} = \frac{10+5+35}{10+39+5+35+35+294+195} = 0.0816$$

$$\hat{p}_{Generator} = \frac{10}{10+184+117+98+235} = 0.0155$$

We note that $\hat{p}_{Brakes} = \hat{p}_{Yaw} = \hat{p}_{Control} = \hat{p}_{Grid} = 0$ because failures in the corresponding subsystems never require a crane. Using the updated trajectories that include crane considerations, we can now run more detailed simulations.

3.5.7 Results from the subsystem model with crane considerations

After a simulation has been completed, plots are provided for the user to asses metrics such as availability and cumulative cost over time, where availability is calculated by taking the difference of the total time and cumulative downtime and dividing that quantity by the total time.

$$Availability = \frac{time - downtime}{downtime} \tag{3.6}$$

Example 6: Illustration using one turbine for 20 years

Using the data from Table 3.1 in Section 3.5.5, Figure 3.9 displays an example of a single run over 20 years for one turbine. The vertical lines denote points where a crane was used for a given repair. In the top of Figure 3.9 the availability is decreasing over time due to the wearing of each subsystem. Such behavior is typical in wind turbines of this size (i.e., 1.5 MW). We note that the four crane events in Figure 3.9 make up a large portion of the cumulative costs over time. Subsequently, we will consider a small fleet of turbines to develop sensible maintenance decisions to lower crane costs over time.

Example 7: Illustration of multiple realizations for one turbine over 20 years

Similar to Example 6, the availability of a single turbine with data from Table 3.1 is considered. Instead of a single realization (i.e., Figure 3.9), the process is simulated over and over. The results

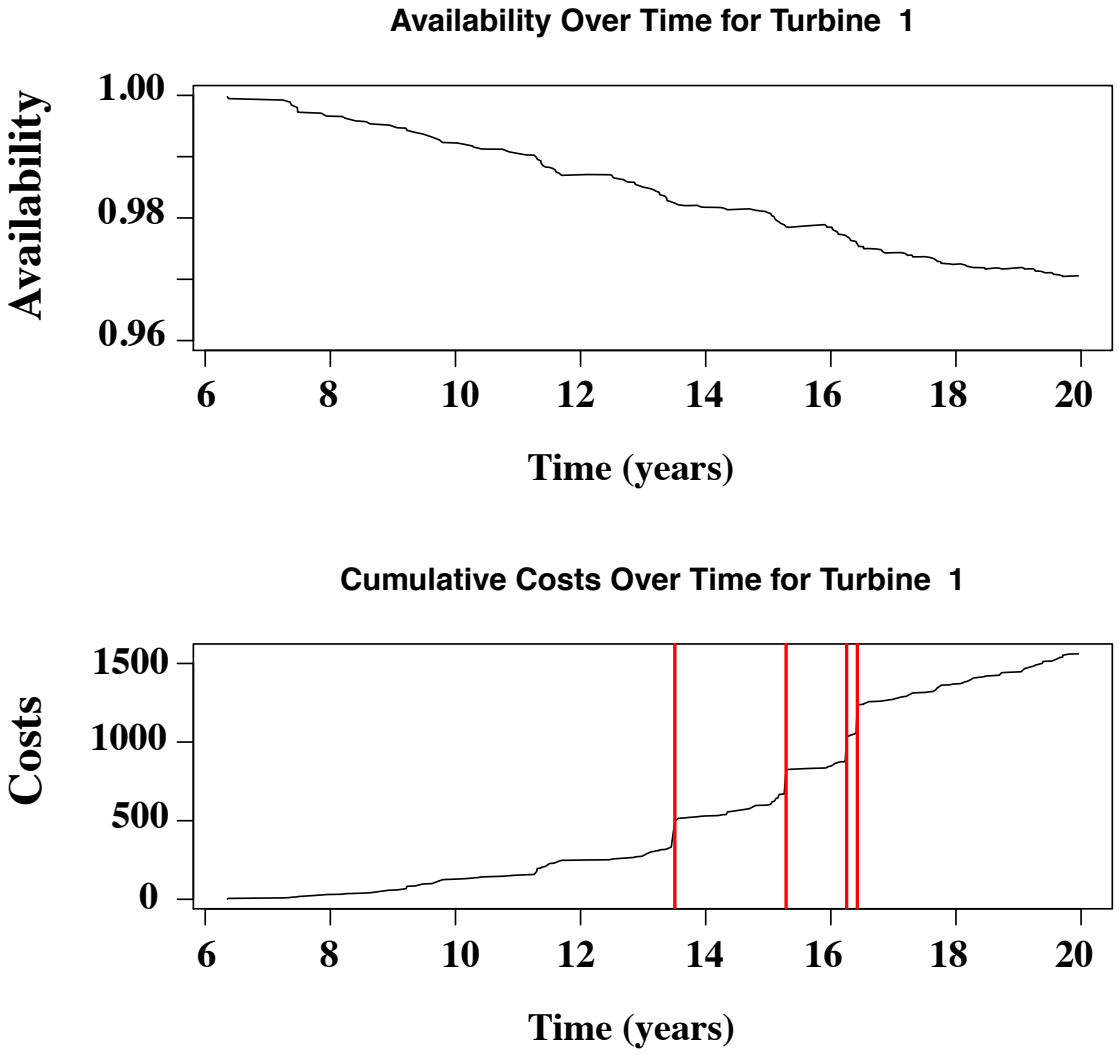

Figure 3.9 Availability (top) and cumulative costs (bottom) over 20 years for a single turbine where the vertical lines indicate crane events.

allow one to visualize the uncertainty. Figure 3.10 displays the median availability from 2000 realizations over a 20 year period, with a corresponding 95% prediction interval that is generated by taking the 0.025 and 0.975 quantiles of the results.

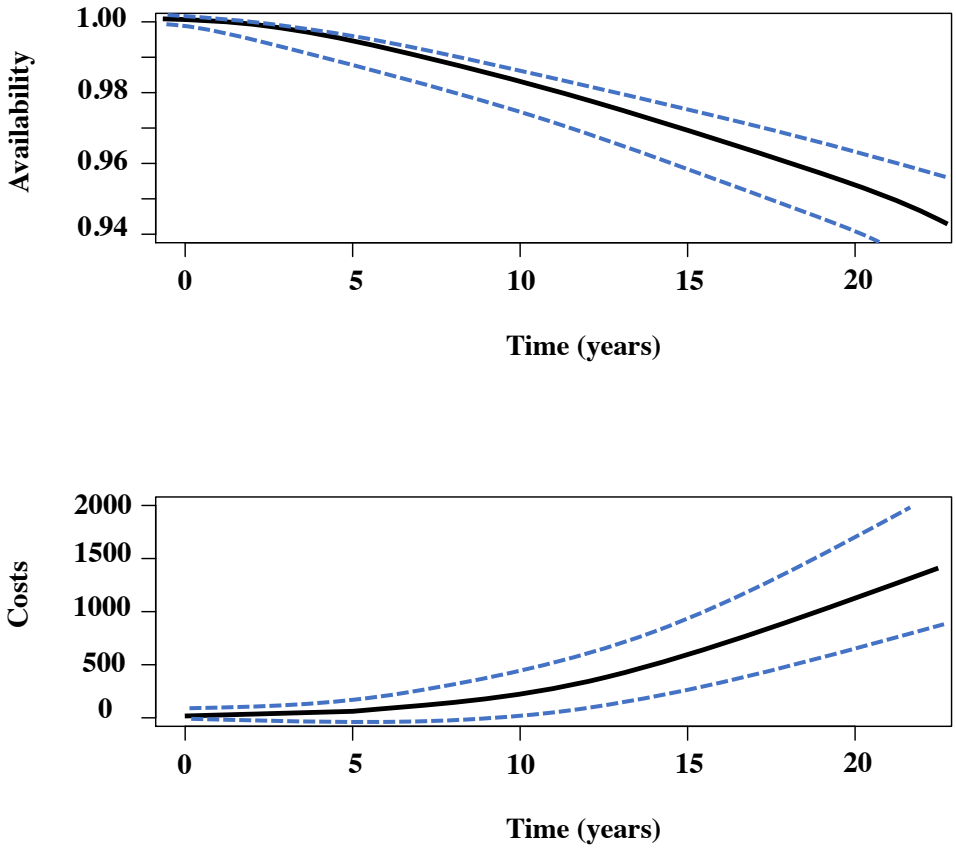

Figure 3.10 Predicted availability, (total time - downtime)/total time, from a single turbine with model parameters given in Table 3.1 (on top). The solid line represents the median availability and the dashed lines represent a 95% prediction interval. The plot on the bottom gives the cost of operation in thousands of USD.

3.6 Illustrative Application: Component-level Model of a Wind Turbine

In this section, we develop a component-level model of a wind turbine, which adds a higher level of detail to the system. Once again, the data for the components within each of the seven subsystems were obtained from Tretton et al. (2011).

3.6.1 Wind turbine components

For the component level structure, we expand Figure 3.7 into a lower-level model as input to the simulation software. Figure 3.11 displays the component level structure inside the 1.5 MW turbine used as an example in this paper. We note that the triangle symbols indicate components that require a crane for repair.

Example 7: Developing component trajectories

Similar to Section 3.5.3, we assign a trajectory to each of the $c = 1, ...C$ components being used in this project. Tretton et al. (2011) provide data on $C = 88$ components that we use for the component level-modeling. The trajectories work in a manner that is similar to the subsystems, except now we have detailed information that is expected to provide more realistic behavior than the high-level model.

3.6.2 Component-level intensity functions

Unlike the subsystem-level failure times that were generated, component-level failure times that cross a specified intensity tolerance will not necessarily be treated as refurbishments, but instead as renewals. We propose an algorithm similar to that given in Section 3.5.4 at the component level after a brief example to motivate components with different intensity functions.

Example 8: Wind turbine component intensities

To motivate a component-level algorithm, consider four of the components in the Gearbox/Drivetrain subsystem and their corresponding intensity function parameters. Parameters for the Main Bearing, Fan Motor, Lube Pump, and High-Speed Gears are:

1. **Main Bearing**: The power law intensity function parameters are $\beta = 3.5$ and $\eta = 39$.
2. **Fan Motor A**: The power law intensity function parameters are $\beta = 2.1$ and $\eta = 16$.
3. **Lube Pump A**: The power law intensity function parameters are $\beta = 2$ and $\eta = 18$.

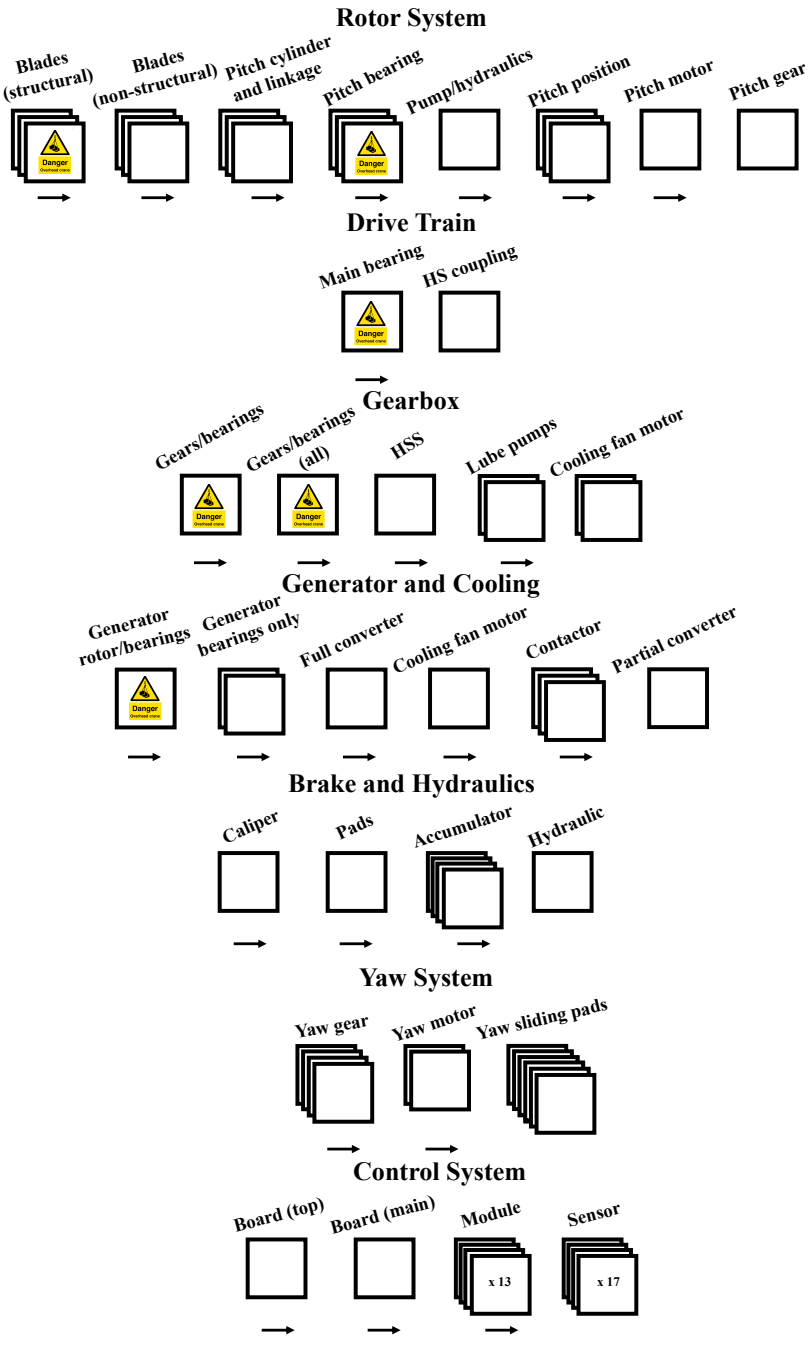

Figure 3.11 Component-level overview where the triangle symbols indicate components that may require a crane for repair.

4. **High-Speed Gears**: The power law intensity function parameters are $\beta = 3.5$ and $\eta = 26$.

Figure 3.12 displays the individual intensity functions versus time over 20 years for these four components. Notice how a component like "Lube Pump A" exhibits a linear increasing behavior in its intensity, whereas the "High-Speed Gear" plot exhibits an exponentially increasing shape. It is clear that these differences need to be taken into consideration with respect to maintenance actions over time.

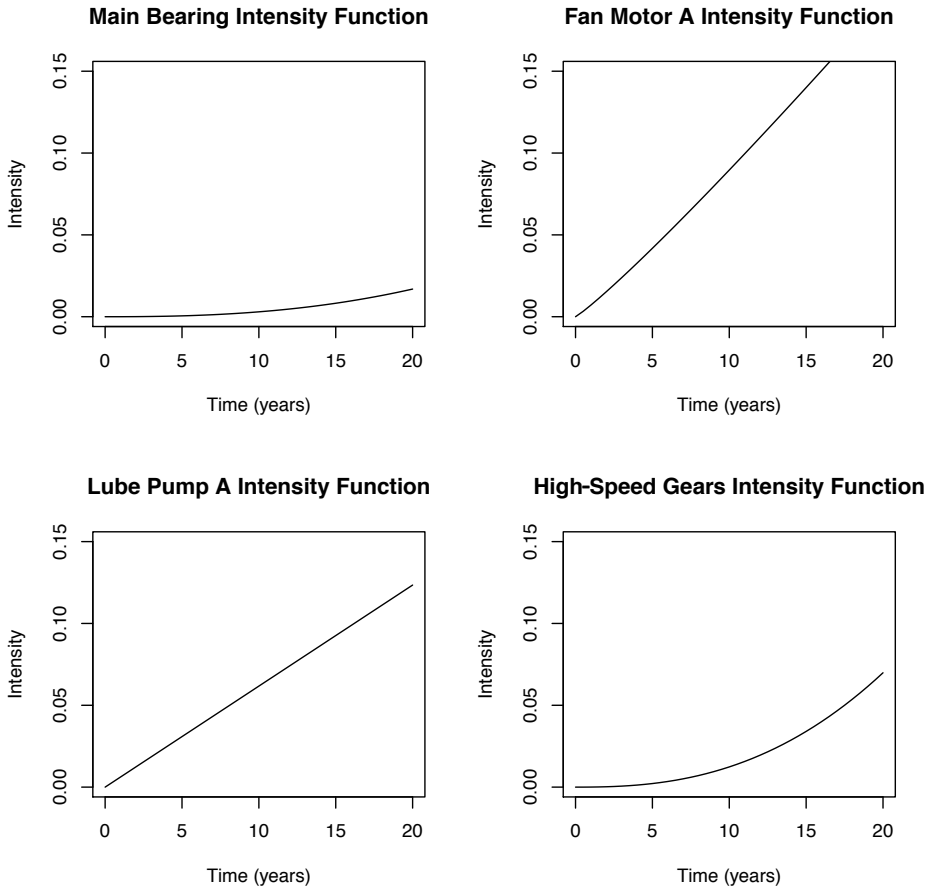

Figure 3.12 Intensity plots of four components within the Gearbox/Drivetrain subsystem.

3.6.3 Generating component failure times

We now describe an algorithm for generating failure times at the component-level. The purpose of this algorithm is to keep performing "minimal repairs" until the intensity level becomes too large

(failures are occurring too frequently) at which time a "renewal" is performed. There are practical implications of performing a "minimal repair" instead of a "renewal." A minimal repair could be thought of as doing something to get the system running with minimal cost, whereas a "renewal" completely replaces the component of interest. Recall that performing a "minimal repair" leaves the intensity unchanged, whereas a renewal returns the intensity to 0. We first define the following terms in the algorithm:

- τ_{ck} is the time of renewal repair l for component c and $\tau_{c0} = 0$.
- ζ_{cl} is the cumulative number of repairs (minimal and renewals) at the time of renewal repair l for component c and $\zeta_{c0} = 0$.
- tol_c is the intensity tolerance for component c. When a component failure occurs at a time t where $\lambda_c(t) > tol_c$, a renewal repair is performed on component c and if a failure occurs at a time t where $\lambda_c(t) < tol_c$, a minimal repair is performed.
- b_l is the number of minimal repairs between times $\tau_{c,l-1}$ and τ_{cl}.
- $V_{c\ell}$ represents the random amount of time needed to effect the repair for failure ℓ for component c.
- ω_ℓ represents the sum of $V_{c\ell}$ values prior to failure ℓ of component c.

For component $c = 1, ..., C$,

1. Starting at $t_0 = 0$, recursively generate NHPP failure times using (3.5) until $\lambda_c(t) > tol_c$.
2. Denote the ordered times from Step 1 by $t_{1+\zeta_{cl}}, ..., t_{b_l+\zeta_{cl}}$. The repairs at $t_{1+\zeta_{cl}}, ..., t_{b_{l-1}+\zeta_{cl}} + \omega_{b_{l-1}+\zeta_{cl}}$ are times of "minimal repair" and $t_{b_l+\zeta_{cl}} + \omega_{b_l+\zeta_{cl}}$ is a "renewal" repair time.
3. When a "renewal" repair occurs, components with a renewal intensity return 0.
4. After a renewal repair is effected, set $\zeta_{cl} = \zeta_{c,l-1} + b_l$ and $\tau_{cl} = \tau_{c,l-1} + t_{b_l+\zeta_{cl}}$.

5. Repeat Steps 1 through 4 until $\tau_{cl} + \omega_{b_l+\zeta_{cl}} > SIMTIME$, where $SIMTIME$ is the length of the simulation.

After $\sum_{c=1}^{C} \zeta_{cl}$ failure times are generated for the C components, they are ordered and then sent to their respective trajectories where each component failure is treated based on the unique component trajectories defined by the user.

Example 9: Single turbine simulation (component-level model)

Before using our component-level model for maintenance decision making at the fleet level, we will demonstrate how the component-level model works for a single wind turbine.

Simulating the need for a crane is more straightforward in the component-level simulation because Tretton et al. (2011) specify which components require cranes. Moreover, the crew and parts costs will now be treated as fixed, based on the data in Tretton et al. (2011).

Case 1: Low-intensity tolerance

Using the component-level information corresponding to inputs defined in Figure 3.6 gives the parameters that are needed to run a single turbine simulation. For the sake of simplicity, we define all of the $C = 88$ intensity tolerances from the algorithm in Section 3.6.3 to be equal to 0.05. A second variable of interest that can be controlled by the owners and operators is a "minimum repair cost ratio," which is the fraction of the cost that a minimal repair costs compared to a renewal. This can be controlled through spare part inventory, quality of part replacement, and cost of labor. The maintenance-action policy choices for of the simulation set up are

- A "minimum repair cost ratio" of 0.20.
- $tol_c = 0.05$ (both for true renewals and TRP model "renewal" components that return the intensity to the trend line).

We run a 20-year simulation with these two choices and display the availability and cumulative costs in the left side of Figure 3.13.

Case 2: High-intensity tolerance

Similar to the left side of Figure 3.13, we run another 20-year simulation. For this simulation, we change the tolerance to now be $tol_c = 0.10$, while holding the "minimal repair" costs ratio to 0.20, as in Case 1. The results of this single simulation are on the right side of Figure 3.13

Case 1 vs. Case 2

As shown in Figure 3.13 the low-intensity tolerance yields better results for both availability and cumulative costs. It is important to note that the low-intensity case is essentially trying to choose the best time to renew, whereas the high-intensity case is fixing the issue quickly and avoiding the cost of a renewal. It is clear in this small example that the cost of many "minimal repairs" can add up quickly. Later in the paper, we will choose different tol_c values for each component to increase the availability and decrease cumulative costs as much as possible over multiple simulations.

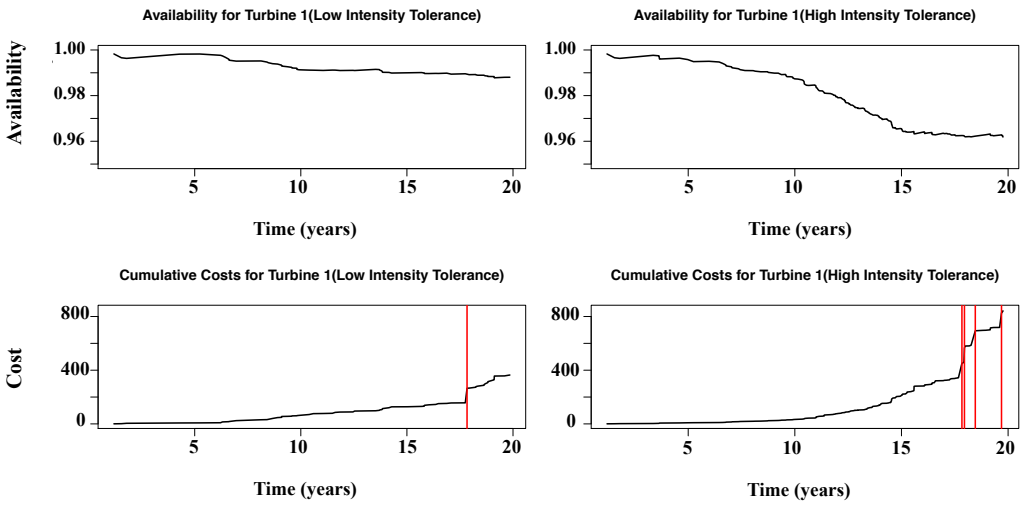

Figure 3.13 One realization of a 20-year simulation for low (left) and high (right) intensity tolerances, where the top and bottom graphs plot the availability and cumulative maintenance costs (in thousands of USD) over time respectively.

Multiple realizations for the availability in Case 1 vs. Case 2

Similar to Case 1 vs. Case 2, the availability of a single turbine with low and high intensities are considered. Instead of a single realization (i.e., Figure 3.13), the process is simulated over and over. The results allow one to visualize the uncertainty. For each intensity case, Figure 3.14 displays the median availability from 2000 realizations over a 20 year period, with a corresponding 95% prediction interval that is generated by taking the 0.025 and 0.975 quantiles of the results.

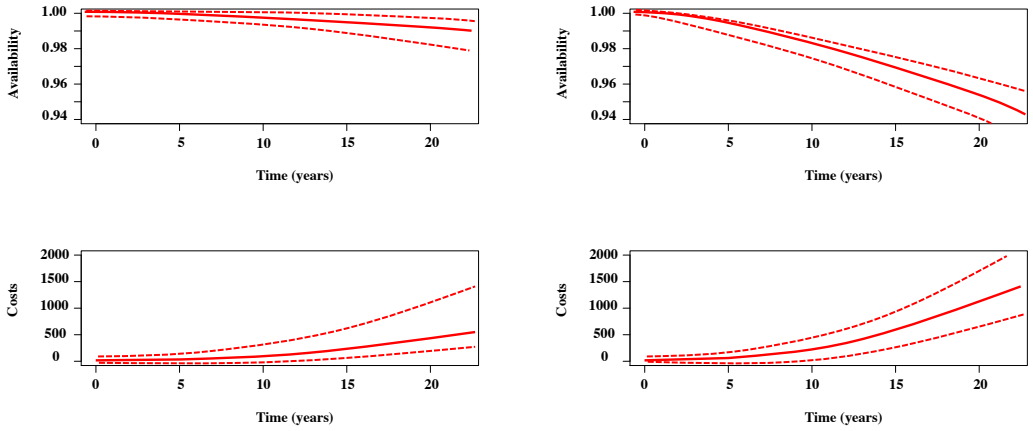

Figure 3.14 Predicted availability over time from a turbine with low (left) and high (right) intensity tolerances. The solid lines represent the median availability and the dashed lines represent 95% prediction intervals, generated by taking the 0.025 and 0.975 quantiles from the 2000 simulations.

3.7 Illustrative Application: Simulation of a Small Wind Farm

In this section, we compare the subsystem-level (Section 3.5) and component-level (Section 3.6) models from Sections 3.5 and 3.6 by applying them to a moderate-sized wind farm. Consider a wind farm with the following characteristics:

- The number of turbines on the farm is $N_{Turbines} = 40$.
- All $N_{Turbines}$ have the same features as those described in Tretton et al. (2011).
- The intensity tolerance for all subsystems and components are equal in each case that we present..

- At the subsystem level, the cost of a minimal repair for subsystem i is $C_{Min_i} = B/(\text{Refurbish Cost})$, where B is a constant that ranges from 0 to 1. As B goes to 1, minimal repair costs approach renewal costs. We will refer to this as the *cost scale*.

3.7.1 Repairable system simulation using a subsystem-level model

This subsection illustrates the use of a repairable system simulation using subsystem-level information. Suppose that the wind farm operator has two maintenance policy decisions, intensity tolerance and cost scale, that can be controlled over the course of the first 20 years of turbine operation. We study how changing the intensity tolerance and cost scale over multiple simulations affects the mean availability and mean cumulative cost of a 40-turbine wind farm using the subsystem-level model from Section 3.5. The simulation set-up includes:

- $I = 7$ subsystems for each of the 1.5 MW turbines on the farm.
- The subsystem intensity tolerances $tol_1 = ..., tol_{40}$ are held equal across the 40 wind turbines.
- Separate simulations were run at each point in a 10×10 grid for cost ratios ranging from 0 to 1 and intensity tolerances ranging between 0 to 0.20 respectively.
- For each combination of cost ratio and intensity tolerance, 1000 20-year simulations of wind turbine operations were run for the fleet of 40 turbines.

Figure 3.15 displays the mean availability over the 10×10 grid. In the grid, the contours show

- The mean availability decreases as the intensity tolerance increases. When minimal repairs are performed, there is an increased number of failures, causing the availability to decrease.
- As expected, the availability is constant as the cost scale increases.

Figure 3.16 shows the mean cumulative cost after 20-years in hundreds of thousands of USD. The contours show

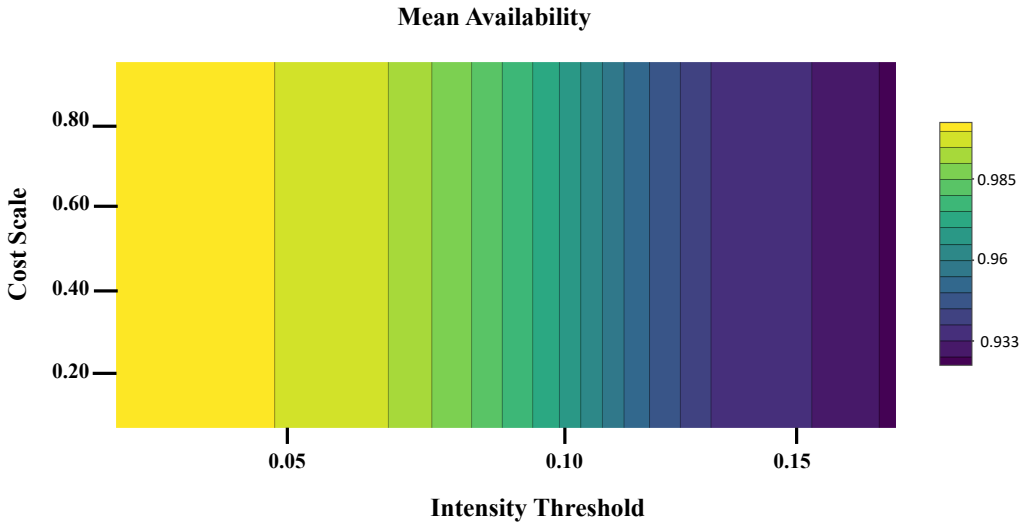

Figure 3.15 Mean availability over a 20-year period using the subsystem-level model for $N_{Turbines} = 40$, with corresponding contours over the 10×10 cost scale by intensity tolerance grid.

- The mean cumulative cost increases as the intensity tolerance increases.
- The mean cumulative cost increases as the cost scale increases.

Intuitively, Figure 3.16 makes sense because increasing the cost of minimal repairs will have a direct effect on raising the overall turbine costs over the 20-year period. Additionally, increasing the intensity tolerance increases the cumulative cost average because more failures occur as the tolerance increases.

Figures 3.15 and 3.16 can be used to help make decisions related to wind farm maintenance policies. In this example, two inputs (cost scale and intensity tolerance) can be controlled by the owner/operator. By varying these two factors in the simulation experiment it is possible to study the effect that these variables have on availability and cumulative cost. The plots can help guide decisions such as, what combination of tolerances will keep the turbines above some availability threshold? This is a prevalent question in industry, as maintenance contracts generally contain an availability threshold that turbines must operate above during particular periods. Corresponding

cumulative costs can help owners and operators plan budgets and comparing preventive maintenance options that could save them money in the long run.

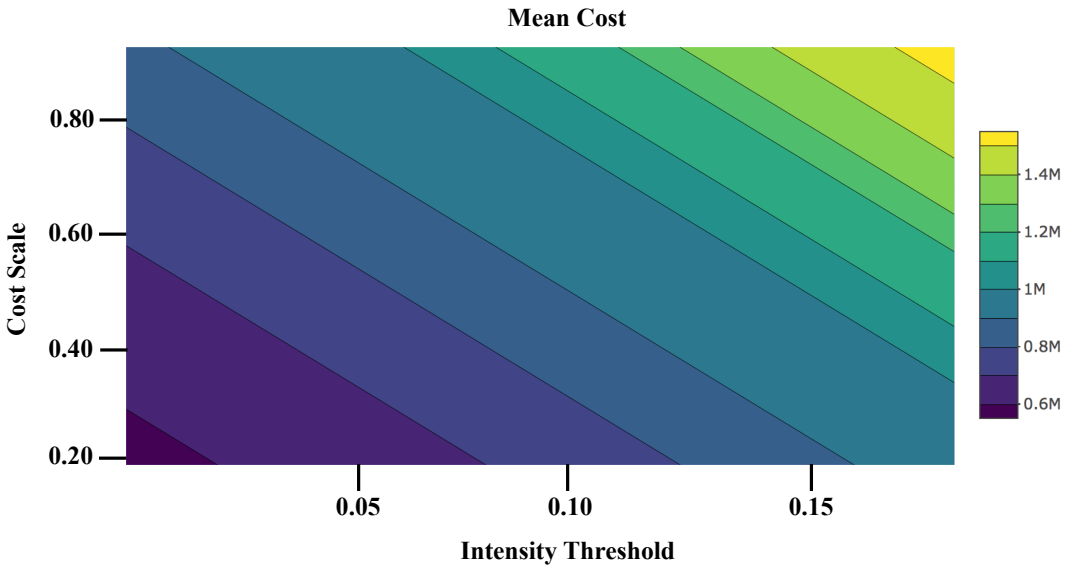

Figure 3.16 Mean cost over a 20-year period using the subsystem-level model for $N_{Turbines} = 40$, with corresponding contours over the 10×10 cost scale by intensity tolerance grid.

3.7.2 Repairable system simulation using a component-level model

A repairable system simulation using the component-level model can be used to visualize the changes in mean availability and cumulative costs over a 20-year period. Recall, the component-level model uses more information, with individual failure rate parameters for each component.

Here, we use the same simulation set-up used in Section 3.7.1, but use the component-level model in place of the subsystem-level model. Figure 3.17 displays the mean availability over the 10×10 grid. In the grid, the contours show

- The availability decreases as the intensity tolerance increases. When minimal repairs are performed, there is an increased number of failures, causing the availability to decrease.
- As expected, the availability is constant as the cost scale increases.
- The availability is slightly lower than the subsystem-level model results.

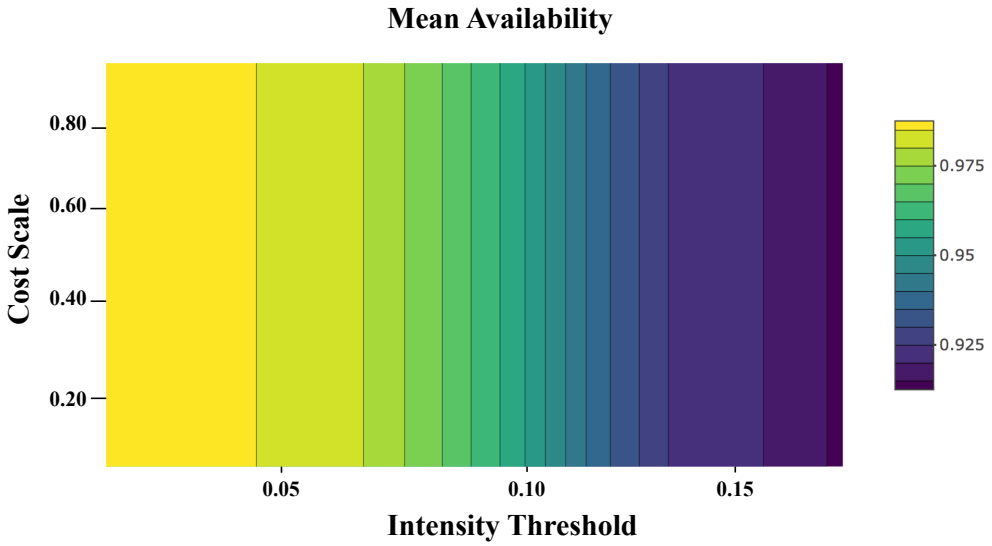

Figure 3.17 Simulated mean availability over a 20-year period using the component-level model for $N_{Turbines} = 40$, with corresponding contours over the 10×10 cost scale by intensity tolerance grid.

In Figure 3.18, the results using the component-level model for the mean cumulative cost after 20-years is displayed in hundreds of thousands of USD. The contours show

- The mean cumulative cost increases as the intensity tolerance increases.
- The mean cumulative cost increases as the cost scale increases.
- The mean cumulative costs are slightly higher than the subsystem-level model results.

3.7.3 Comparing the results from the subsystem-level and component-level models

The results from Sections 3.7.1 and 3.7.2 are similar, but have some interesting differences for this application. First, we notice the difference in mean availability and mean cumulative cost between the subsystem-level and component-level models. This difference is more than likely driven by the crane events. Recall, crane events are estimated by a Bernoulli distribution at the subsystem-level and occur conditional on particular component failures within the component-level model.

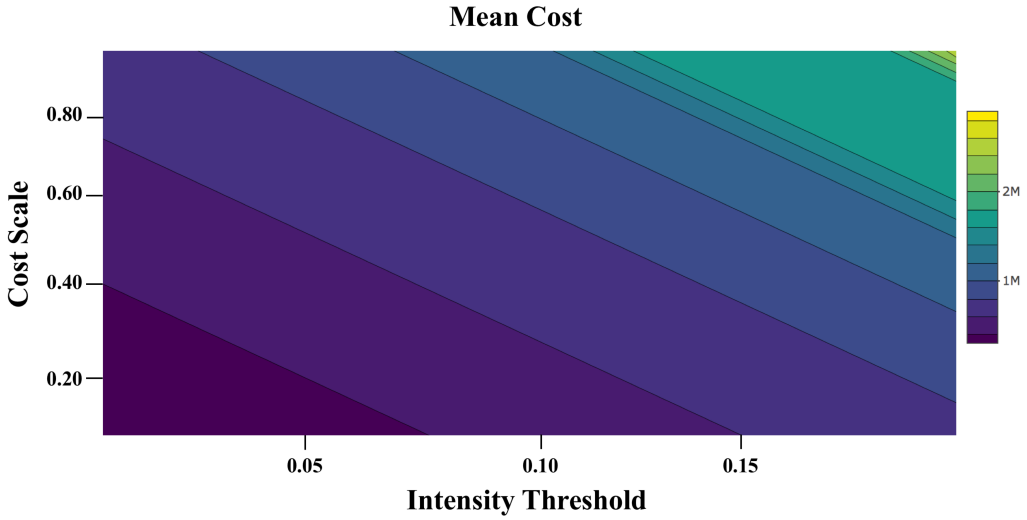

Figure 3.18 Simulated mean cost over a 20-year period using the component-level model for $N_{Turbines} = 40$, with corresponding contours over the 10×10 cost scale by intensity tolerance grid.

Another difference is the number of events that occur using each model. Recall the subsystem model simulates downtimes based on individual lognormal distributions, since some components within the subsystem take longer to repair than others. For that reason, we see fewer events, that have downtimes which have less variability per event than that of the component-level model.

Overall, the simpler subsystem-level model serves as a good approximation to the component-level model. To decide between models, one should consider the application. For example, if one chooses to assign all system components to have the same intensity tolerance, then the component-level model will not provide much additional information about the availability changes over times. Additionally, if one chooses to assign different cost scales to each component, the component-level model would be appropriate to better understand that these different cost scales will have on the expected cumulative costs over time.

3.7.4 Implementing a crane policy using the component-level model

Similar to Section 3.7.2, the component level-model is now used to make an important policy-based decision on a wind farm: when to deploy a crane. Recall, crane rentals and daily usage rates contribute substantially to the overall operation and maintenance costs on a wind farm.

How many turbines should require a crane before a crane is deployed to a wind farm? To answer this turbine downtime must be taken into consideration, as lost revenues from letting a failed turbine remain non-operational can add up quickly. According to the Electricity Information Administration, the average cost to generate electricity in 2017 was 5.72 cents per kilowatt-hour (kWh) and according to Pacificorp (annual reports), the average revenue is 7.2 cents/kWh. The cost for transmission is not considered in this paper.

To quantify downtime costs we use a formula provided by the National Renewable Energy Lab (NREL), starting with the cost to generate power from a turbine or wind farm:

$$P_{gen} = \big[(FCR \times IC)/AEP\big] + \big[(LRC + O\&M + LLC)/AEP\big] \tag{3.7}$$

where:

- FCR is a fixed charge rate (i.e., the fraction of total installed cost that must be set aside each year to retire capital costs).
- IC is the initial capital expenditure in USD.
- AEP is the net annual energy production in kWh.
- LRC is the levelized replacement cost, which captures the anticipated costs of replacing major components over the project lifetime, in USD.
- $O\&M$ is the cost for operations in maintenance (turbine maintenance, USD over the project lifetime).
- LLC is the land lease cost in USD over the project lifetime.

Annual profit, P_a, can be calculated by using the result from (3.7) where

$$P_a = (P_{selling} - P_{gen}) \times AEP$$

Using the component-level model, multiple scenarios are considered where the variables input to each simulation include:

1. $P_a = P_{selling} - P_{gen} = 0.02, 0.03, 0.04, 0.05$, which are assumed profits in dollars per kilowatt hour.

2. $CapFac = 0.30, 0.32, 0.34, 0.36, 0.38, 0.40$, which are capacity factors (the average power generated divided by the rated peak power) that directly affect the AEP.

3. $tol_c = 0.13, 0.14, 0.15, 0.16$, which are intensity tolerances for the components of each wind turbine.

4. $N_{turb} = 1, 2, 3, 4, 5$, which is number of turbines that require a crane before a crane is deployed.

The 480 possible combinations of these variables are input into the component model simulation to assess the median crane cost and median downtime cost over 20 years for the wind farm. As an example, Figure 3.19 displays the results from the following combination:

- $P_{selling} = 0.03$ USD.
- $CapFac = 0.34$.
- $tol_c = 0.13$.

In Figure 3.19, the results show that the best option is to deploy a crane when two turbines require a crane. This policy-based graphic can help plan for future crane events and implement future preventive maintenance strategies to guard against crane events in general.

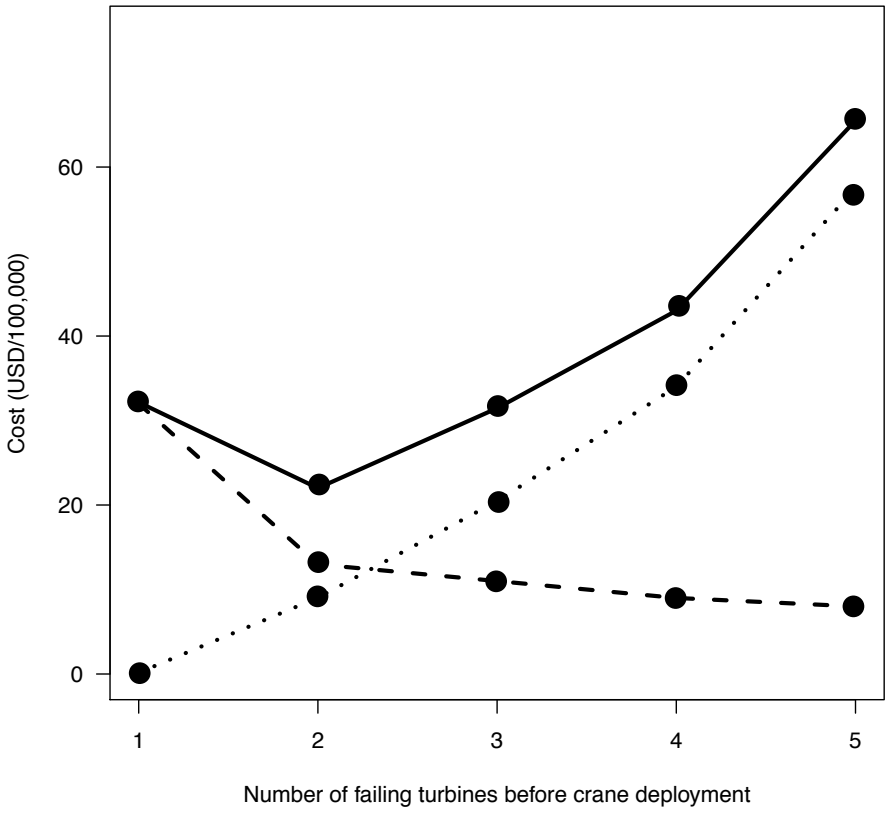

Figure 3.19 Output from the component-level model where the dashed line represents crane costs, dotted line represents downtime costs, and solid line represents the total costs accrued from crane-based events. In this example, two cranes minimize the median cost over 2,000 component model simulations.

3.8 Concluding Remarks and Areas for Future Research

3.8.1 Key takeaways

3.8.1.1 Using the repairable systems simulation results

Figures 3.15, 3.16, 3.17, and 3.18 can assist in decision making across different industries. Having insight to the effects inputs that are controlled by an owner/operator can guide maintenance-based decisions. For example, in the wind energy industry availability contracts generally call for wind turbine availability to stay above some level over some period of time. Owners and operators can run simulations to better understand how a variable like intensity threshold effects turbine availability.

3.8.1.2 The cost scale of spare parts

In this paper, we presented a useful tool for evaluating maintenance policies with repairable system simulation. The simulation tool allows users to better understand how the cost of "minimal repairs" will affect the cumulative costs for a fleet of systems. What is a minimal repair? Consider spare part inventory, where a spare part costs money to purchase and store. The overall cost of a spare part will cost some fraction of completely replacing a component with a new part. If one is able to estimate these costs, the overall budget for a fleet of systems can be estimated with more accuracy.

3.8.1.3 Availability contracts

Specific to the wind energy industry, methods to analyze the decrease in availability over time for a fleet of systems were developed in this paper. Being able to predict (and perhaps mitigate) the decrease in availability is important for wind turbines, as contracts generally guarantee a sustained level of availability over some initial period of each turbine's life. Having these availability predictions can help owners and operators implement preventive maintenance strategies that target components that are significantly affecting the availability decrease.

3.8.2 Concluding remarks

Repairable systems simulation is an important tool used in the reliability discipline. Advancements in technology will provide important opportunities for statisticians to collaborate with engineers and policy makers to make important contributions in the field of engineering.

3.8.3 Future research

Models that use rate/environmental data have the potential to explain much more variability in failure processes that affect availability and cumulative costs. This information can be used to predict future turbine lifetimes at the individual unit level, leading to maintenance policies structured around increasing the remaining useful life of each unit.

Acknowledgments

This work was completed under an IGERT program funded by the US National Science Foundation, Award 1069283.

Bibliography

Bangsow, S. (2012). *Use Cases of Discrete Event Simulation.* Springer.

Brailsford, S., Churilov, L., and Dangerfield, B. (2014). *Discrete-Event Simulation and System Dynamics for Management Decision Making.* Wiley.

Cook, R. J., and Lawless, J. F. (2007). *The Statistical Analysis of Recurrent Events.* Springer.

Ding, F. and Tian, Z. (2012). Opportunistic maintenance for wind farms considering multi-level imperfect maintenance thresholds. *Renewable Energy, 45,* 175–182.

El-Thalji, I., and Liyanage, J. (2012) On the operation and maintenance practices of wind power assets. *Journal of Quality in Maintenance Engineering, 18,* 232–236.

Hill, R., Stinebaugh, J., and Briand, D. (2008). Wind turbine reliability: A database and analysis approach. Technical report, 0983, Sandia National Laboratories. https://windpower.sandia.gov/other/080983.pdf. Last accessed November 21, 2018.

Lindqvist, B. H., Elvebakk, G., and Heggland, K. The trend-renewal process for statistical analysis of repairable systems. *Technometrics, 45,* 31–44.

Meeker, W. Q., and Escobar L. A. (1998). *Statistical Methods for Reliability Data.* Wiley.

Rausand, M., and Hoyland, A. (2007). *System Reliability Theory Models, Statistical Methods, and Applications.* (Second Edition). Wiley.

Trabish, H. (2010). *Operations and Maintenance: Keys to Wind Farm Profitability.* Greentech Media.

Tretton, M., Reha, M., Drunsic, M., and Keim, M. (2008). Data Collection for Current U.S. Wind Energy Projects: Component Costs, Financing, Operations, and Maintenance. Technical report, 52707, NREL. https://www.nrel.gov/docs/fy12osti/52707.pdf. Last accessed November 21, 2018.

Ucar, I. and Smeets, B. (2018). *Discrete-Event Simulation for R (3.6.5 Edition).* https://CRAN.R-project.org/package=simmer.

Vachon, W. (2006). *Crane Considerations Related to Maintaining Wind Turbines.* W. A. Vachon and Associates, Inc. https://windpower.sandia.gov/2006reliability/wednesday/10-billvachon.pdf. Last accessed November 21, 2018.

Yildirim, M., Gebraell, N., and Sun, X. (2017). Integrated predictive analytics and optimization for opportunistic maintenance and operations. *EEE Transactions on Power Systems, 32,* 4319–4328.

CHAPTER 4. PREDICTION OF SPARE PART REQUIREMENTS BASED ON RECURRENT -EVENT MAINTENANCE DATA

A paper being submitted to *the International Journal of Health and Prognostics*

Michael S. Czahor and William Q. Meeker

Department of Statistics

Iowa State University

Ames, IA, 50011, USA

Abstract

When a repairable system fails during operation, part replacement(s) are required to return the system to operational status. Part consumption data provide a useful resource for obtaining information on support activities such as financing, storage and supply of spare parts, and maintenance activities. It is common nowadays to dynamically record part consumption data at the individual system level. In this paper, we introduce a nonparametric algorithm for predicting future part consumption in systems that fail from multiple failure types. We use a nonhomogenous Poisson process model to describe each failure process for the failure types. Using historical data, point estimates of the shape and scale parameters for each failure model are used to generate future failure times. We describe the prediction algorithm for computing future part consumption needs for multiple part types. The proposed methods are illustrated with an application for predicting part consumption needs for a fleet of systems with three failure types and 24 unique part types.

Key Words: repairable systems, nonhomogenous Poisson process, nonparametric, part consumption data.

4.1 Introduction and Motivation

4.1.1 Background

In large fleets of repairable systems, parts often need to be replaced when failures occur. Having the ability to predict the parts needed for future repairs can benefit operational strategies developed by the owners/operators. Characteristics that influence the part types and the number of parts needed for system repairs include the system makeup, operational environment, maintenance policy, etc. However, minimal work has been done developing methods for predicting individual part demand when both limited field information is available and the predictions occur during the middle of a system's life.

4.1.2 Motivation

Complex repairable systems with different failure modes and with different kinds of parts that can fail present difficulties in predicting the number of spare parts that will be needed for future repairs. With the need to effect timely repairs, the availability of spare parts becomes a critical component of maintenance operations. Being able to predict the demand for specific part types can assist in optimizing the management of spare parts for a fleet of systems. We consider several models for predicting spare part needs.

Recurring events can be observed over a monitoring period and at each event the number of parts and type of parts used for the repair are recorded. Part number prediction for corrective maintenance (CM) actions that result from failures are difficult to plan for when competing causes drive the failures. A generalized reliability analysis procedure that takes multiple failure causes and part counts into account is needed. This paper develops a procedure to predict part demand for effecting repairs for a fleet of similar systems.

4.1.3 System failures

The focus of this paper is on failures that require corrective maintenance (CM) actions. When systems operate over time they are subject to failures that require maintenance to return the system

to an operational status. Such systems are known as *repairable systems*. Different subsystem failures could require different part types for the necessary maintenance actions, depending on what caused the failure.

4.1.4 Related work

Barabadi, Barabday, and Markeset (2014) present a case study where they apply reliability models with covariates to make predictions for spare part needs. Qian et al. (2017) analyze factors such as financing and storage of spare parts and develops a prediction model for spare parts consumption under small sample conditions using an engineering analysis method that is comprised of: failure mode analysis, frequency ratio analysis, and unit failure rate calculations.

4.1.5 Overview

The rest of this paper is organized as follows. Section 4.2 introduces the a part consumption dataset and describes a simple time series prediction method. Section 4.3 outlines a general approach to predictions and provides examples of applying such methods to predicting future part consumption. Section 4.4 fits our model across different training cases. Section 4.5 presents an error analysis and explores the sensitivity of changing the length of the training period. Last, Section 4.6 discusses alternative approaches and highlights key takeaways from this research.

4.2 Data

4.2.1 The part consumption data

System repairs frequently require part replacements. Such parts could be as minor as nuts and bolts and as major as large bearings in wind turbine gearboxes. Being able to predict the number of parts and part types of a future period has the potential to benefit owners and operators of systems (or fleets of systems), as one can use such information to plan future inventory and budgets.

The dataset used in our study contains 4,717 events corresponding to corrective maintenance actions, triggered by a system failure, for a fleet of 1213 systems during 24 months of operation.

There were 24 unique part types used for three failure types in this dataset. Details about the system are proprietary. For each system failure, the data records contain the

- System ID
- Time of failure
- Failure type, and
- Part Number and quantity of each part number needed for each repair.

Table 4.1 An example of the data for four system failures for system ID A000204.

System ID	System failure time (days)	System failure cause	Part ID	Part quantity
A000204	167	R193	P169319	5
A000204	167	R193	P991287	1
A000204	171	R193	P573388	1
A000204	196	R193	P991287	1
A000204	276	R193	P097048	1
A000204	276	R193	P168211	1
A000204	276	R193	P169319	1
A000204	276	R193	P610186	1
A000204	276	R193	P843990	3
A000204	276	R193	P953340	3

Table 4.1 shows the data for four failures for system ID A000204. The first two rows of Table 4.1 represent a single failure, where each row identifies the quantity of a unique part ID needed for the repair. The last column of Table 4.1 displays the number of parts needed for the failure event. Forecasting the quantity of parts needed in the future is of interest.

Although there are 24 months of data for the fleet of systems, we will initially do our modeling and prediction using the first 18 months of data so that we can use the last 6 months of data to assess the accuracy of our predictions.

4.2.2 Multiple failure causes in repairable systems

To better describe the dataset, consider a system where failures are classified into J different types. Suppose that a continuous process where after each failure time a system is repaired. For each

failure, a failure cause, the number of part types, and the part counts for each part type needed to effect the repair are recorded. Also suppose that the repair times are negligible, such that a failed system is restarted immediately after a maintenance action is performed. Modern maintenance databases generally contain failure times and other additional information. For example, there may be information on the identity of a failed component, failure cause, repair cost, part types used for the repair, etc. Thus we shall more generally assume that observations from repairable systems are represented as marked point processes where each mark label represents a type of event. For example, the marks may represent three failure causes and other information about the failure/repair. In this research, the data $(T_1, C_1), (T_2, C_2), ...,$ is referred to as a marked point process with successive failure times $0 < T_1 < T_2 < ...$ and marks C_j in $1, .., J$, where J is the number of failure types.

4.2.3 Exploratory analysis and mean cumulative functions for multiple failure causes

When initially observing failure data, non-parametric methods are useful for obtaining a graphical representation of the number of recurrences for a fleet of systems and/or individual units versus the time in service (i.e., weeks). In this paper, the model used to describe failures for the population of systems is based on a mean cumulative function (MCF) as a function of system age t. Nonparametric MCF estimation requires no assumptions about the form of the individual system event recurrence rates. MCF graphs provide a summary of recurrent-event data, where trends and unusual behavior can be identified. When a fleet of systems has different failure causes, multiple MCFs can be estimated. For each failure cause, the MCF method assumes that the time that observation of a system is terminated does not depend on the system's history. An algorithm in Chapter 16.1 of Meeker and Escobar (1998) is outlined and can be used to estimate MCFs for each failure type. Further information also can be found in Nelson (2003).

4.2.3.1 Example 1: Mean cumulative function for multiple failure types using the part consumption data

Three failure causes that recur for the fleet of systems in the part consumption data are observed during an 18-month window of system operation. We compute the sample MCF for each failure type along with the standard errors that allow us to compute pointwise approximate confidence intervals for the population MCFs. Figure 4.1 displays the MCFs for each failure type during an 18-month window of operation. Characteristics observed in the sample MCF plot include:

- R193 and R446 MCF function are increasing approximately at a constant rate.
- R364 MCF functions are increasing at an increasing rate.

Having information on the rate of recurrence by failure type can provide a better understanding of the part consumption data, as some parts may be used more frequently for particular failure types. A resampling model can be used to assist in modeling part-specific information for each system failure.

4.2.4 Prediction with a simple time series model

A time sequence of observations is a time series. Figure 4.2 displays the time series for the quantity of each part number needed during 80 weeks of operation. In this case, the part counts for each part type appear to be independent and identically distributed (iid) over time. In particular, there is no evidence of trend or autocorrelation in the time series data. Thus the model is simple and can be described by a sample mean and standard deviation. For each part, we can let the part predictions be represented by the historical part count mean and standard deviation. For example, if we let the historical data for part type $p = 1, ..., P$ be denoted by $y_{p,1}, ..., y_{p,T}$, then we can write the forecasts as

$$\hat{y}_p = \bar{y}_p = (y_{p,1} + ... + y_{p,T})/n$$

where $\hat{y}_p$ is an estimate of future values of y_p given the history for part p. For a normal distribution, Meeker, Hahn, and Escobar (2018) show the two-sided $100(1-\alpha)\%$ prediction interval for a single

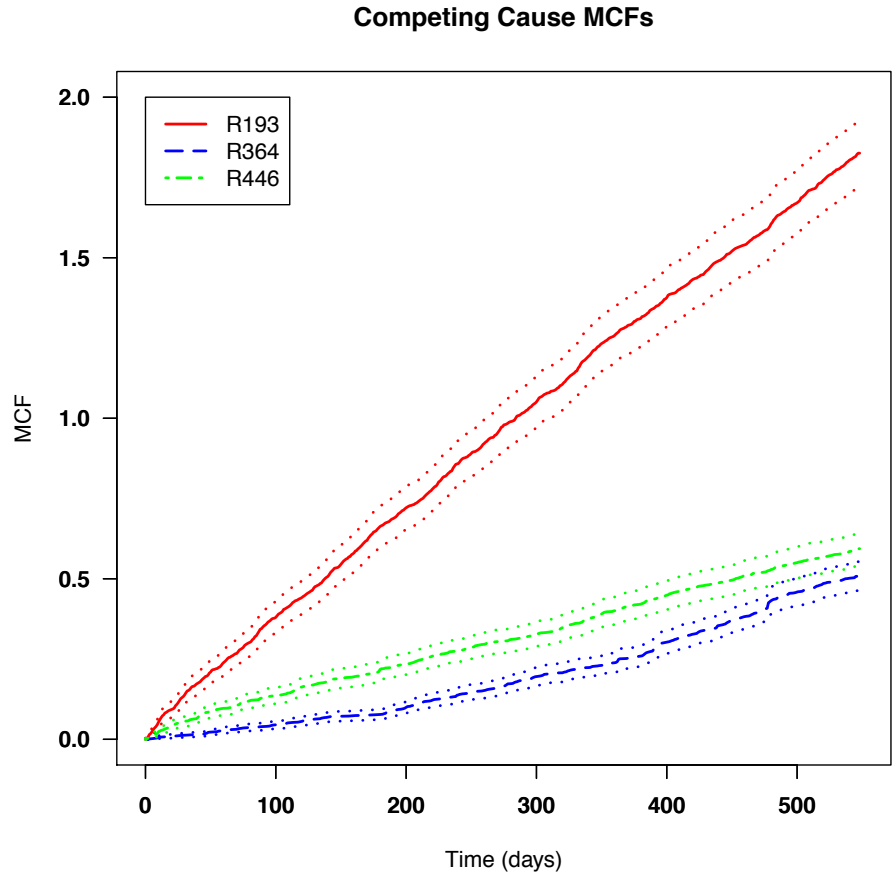

Figure 4.1 Sample MCFs and 95% pointwise confidence intervals for the three different failure causes.

future, independently and randomly selected observation, based upon the results of a previous independent random sample of sample size n from the same normal distribution to be

$$\bar{y}_p \pm t_{(1-\alpha/2;n-1)} \left(1 + \frac{1}{n}\right)^{1/2} s_p \tag{4.1}$$

where s_p is the sample standard deviation of part p and $t_{(1-\alpha/2;n-1)}$ is the $(1-\alpha)$ quantile of a student's t distribution with $n-1$ degrees of freedom. Because n is large in the part consumption data, a good approximation to the exact prediction interval is

$$\bar{y}_p \pm z_{(1-\alpha/2)} s_p \tag{4.2}$$

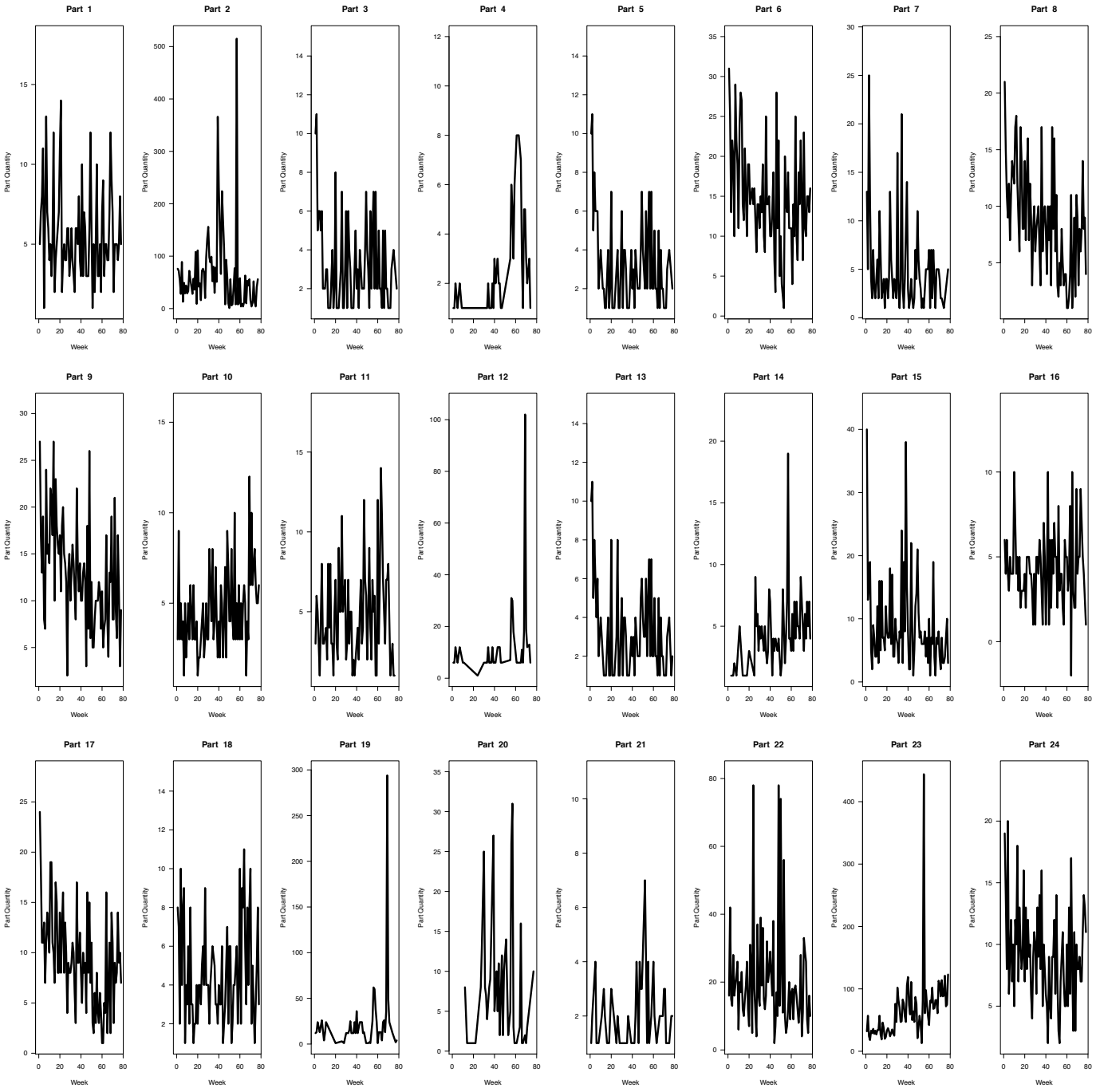

Figure 4.2 Part requirement quantities time series (by week) for all 24 parts used for the fleet of systems.

where $z_{(1-\alpha/2)}$ is the $1-\alpha/2$ quantile of the standard normal distribution and the choice of α depends on the desired coverage probability.

4.2.4.1 Example 2: Predicting parts by using the sample mean

Suppose that for part number 1 we want to predict the number of parts needed for the fleet of systems in the next six months, given 18 months of data. The sample mean and standard deviation from the historical data are $\bar{y}_1 = 5.32$ and $s_1 = 1.34$ respectively. A 95% prediction interval for Part 1 quantity predictions is constructed in Figure 4.3 by substituting these values into (4.2) and setting $z_{(1-\alpha/2)} = 1.96$, resulting in

$$5.32 \pm 1.96 \cdot 1.34 = [2.69, \quad 7.95].$$

4.3 Alternative Statistical Methods for Predicting Future Part Consumption

4.3.1 A general approach to prediction

As an alternative to the simple time series model for part consumption forecasts, we now suggest a nonparametric method to predict part consumption. With the goal of prediction, it is necessary to have a probability model for the random variable of interest. A point prediction for the random variable can be generated by using the mean or median of the probability distribution. Then an approximate $100(1-\alpha)\%$ prediction interval can be obtained by using the $\alpha/2$ and the $1-\alpha/2$ quantiles of this distribution.

4.3.2 An application of the general approach to predicting future part consumption

Recalling the general approach from Section 4.3.1, we start by defining the random variable of interest in our application as the number of parts needed for each part type in a given week. Because there is a complicated joint distribution for the number of parts needed for each week/part number combination for the fleet in our application, it would be difficult to obtain an analytical form for the needed marginal probability distributions because of the non-stationarity in the time

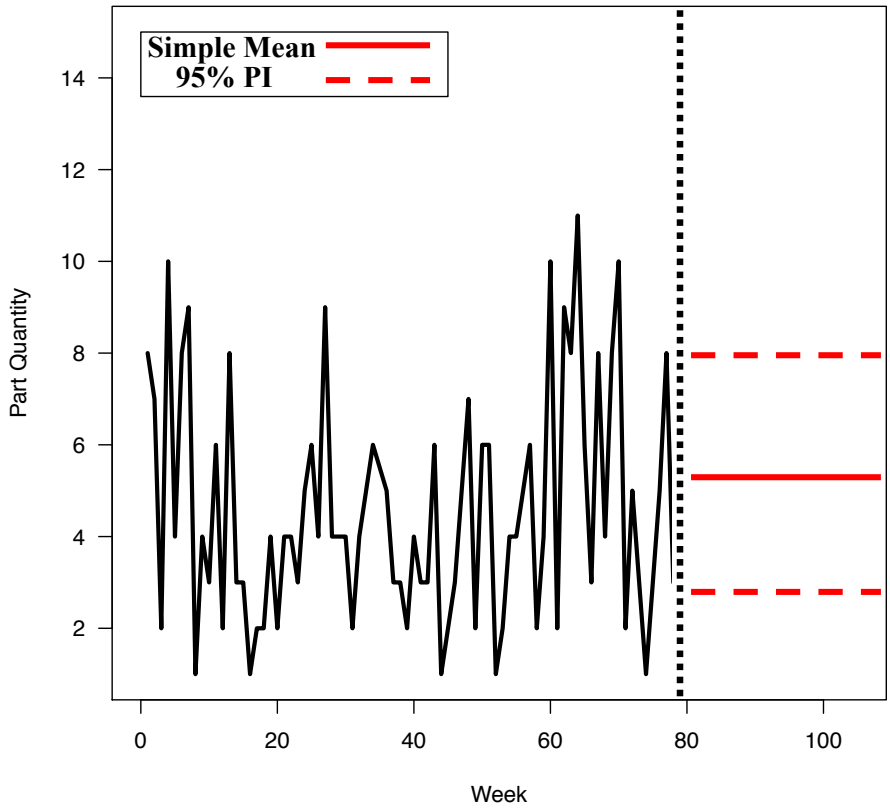

Figure 4.3 Simple time series model for predicting part quantity for part number 1 with 95% prediction intervals.

series structure, in addition to the dependencies on part type combinations used for particular repair types.

As an alternative, we can use a simulation-based method to obtain the number of parts probability distributions for each part type/week combination. To do this, the entire part demand process can be simulated over and over again, where a single run of the simulation for a given part type/week combination represents the number of a specific part needed for a given week across all systems in the fleet. Prediction intervals for the number of parts needed in each week can be generated with the method discussed in Section 4.3.1, based on the simulated empirical distributions.

4.3.3 Notation

We use the following indices and other notations:

- $j = 1, .., J$ indexes the failure types, where $J = 3$ is the number of failure types for the part consumption data.
- $p = 1, ..P$ indexes the unique part types used to repair the systems, where $P = 24$ is the number of part types for the part consumption data.
- $n = 1, ..N$ indexes the events in the part consumption data frame, where $N = 4,717$ is the number of events for the part consumption data.

4.3.4 Modeling and simulation of failure times for the different failure types

We use a nonhomogenous Poisson process (NHPP) model to describe intensity functions for each independent failure type. An NHPP model has a non-constant recurrence rate $\nu(t)$. Further information about the Poisson process is given in Section 2.2 of Cook and Lawless (2007). For each failure type, we define the intensity function to be the well-known power law model

$$\lambda(t) = \frac{\beta}{\eta}\left(\frac{t}{\eta}\right)^{\beta-1} \tag{4.3}$$

where β and η need to be estimated for each failure type, based on the observed failure times.

Once the parameters in (4.3) are estimated, a simple algorithm from Section 16.7 of Meeker and Escobar (1998) can be used to generate a sequence of failure times for each failure type recursively. An explicit formula for this algorithm using the intensity in (4.3) is

$$T_i = \left[T_{i-1}^{\beta} - \eta^{\beta} \times \log\big(U_i\big)\right]^{1/\beta} \tag{4.4}$$

where $t_0 = 0$ and $U_i, i = 1, ...,$ is a pseudorandom sample from a UNIF$(0, 1)$ distribution. This algorithm is used for each failure type independently, where (β_1, η_1), (β_2, η_2), and (β_3, η_3) represent the NHPP parameters for R193, R364, and R446 failures, respectively.

4.3.5 Using a sampling structure to model the part consumption for each failure conditional on failure type

A second level of the model is needed to generate the part quantities and types needed to effect each repair in the simulation. To generate a single realization of the future-failure/repair process, we first merge and reorder the failure times from all failure types that were generated as described in Section 4.3.4. Then for each generated failure time, we sample an observed event from the original dataset conditional on the failure type.

Let **Z** represent a random vector listing all parts needed for a simulated repair time conditional on failure type. For example, for each simulated failure, one can sample a random vector **Z** from the historical data.

4.3.5.1 Example 3: Sampling a vector of parts conditional on failure type

Recall the example data presented in Table 4.1. Suppose that an R193 failure occurred and we wanted to generate a realization for the parts needed to complete the repair. We would sample, with replacement, a failure event from all of the previously observed R193 failures. For example, suppose our sampled **Z** selected the R193 event where System ID A000204 failed at time 167, then the realized value of **Z** would be a vector with the following elements

$$Z = \begin{bmatrix} P169319 \\ P169319 \\ P169319 \\ P169319 \\ P169319 \\ P991287 \end{bmatrix}$$

.

4.3.6 Motivating an empirical distribution matrix

Once part-need realizations are made over the entire period of interest, it is necessary to bin the part-need counts into categories corresponding to part number and time intervals and to aggregate over all systems. With observed random variables for each part number, a prediction can be made for the total number of parts needed on a week-to-week basis.

To do this we generate a matrix, where the rows and columns are represented by weeks and part numbers respectively. We call this matrix Q, where $Q_{p,w}$ represents a single value from the empirical distribution of total part p's needed during week w. In the next subsection, we present an algorithm to simulate multiple Q matrices to obtain the empirical distributions of part counts for each part type during each future week of interest.

4.3.7 Structure of the resampling prediction algorithm

In summary, the prediction method suggested in this section is implemented by doing the following:

1. Simulate failure times for each failure type over the period of prediction.

2. Combine and reorder the failure times from Step 1.

3. For each failure time, sample a part vector for each simulated failure by sampling, conditional on failure type, a failure from the available data.

4. Accumulate part counts for each combination of week and part type to generate the probability distributions of interest on a week-to-week basis. Save these results as $q_{w,p,\ell}$, where ℓ indicates the draw number from the empirical distribution.

5. Repeat Steps 1 through 4 B (e.g., 2000) times to generate the accumulated part distributions each week (i.e., generate $q_{p,w,1}, ...q_{p,w,B}$).

6. Calculate the medians from each probability distribution of accumulated parts each week to be used as point predictions.

7. Calculate 0.025 and 0.975 quantiles for each week and part type combination to provide 95% prediction intervals.

4.4 Applying the Part Consumption Prediction Resampling Algorithm

This section applies the resampling prediction algorithm from Section 4.3.7 to the part consumption data and analyzes the algorithm's predictive accuracy with different amounts of historical information. In Step 1, failure times for three different failure types need to be simulated. Given that the power-law parameters for each failure type are estimated from the observed history, we consider the implications of having different amounts of information prior to using the part consumption resampling prediction algorithm outlined in Section 4.3.7. More information is expected to enhance the algorithm's accuracy because an increased amount of historical data will reveal part combinations that might exist given a particular failure type. For that reason, we apply the resampling prediction algorithm to different amounts of training data to compare the predictive ability of the procedure as a function of the amount of training data.

4.4.1 Defining the training and testing data

4.4.1.1 Train-test split

We start by splitting the dataset into training and testing subsets, where the prediction method is based on the training set and predictions are evaluated on the testing set. Split points in the ordered list of observations in the part consumption data (equivalent to points in time) are selected as a cutoff to create two datasets.

4.4.1.2 Splitting the data

Recall the system-repair dataset has 104 weeks of data and we want to create four splits. A proposed first split could be the part consumption from the first 78 weeks being used to predict the part consumption for the next 26 weeks for each part type/week combination. A second split can

be calculated by using the part consumption from weeks 26 to 78 to predict the part consumption for the next 26 weeks for each part type/week combination.

Notice that the testing data stays the same. Then the performance statistics calculated on the predictions for each split will be consistent and can be compared. Here, the number of records used in the resampling prediction algorithm for each split is different, offering a larger and larger history to sample from in the simulation that generates the probability distributions of interests.

4.4.1.3 Example 3: Splitting the part consumption data

The system-repair dataset has 104 weeks of data. The following splits will be used to evaluate the validity of the resampling prediction algorithm:

- Split 1: weeks 66 - 78 (train), weeks 79 - 104 (test).
- Split 2: weeks 53 - 78 (train), weeks 79 - 104 (test).
- Split 3: weeks 27 -78 (train), weeks 79 - 104 (test)
- Split 4: weeks 1 - 78 (train), , weeks 79 - 104 (test)

Using different splits within the resampling prediction algorithm allows one to assess the performance in comparison to a historical mean with different amounts of information. One would expect that the predictive ability of smaller splits will yield poor estimates of the number of parts for each part type/week combination probability distribution in comparison to larger splits because limited information to estimate the NHPP parameters and because fewer part combinations are observed.

4.4.2 Forecasting future recurrences for each failure type

Separate estimates of the parameters used in the power law process defined in (4.3) are calculated for each split. Future failure times are simulated for each split case across all three failure causes. Table 4.2 shows the estimated power-law parameters for each split case in Example 3.

Table 4.2 Power-law parameter estimates for each split case.

Split (weeks)	$\hat{\beta}_{R193}$	$\hat{\beta}_{R364}$	$\hat{\beta}_{R446}$	$\hat{\eta}_{R193}$	$\hat{\eta}_{R364}$	$\hat{\eta}_{R446}$
66-78	0.970	1.104	0.885	286.55	861.39	992.22
53-78	0.960	1.003	0.838	306.14	880.49	981.40
27-78	0.952	1.349	0.867	277.44	824.15	977.42
1-78	0.933	1.517	0.884	290.42	858.77	985.81

4.4.3 Applying the algorithm to obtain part quantity forecasts

The methods outlined in Section 4.3.7 are used to generate accumulated part distributions for each part type/week combination and to predict the median number of parts needed each week for all part types. Given the stochastic framework in Sections 4.3.4 and 4.3.5, we implement the iterative simulation approach to generate part count predictions. We run the simulation $B = 2000$ times on each split case and use the results to predict the vectors of parts needed for all failures.

4.4.3.1 Example 4: Illustrating part predictions for a single part for each split

As an example, consider the demand for Part ID 6 during each split case. Over each period, the fleet experiences failures, some of which need one or more of Part ID 6 to complete the repair. In Figure 4.4, predictions (i.e., medians from the part/week probability distribution) for the quantity of Part ID 6's needed in the next 26 weeks are displayed with a solid line. Corresponding 95% predictions intervals are displayed as well, in addition to the historical mean (horizontal solid line). The vertical dashed line represents the right endpoint of the split used within the simulation. Note, in this case the prediction for each week from the algorithm can be denoted as $\hat{y}_{6,w}$ and computed as the median of $(q_{6,w,1}, ..., q_{6,w,2000})$. A 95% prediction interval is generated by using the 0.025 and 0.975 quantiles of the distribution to obtain $[\underset{\sim}{y} \ , \ \widetilde{y} \ ]$.

4.5 Results

In this section, we present the results for predicting the cumulative number of parts needed for the fleet of systems for each part type/week combination.

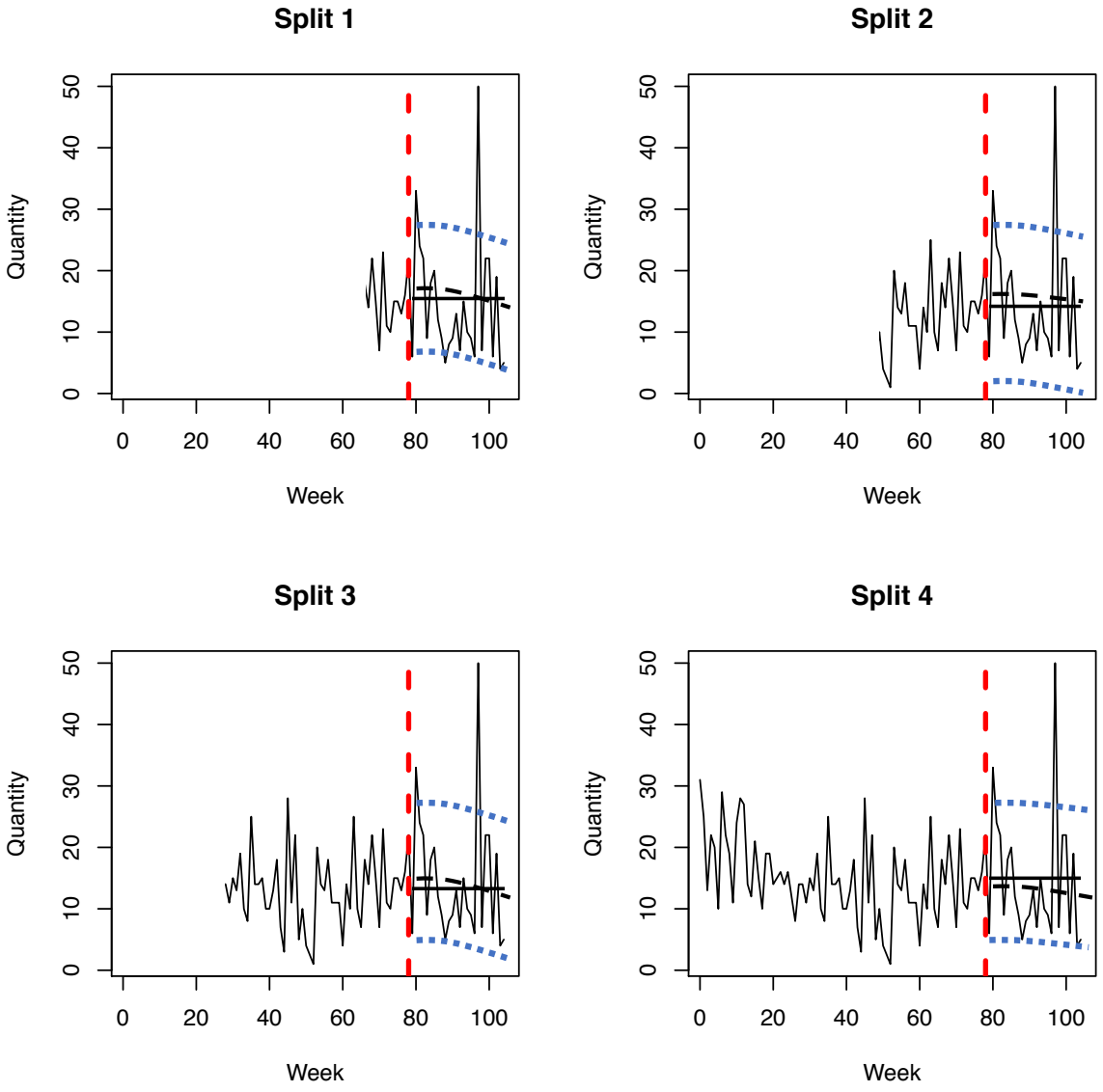

Figure 4.4 Results from the part consumption resampling prediction algorithm for each split case for part type ID 6 probability distributions across 26 testing weeks. The dashed lines represent the median number of part ID 6's needed in each week and the dotted lines represent corresponding 0.025 and 0.975 quantiles. The vertical line represents the right end point of each split. The horizontal solid line represents the historical mean.

4.5.1 Computing sample means and predictions from the part consumption algorithm

Similar to Example 4, predictions for each $q_{p,w}$, combination are made for each split, where all splits include parts $p = 1, ..., 24$. Table 4.3 shows the start and end times for four separate splits, where the *train* times indicate the period of observations, *test* times indicate the prediction period, and N_s represents the number of weeks in each prediction period.

Table 4.3 Training and testing periods for each split.

Split	Train start (week)	Train end (week)	Test start (week)	Test end (week)	N_s
1	66	78	79	104	26
2	53	78	79	104	26
3	27	78	79	104	26
4	1	78	79	104	26

The prediction $\hat{y}_p$ for each part/week probability distribution is computed as the median of $M(q_{p,w,1}, ..., q_{p,w,2000})$. These medians result in $N_i = 26$ predictions for each split. Similarly, a historical mean is calculated for each split and is used as a prediction for each $q_{p,w}$ combination where:

- Split 1 historical mean for part p: $\bar{y}_{p1} = \sum_{w=66}^{78} \frac{q_{p,w}}{13}$
- Split 2 historical mean for part p: $\bar{y}_{p2} = \sum_{w=53}^{78} \frac{q_{p,w}}{26}$
- Split 3 historical mean for part p: $\bar{y}_{p3} = \sum_{w=27}^{78} \frac{q_{p,w}}{52}$
- Split 4 historical mean for part p: $\bar{y}_{p4} = \sum_{w=1}^{78} \frac{q_{p,w}}{78}$.

4.5.2 Comparing the resampling prediction algorithm to a historical mean

This section compares the performance of the two different prediction methods: the resampling prediction algorithm and a historical mean. To assess how well each prediction method performs, the root mean squared error for each can be calculated to assess predictive accuracy. For part p and split i, where $i = 1, ..., 4$, the root mean squared error for the simple sample mean method and the resampling algorithm are defined, respectively, as:

$$SM_{RMSE_{ip}} = \sqrt{\sum_{w=ts_{start_i}}^{ts_{end_i}} (q_{p,w} - \bar{y}_{i,p})^2 / N_s} \tag{4.5}$$

$$RS_{RMSE_{ip}} = \sqrt{\sum_{w=ts_{start_i}}^{ts_{end_i}} (q_{p,w} - \hat{y}_{p,w})^2 / N_s} \tag{4.6}$$

where $q_{p,w}$ represents the observed number of parts for a given part type and week combination and $\hat{y}_{p,w}$ is the predicted number of parts for a given part type/week combination.

The RMSE for each split can be calculated using the prediction algorithm and historical mean. The results can be summarized by calculating the percent change in RMSE for parts $p = 1, ..., 24$ for each split case, where the percent change in RMSE for part p and split i across the entire prediction can be calculated by

$$PC_i = 100 \left(\frac{RMSE_{sm} - RMSE_{rs}}{RMSE_{sm}} \right) \tag{4.7}$$

where $RMSE_{sm}$ represents the RMSE using the historical mean and $RMSE_{rs}$ represents the RMSE using the resampling algorithm. Below, the number of parts which saw a reduction in RMSE using the resampling algorithm are summarized:

- Split 1: 14 out of 24 parts saw a reduction in RMSE when using the prediction algorithm.
- Split 2: 18 out of 24 parts saw a reduction in RMSE when using the prediction algorithm.
- Split 3: 19 out of 24 parts saw a reduction in RMSE when using the prediction algorithm.
- Split 4: 20 out of 24 parts saw a reduction in RMSE when using the prediction algorithm.

Figure 4.5 displays the results using (4.7). A five-number summary of the percent change results can be seen in Table 4.4. This information can be used to assess whether more historical information assists in reducing the RMSE for each part number. In addition, one can use Figure 4.5 as an exploratory tool to analyze the shapes of each RMSE distribution.

Table 4.4 A five number summary for the percent change part number MSEs.

Split	Min.	Q1	Median	Mean	Q3	Max.
1	-32.31	-11.23	6.14	6.14	26.01	41.47
2	-39.18	-2.33	3.90	3.40	11.56	54.51
3	-38.36	-9.13	6.05	7.26	22.01	56.30
4	-25.37	3.92	13.83	20.17	41.79	69.92

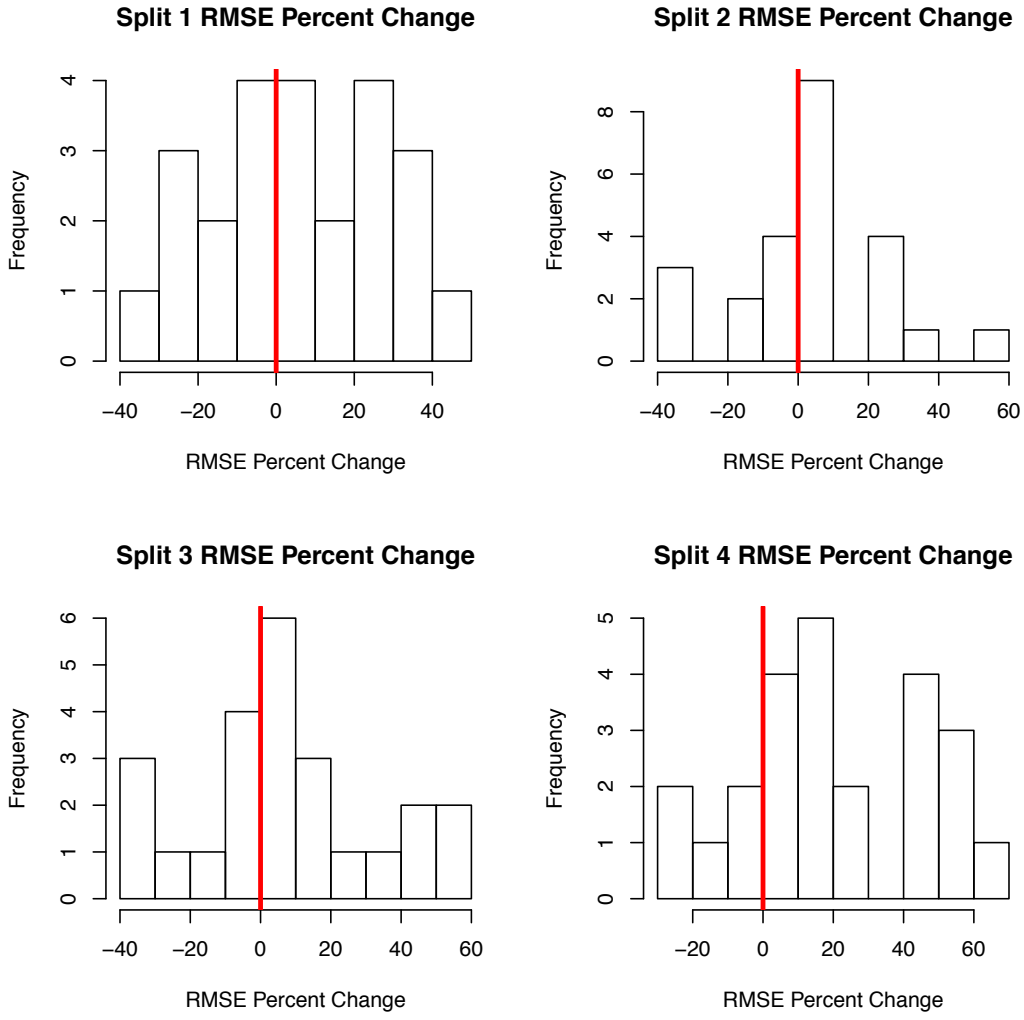

Figure 4.5 The percent change in RMSE in each part type for splits 1-4. Positive percent changes indicate that the prediction algorithm performed better than the historical mean. The solid vertical lines represent the point of no difference between the historical mean and prediction algorithm.

4.5.3 Evaluating prediction interval performance

To assess the accuracy of the prediction intervals for the historical mean and resampling algorithm methods, we calculate how often each interval captures the truth within each split/week/part combination. For each split, prediction intervals were generated for 24 parts in each of the 26 respective testing weeks, resulting in 624 intervals for each split. Table 4.5 and Figure 4.6 summarize how often the prediction intervals capture the truth across the 624 cases in each each of the four splits. Supplementary plots illustrate lower bounds for the prediction intervals for the resampling algorithm never going below 0, a major benefit of the resampling algorithm (i.e., lower bounds for the historical mean can go below 0).

One can use Figure 4.6 and Table 4.5 to assess how frequently the percent of observations captured falls above or below the nominal coverage probability. In addition, the percent difference between each method can be calculated at each split, to assist in understanding why one method does better in a particular split.

Table 4.5 Percentage of holdout observations captured by 95% prediction intervals across each split

Split	Resampling	Historical mean
1	94.71	92.47
2	96.31	95.35
3	96.47	95.83
4	98.56	97.44

4.6 Discussion

In this paper, we developed a generic statistical part-demand prediction algorithm for the part consumption prediction problem. This method can be used with complicated distributions that do not have a closed form.

In our data analyses, we found that some systems experienced particular failure types more often than others. With limited information on the system makeup, high failure rates might suggest that there are subsystems with defective components or being operated in harsher operating conditions.

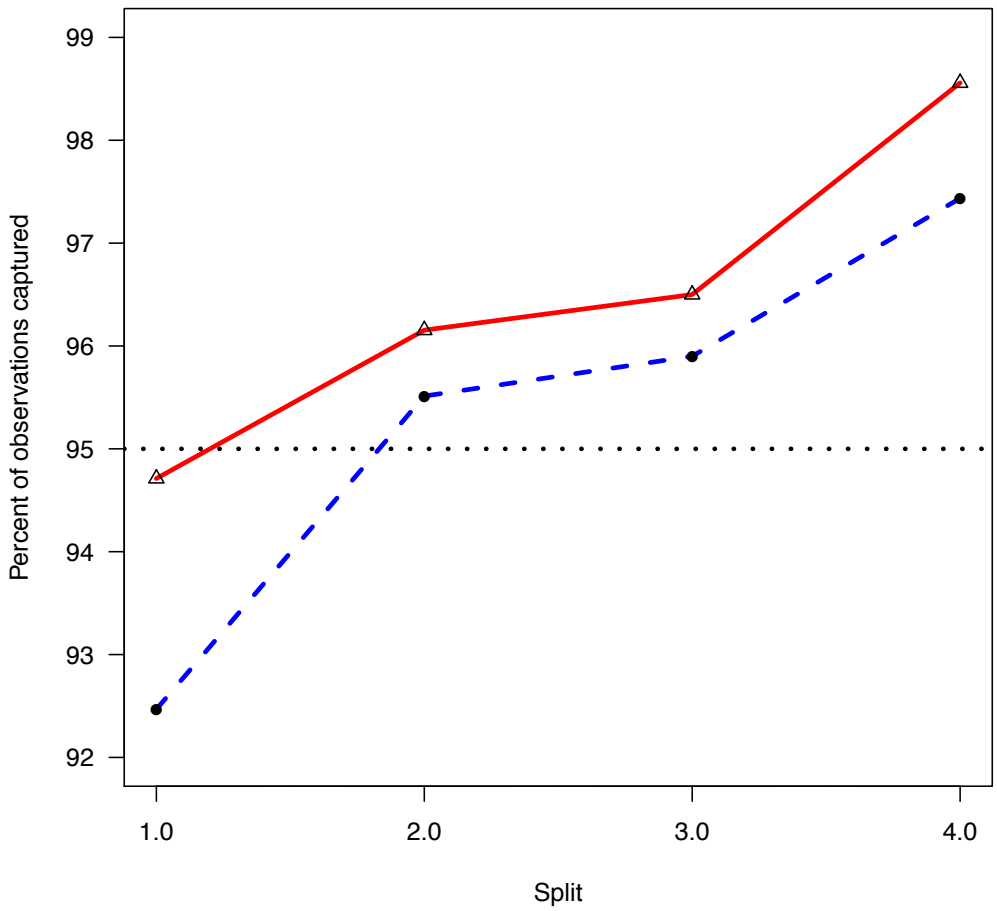

Figure 4.6 The percentage of observations captured using 95% prediction intervals in each split using the historical mean (dashed line with circular points) and resampling algorithm (solid line with triangular points). A dotted horizontal reference line is plotted at 95%.

Although the prediction intervals for the individual part type/week combinations are often too wide to be directly useful in determining the number a specific part type in a given week for a fleet of systems, the quantitative information does provide a useful ranking for setting priorities in maintenance scheduling and for ordering spare parts for the systems that need more frequent part replacements. The prediction intervals for the cumulative number of parts over time for the fleet of systems is useful for capital planning.

4.6.1 Alternate approaches: individual system predictions

The prediction intervals for individual systems tend to be wide. If usage and/or environmental information for the individual systems were available (e.g., load or ambient temperature history), it would be possible to build a better predictive algorithm that would more accurately predict individual part consumption needs. Models in Nelson (2001) and Duchense (2005) use such methods. Hong, Meeker, and McCalley (2009) state that further developments would, however, be needed to develop appropriate prediction interval procedures.

4.6.2 Improvements and limitations

The proprietary nature of the data used in this paper restricts the ability of to use engineering knowledge for building the predictive model. With engineering or problem-specific knowledge, information about parameters used in the prediction algorithm could be used within a Bayesian approach to take advantage of the prior information to narrow the width of the prediction intervals. This parametric approach would add interpretability in comparison to the algorithm used in this paper, but would require additional modeling assumptions.

Acknowledgements

This work was completed under an IGERT program funded by the US National Science Foundation, Award 1069283.

Bibliography

Barabadi, A., Barabady, J., and Markeset, T. (2014). Application of reliability models with covariates in spare part prediction and optimization: a case study. *Reliability Engineering and System Safety, 123,* 1–7.

Cook, R. J. and Lawless, J. F. (2007). *The Statistical Analysis of Recurrent Events* Springer.

Duchense, T. (2005). Regression models for reliability given the usage accumulation history. In A. Wilson, N. Limnios, S. Keller-McNulty, and Y. Armijo (Eds.). *Modern Statistical and Mathematical Methods in Reliability, 10,* 29–40. World Scientific, Singapore.

Hong, Y., Meeker, W. Q., and McCalley, J. (2009). Prediction of remaining life of power transformers based on left truncated and right censored lifetime data. *The Annals of Applied Statistics, 3,* 857–979.

Meeker, W. Q., and Escobar L. A. (1998). *Statistical Methods for Reliability Data.* Wiley.

Meeker, W. Q., Hahn, G. J., and Escobar L. A. (2017). *Statistical Intervals: A Guide for Practitioners and Researchers.* (Second Edition) Wiley.

Nelson, W. (2001). Prediction of field reliability of units, each under differing dynamic stresses, from accelerated test data. In *Handbook of Statistics, 20,* 611–621. Elsevier.

Nelson, W. (2003). *Recurrent Events Data Analysis for Product Repairs, Disease Recurrences, and other Applications.* ASA-SIAM.

Qian, Z., Shenyang, L., Zhijie, H., and Chen, Z. (2017). Prediction model of spare parts consumption based on engineering analysis method. *Procedia Engineering, 174,* 711–716.

CHAPTER 5. SUMMARY AND CONCLUSIONS

In this dissertation, we developed general statistical methodology for real problems facing the wind energy industry.

In Chapter 2, we developed a generic statistical procedure using a Bayesian hierarchical structure for a downtime prediction problem that can be used with truncated data. The methods were applied to a fleet of wind turbines, using data that was provided from a United States power company.

The hierarchical modeling of the fleet of turbines as related but distinct made sense from a practical standpoint. We showed the ability to predict future downtime through simulation and borrowing strength properties of a hierarchical model, which proved to have an advantage in comparison to modeling each turbine separately. After a service event, the power law process was considered to be "as-bad-as-old" because its intensity is approximately constant during small time intervals. One could argue that the plausibility of "as-bad-as-old" due to the multiple failure modes associated with wind turbines. Checking this assumption requires additional research.

In Chapter 3, we developed a repairable systems R tool that offers multiple models to understand how engineering assets perform over time. The R tool was applied to data from a publicly available technical report to highlight the maintenance decision benefits that result from predicting system behavior at the subsystem and component levels.

We showed the ability to predict system behavior under both component and subsystem level models. The developed R tools were used to better understand how specific inputs (i.e. intensity threshold) affect wind turbine availability. We also found that the simulation tool allows users to better understand how the cost of "minimal repairs" will affect the cumulative costs for a fleet of systems. Finally, we presented a prediction method for wind turbines, which is a valuable tool in the wind energy industry since contracts generally guarantee a sustained level of availability over some initial period of each turbine's life. The availability predictions are expected to assist owners

and operators in implementing preventive maintenance strategies that target components that are significantly driving down turbine availability.

In Chapter 4, we developed models and methods to incorporate part consumption data that is dynamically logged in the field . A nonparametric algorithm for predicting future part consumption in systems that fail from multiple failure types was presented to deal with problems that have complicated time series structures. The methods were illustrated with an application for predicting part consumption needs for a fleet of systems with three failure types and 24 unique part types.

With limited information on the system makeup in this research, we concluded that high failure rates might suggest that there were subsystems with defective components or experienced a harsher operating environment. The prediction intervals were wide, but we suggest that they can be useful for ranking the assets with respect to maintenance scheduling and for ordering spare parts for the systems that need more frequent part replacements. Finally, we concluded that with engineering or problem-specific knowledge, we could have used a Bayesian approach to take advantage of prior information to narrow the width of the prediction intervals. Such a parametric approach would add interpretability in comparison to the algorithm developed in Chapter 4, but would require additional modeling assumptions.